EMRAS Tritium and C14 Working Group

PINE TREE SCENARIO

Final Report
June 2008

1. BACKGROUND AND OBJECTIVES

1.1. Introduction

In the Tritium Working Group (TWG) of the IAEA BIOMASS program from 1996 to 2000, two atmospheric source scenarios for model-data comparison exercises were proposed by Canada and France. Both were concerned with the transport of tritium in the vicinity of long-term or chronic atmospheric sources of tritiated water vapour (HTO). The sites were located in inland areas subject to temperate climates. Modelers were requested to predict tritium concentrations in sample species such as air, rain, soil water and plant water, with special focus on organically bound tritium (OBT) in plants and on the relationships between air HTO, plant tissue free water tritium (TFWT) and plant OBT concentrations. Compared with these two scenarios, the EMRAS pine tree scenario has unique features in the following aspects. First, it deals with a sub-tropical climate, which may affect the tritium behavior in the environment differently from a temperate climate. Secondly, the tritium sources are located along the Pacific coast, which may have a specific influence on atmospheric dispersion. Thirdly, it is the first model-data intercomparison exercise that treats sub-surface infiltration (groundwater) pathways following long-term atmospheric releases. Finally, it involves monthly variations of plant OBT concentrations over a few years, which may help to understand the seasonal variations of OBT in an evergreen pine tree. If we take into account the long residence time and translocation of OBT in plants, it is useful to compare OBT concentrations in four seasons in consecutive years. The Canadian BIOMASS scenario requested OBT concentrations in grass only at three times in a 2-month period in the summer, and the French scenario requested annual average OBT concentrations in a deciduous birch tree. Thus neither scenario addressed the long-term behavior of plant OBT, including winter seasons, a deficiency that is rectified in the EMRAS Pine Tree scenario.

1.2. Need for the Present Study

We learned from the BIOMASS scenarios that the uncertainty associated with the prediction of OBT concentrations in plants depends largely on the uncertainty in the tritium concentration in air moisture. The plant OBT concentration is calculated by multiplying the plant TFWT concentration by a discrimination factor, while the TFWT concentration is usually expressed as a function of the HTO concentrations in air and soil. These relationships have been validated in temperate climates and inland areas such as Europe and North America, where rainfall, air temperature and air humidity are all relatively low. For tritium discharge sources located along the sea coast, alternating wind directions between day and night time are common and may affect the atmospheric dispersion of the airborne plume. Especially during the day, onshore winds sometimes result in trapping conditions that have never been considered in past modeling scenarios. The Pine Tree scenario provides the opportunity to test models that predict tritium concentrations in various sample species (endpoints) due to multiple tritium sources located along the Pacific coast in Tokaimura, Japan.

In the French scenario of BIOMASS, the OBT concentrations measured in the leaves of one plant type were a factor of two different from the concentrations in the annual rings of a second plant type. There is a need to confirm this difference for different components of the same plant species, and to provide possible explanations for the difference. Since humans and animals eat

different components of plants (leaves, stems, fruits and roots), it is important to take into account differences of OBT concentration between the various plant parts for reliable tritium dose assessments.

In BIOMASS, two exercises on sub-surface pathways were conducted as model inter-comparison exercises without observational data. Suitable test data, which are essential for validating soil and hydrological models, were not found despite a concerted search at the time. The EMRAS Pine Tree scenario includes a dataset of monthly HTO concentrations in groundwater for a few years and meets the need not realized in the BIOMASS program.

1.3. Specific Objectives

The Pine Tree scenario was provided to evaluate the suitability of current modeling approaches for predicting monthly and yearly mean tritium concentrations in sample species (air moisture, rain, pine needle TFWT and OBT, pine annual ring OBT, and groundwater) in the vicinity of multiple tritium sources, taking into account such features and conditions as i) a short-term incidental release from one of the tritium sources, ii) a sea coast location for all sources, which were subject to diurnal wind direction changes, iii) a sub-tropical climate characterized by high humidity and rainfall intensity, iv) OBT production and translocation related to pine tree physiology and v) groundwater and tritium movement through a shallow sandy gravel layer.

2. SCENARIO DESCRIPTION

The Pine Tree scenario involved the continuous release of tritium from four sources near Tokaimura, Ibaraki Prefecture, Japan, and requested the calculation of tritium concentrations in air moisture, rain, pine trees and groundwater in the vicinity of the sources. As shown in Fig.1, two heavy water moderated research reactors (JRR2 and JRR3) and a waste treatment facility (WTF) are located at the JAERI* site and the Tokai Reprocessing Plant (called the Nuclear Fuel Reprocessing Plant, NFRP in this report) is situated at the JNC* site in Tokaimura. These facilities have released HTO vapor into the atmosphere continuously for many years. The most frequent wind direction at the site is north-east to south-west, as shown in Figs. 6a and 6b in the scenario description. Since 1981, the National Institute of Radiological Sciences (NIRS) has conducted a monthly monitoring program, including measurements of tritium concentrations in rain, groundwater and pine trees in the vicinity of JAERI and JNC. Among many sampling points, data from P3, MS2 and G4 were selected for the scenario because of their distinct source-distance relationships.

Since 1984, JAERI has conducted a monthly monitoring program including measurements of HTO concentrations in air, rain and pine needles at MP7, and HTO concentrations in rain at MS2.

All the main tritium sources as well as the sampling points P3, MS2 and G4 in the scenario were located within a rectangle measuring 1.0 km east-west and 2.0 km north-south (Fig. 1). The area is covered with sand dunes, the height of which increases away from the coastline to about 24 m above the sea level. A detailed description of the area, including the direction and distance of the sampling points from the sources, soil characteristics, geological structure (including parameter values for groundwater flow calculation), meteorological data and atmospheric tritium discharge rates from the four sources were provided in the scenario description.

* The Japan Atomic Energy Research Institute (JAERI) and the Japan Nuclear Cycle Development Institute (JNC) were unified into the Japan Atomic Energy Agency (JAEA) on 2005 October 1. The old names of JAERI and JNC are used in this report to maintain consistency with the organization names used in published papers related to this report.

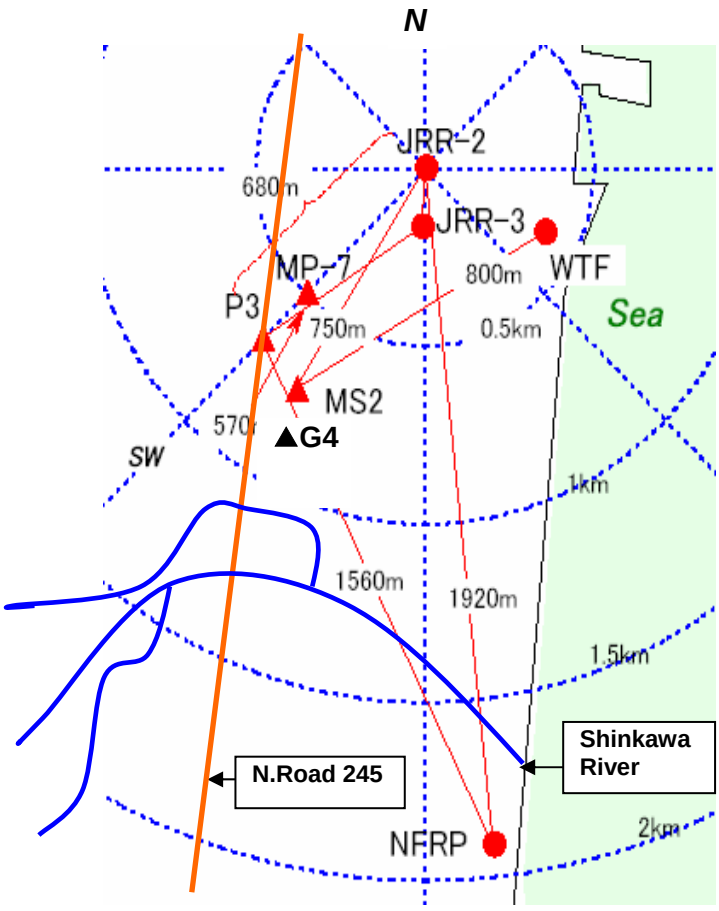

Figure 1. Map of the four tritium sources JRR2, JRR3, WTF of JAERI, and NFRP of JNC (closed circles) and the four tritium sampling points MP7 of JAERI and P3, MS2 and G4 of NIRS (triangles) in Tokaimura, Japan.

Modelers were requested to calculate the following endpoints:

1) Monthly-average HTO concentrations in air moisture and precipitation, and TFWT and non-exchangeable OBT (nOBT) in pine needles from 1982 to 1986 at sampling point P3;
2) Annual-average HTO concentrations in air moisture and precipitation, OBT in pine tree rings, and TFWT and OBT in needles of pine trees separately collected from the tree at the sampling point MS2. All predictions were to be for the period 1984 to 1987 at MS2;
3) Monthly-average tritium concentrations in groundwater at the well G4 from 1984 to 1987; and
4) 95% confidence intervals on each prediction.

The full scenario description is provided in Appendix A.

3. OBSERVATIONS

3.1. Sampling

From 1981, NIRS collected monthly rain water using a funnel attached to a long pipe. No effort was made to avoid tritium exchange between air moisture and the rain water accumulated in the pipe. Groundwater samples were collected from the taps of residents. New pine needle samples

were collected from new growth branches at heights of 1.0 to 1.5 m above the ground; these samples were stored in double-sealed plastic bags until they could be analyzed. The red pine trees in the Tokaimura area are up to 10 m high. For the annual-ring OBT analysis, a pine tree trunk sample was collected in December 1987 close to MS2.

3.2. Background samples

The contribution of tritium discharged from the tritium sources to the environmental concentrations was calculated from the observations by subtracting the background tritium levels. The background concentrations in rain, groundwater and annual-ring samples were determined by NIRS at locations far from nuclear facilities. Background concentrations in air moisture, pine needle TFWT and pine needle OBT in Japan were taken from published papers. These background data are shown in Table 1.

Table 1. Background tritium concentrations in Japan from 1982 to 1987.

	Air moisture	Rain	Pine needle TFWT	Pine needle OBT	Groundwater
	1984-1988	1982-1987	1983	1983	1980-1988
Mean (Bq/L)	1.9	1.1	1.7	2.4	2.2
2SD*	0.2	0.4	1.1	1.3	0.6
Location	Fukuoka	Chiba	Whole of Japan	Whole of Japan	Ibaraki

*SD: standard deviation of the mean

3.3. Experimental Procedures

Rain samples were purified by distillation and counted by low background liquid scintillation counting (LSC) techniques. Groundwater samples were normally electrolytically enriched before LSC. Needle TFWT was extracted on a cold finger as ice by vacuum distillation, purified by distillation by adding a small amount of $KMnO_4$, and counted by LSC. OBT concentrations in pine needles were obtained from the combustion water of the dry samples using an oxygen plasma asher (oxidizer) and purified by distillation. Detailed techniques of analysis are published elsewhere (Iwakura et al., 1979; Tanaka-Miyamoto et al., 1987, Inoue and Iwakura, 1990; Hisamatsu et al., 1990; Fuma and Inoue, 1995).

3.4. Uncertainties in Counting

The lower detection limit was estimated to be 1.2Bq/L, a value 3 standard deviations (SD) below the net counting rate when 8 ml of water was directly counted. The OBT concentrations in all samples exceeded this limit except for the concentrations in the tree rings collected in Chiba city in the late 1980s. The precision (reproducibility) was estimated to be 11-20% (2SD of the mean) by analyzing identical samples of two different tree rings two to three times. Uncertainties as 2 SD of the mean ranged from 11% to 31% for the OBT concentration in tree rings at MS2 from 1984 to 1987 (Fuma and Inoue, 1995).

3.5. Air Moisture Estimates at P3 and MS2

NIRS did not carry out air moisture sampling at P3 or MS2. JAERI collected air moisture continuously using molecular sieve columns at MP7, but not at MS2. JAERI also collected monthly rain at MP7 and MS2 (Matsuura et al., 1995). The air HTO concentration in Bq/m^3 reported by JAERI was converted to Bq/L water using the absolute humidity of each month averaged over the six years from 1982 to 1987. This conversion may have introduced an error of about 10% into the observed air moisture concentration in Bq/L water at MP7.

Ratios of annual mean tritium concentration in rain at P3 and MP7 and at MS2 and MP7 from 1984 to 1987, which were calculated from NIRS data for P3 and MS2 and JAERI data for MP7,

are shown in Fig. 2. The rain concentrations are similar at the three sites, suggesting that the concentrations in air moisture are also similar. Thus it is reasonable to assume that JAERI's air moisture data at MP7 apply also at P3 and MS2 as reference values, with uncertainties of about 30% for P3 and 80% for MS2.

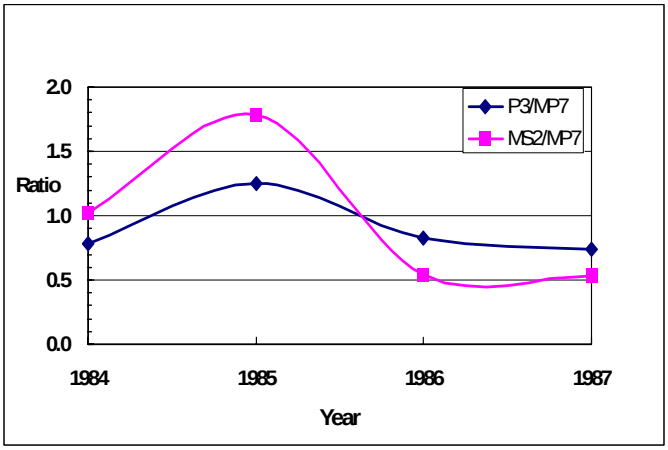

Figure 2. Ratios of yearly tritium concentration in rain at P3 and MP7, and at MS2 and MP7 from 1984 to 1987.

4. PARTICIPANTS AND THEIR MODELS

4.1. Participants and Model Names

The five modeling groups that submitted results for the Pine Tree scenario are shown in Table 2, together with affiliations, model names and designations used in text. The endpoints calculated by each group are shown in Table 3. Observed values were revealed after the submission of the second set of results.

Table 2. Participants and the models in the Pine Tree scenario

Participating Group	Affiliation	Model name	Designation used in text
K. Miyamoto K. Yamamoto	NIRS, Japan Y First, Japan	Tritium-EESAD ERMA	NIRS
M. Saito	Safety Reassurance Academy, Japan	TriSat	SRA
S.R. Peterson	Lawrence Livermore National Lab, USA	DCART	LLNL
D. Galeriu A. Melintescu	Institute of Atomic Physics and Nuclear Engineering, "Horia Hulubei", Romania	DISPT	IFIN
F. Siclet E. Gilbert T. Kestens	Electricité de France, France	ADMS3, ARGUS	EDF

Table 3. Participants and their calculated endpoints.

Participant	Number of calculations until final results	Air	Rain	Needle TFWT	Needle nOBT	Ring nOBT	Ground-water
NIRS	2	○	○	○	○	○	○
SRA	3	○	○	○	○	○	○
LLNL	1	○	○	○	○	○	-
IFIN	1	○	○	○	○	○	○
EDF	1	○	○	-	-	-	○

4.2. Modeling Approaches

The detailed approaches used in each model are described in Appendix B. The models and calculation conditions assumed for pathways from air to pine tree are summarized in Table 4 and those from air to groundwater in Table 5.

4.2.1. Modeling approaches for atmospheric dispersion

Most modelers used a Gaussian plume model to calculate atmospheric dispersion. The exception was NIRS, which applied a random walk model that has been proven to generate results essentially identical to those of the Gaussian model for steady-state conditions. Within this overall similarity in approach, there were some differences in the way individual dispersion processes were treated. All modelers except NIRS considered all four HTO sources separately. In contrast, NIRS ignored the NFRP at JNC on the assumption that it makes a minor contribution at the sampling (target) sites due to its large effective release height, its location in a sector into which the wind blows infrequently and its large distance from the target sites.

SRA, IFIN and LLNL used the sector-averaged form of the Gaussian plume model and calculated air concentrations averaged over the sector. On the other hand, NIRS and EDF used an averaging area of 100 m x 100 m, which was smaller than that of the Gaussian model at the downwind distances of the target sites.

NIRS and SRA did not take plume rise into account while other modelers estimated plume rise by different methods. LLNL used the momentum driven plume rise model in the dispersion code CAP88-PC, where plume rise = 1.5VD/U, where V is the stack gas exit velocity (m/s), D is the inside stack diameter (m) and U is the wind speed (m/s). The wind speed used in the models should ideally be the speed at the effective release height (physical stack height + plume rise) of the plume. Since they did not calculate plume rise, NIRS and SRA used the wind speed at the physical stack height. Using the ADMS3 code, EDF recalculated the wind speed at the emission height of each stack based on meteorological data observed 10 m above ground on the JNC meteorological tower.

The vertical dispersion parameter, σ_z, is important in predicting tritium concentrations in air at the target points. The modelers used a number of different approaches to calculating σ_z, as presented in Table 4.

Washout of HTO from the air to the ground by rain is an important process for determining tritium concentrations in rain, soil and groundwater. Most modelers calculated wet deposition and rain concentrations using a washout coefficient, although the value of the coefficient differed from modeler to modeler, as shown in Table 4. Consideration of dry deposition and re-emission of HTO from the ground surface depended on each model.

4.2.2. Modeling approaches for pine trees
All modelers estimated the concentration of TFWT in pine needles using an equation of the form:

$$C_{TFWT} = \gamma \{RH*C_a+(1-RH)*C_s\}, \quad (1)$$

where γ (=1.1) is an isotopic discrimination factor,
RH is the relative humidity,
C_a is the HTO concentration in air moisture, and
C_s is HTO concentration in soil moisture,

NIRS adopted a mean equivalent value for RH based on reference searches as presented in Table 4. Modelers calculated C_{OBT} in pine needles by multiplying C_{TFWT} by a proportionality constant of 0.6 to 0.8, which is considered an isotopic discrimination factor in the photosynthesis process. The modelers made different assumptions about the period of OBT photosynthesis, ranging from five months (from April to August) by SRA to the full year by NIRS and LLNL. NIRS assumed that the pine needle OBT concentration equaled the average value over the six months before sampling. Although new-growth needles were always collected from new-growth branches, IFIN assumed that half the needle OBT concentration was made up of old OBT produced in the previous year and translocated to the new growth.

The OBT concentrations in the annual rings of the pine tree were calculated by multiplying the needle OBT concentrations by values ranging from 1.0 (no isotopic discrimination) to about 0.5. LLNL and NIRS applied values of 0.57 and 0.50, respectively, which are assumed to be isotopic discrimination factors in a metabolic translocation process of OBT from pine needles to the woody parts of the annual rings (Inoue et al, 2005).

4.2.3. Modeling approaches for groundwater
Four models participated in the prediction of HTO concentration in groundwater. The models and parameter values for the pathway from soil surface to groundwater are presented in Table 5. The models fall into two categories. The first is a compartment model, where wet deposited HTO infiltrates the unsaturated soil layer and, after a certain travel time, reaches the saturated layer of the groundwater aquifer where instant mixing is assumed. NIRS and SRA adopted this simple approach, which requires few parameters. They assumed that the tritium concentration in groundwater at G4 equaled the monthly-average concentration in rain deposited on the soil surface at MS2, with a travel time of about 2.7 – 3 years to reach the water table after wet deposition. Another parameter required by NIRS is the turnover rate (0.17 a^{-1}) of water in the groundwater aquifer. SRA used a factor of 0.3 as a dilution factor for tritium in the pathway from soil surface to groundwater.

The second category of groundwater model, as adopted by IFIN and EDF, was relatively more complex and required many parameters to run. EDF fully utilized the information given in the scenario description regarding the geological formation and the groundwater flow, with the assumption that the model area was limited to a region 500 m long by 200 m wide starting 300 m southwest of JRR2 and JRR3. Only tritium deposited in this limited area by precipitation affected the tritium concentration in the groundwater at G4. EDF needed many parameter values to solve their dispersion model as listed in Table 5. On the other hand, IFIN assumed a different groundwater scenario in which the aquifer started 2 km north of JRR2 and flowed south through G4. In this case, wet-deposited tritium from a wide area affected the tritium concentration in groundwater at G4.

Table 4. Models and calculation conditions for pathways from air to pine tree*

Organization		NIRS	SRA	IFIN	LLNL	EDF
Type of dispersion model		Random walk	Sector-averaged Gaussian plume	Sector-averaged Gaussian plume	Sector-averaged Gaussian plume	Advanced Gaussian plume
Code name		Tritium-EESAD	TriSat	DISPT	CAP88-PC, DCART	ADMS3
Number of sources		3 (NFRP ignored)	4	4	4	4
Receptor size		100 m x 100 m	Sector-averaged	Sector-averaged	Sector- averaged	100 m x 100 m
Roughness length, m		-	-	-	0.01	0.5
Wind data used to estimate wind speed at stack height		JAERI:40m	JAERI:40m, JNC:70m	JAERI:40m, JNC:70m	JAERI:10m, JNC:10m	JNC 10m
Plume rise		Not calculated	Not calculated	Equation in the scenario	Equation in the scenario	ADMS3 equations
Dispersion parameter, σ_z		Pasquill-Gifford	Briggs	$ax^{0.711}$	Briggs	Based on Monin-Obukhov theory
Dry deposition velocity, m s^{-1}		0.005	0.003	Soil concentration includes $0.1C_{air}$	Dry deposition not calculated	Dry deposition not calculated
Washout coefficient, s^{-1} (J= rain intensity, mm h^{-1})		$5.0E\text{-}5J^{0.8}$	7.3E-5	$1E\text{-}4\ J^{0.8}$	Variable from 7E-6 to 1.3E-4	7.3E-5
Re-emission		Considered	Considered	Considered	Not calculated	Not calculated
Soil concentration		$0.3C_{air}$	Equal to rain concentration	0.9 x rain concentration + 0.1 x air concentration	Equal to rain concentration	Not calculated
Needle TFWT concentration		$0.57C_{air}+0.43C_{soil}$	1.1 [RH x C_{air} + (1-RH) x C_{soil}]	1.1 [RH x C_{air} + (1-RH) x C_{soil}]	1.1 [RH x C_{air} + (1-RH) x C_{soil}]	Not calculated
Needle OBT	Equation	0.8 x C_{TFWT}	0.73 x C_{TFWT}	0.5 oldOBT+ 0.5 newOBT (newOBT = 0.6 x C_{TFWT})	0.7 x C_{TFWT}	Not calculated
	Photosynthesis period	Entire year	April - August	April - October	The entire year	-
	Retention period	6 months	2 years	Equilibrium	Equilibrium	-
Ring OBT		0.5 x needle OBT	1.0 x needle OBT	1.0 x needle OBT	0.57 x needle OBT	Not calculated

*Some expressions or units in this table differ from those in the model descriptions to aid in the comparison

Table 5. Models and parameters for the groundwater (GW) pathway

Organization	NIRS	SRA	IFIN	EDF
Modeler	K. Miyamoto	M. Saito	D. Galeriu	T. Kestens
Code name	ERMA	TriSat		ARGUS
Input data or wet deposition area	Rain concentration at MS2	Rain concentration at MS2	From 2 km north of JRR2 to 800 m south (G4) of JRR2	Area 200 m wide by 500 m long, 300-800 m south of JRR2-3
Unsaturated soil layer Total porosity of surface soil	-	-	-	0.53
Water content, %	-		-	28.4
Thickness of unsaturated layer, m	15	15	-	15
Vertical water velocity, m a^{-1}	5.5	5	-	5.5
Vertical dispersivity, m	-	-	-	1
Travel time of HTO from soil surface to GW table, a	2.7	3	1	2.7
Saturated layer Thickness of water table, m	-	-	1m at 2 km N of JRR2 to 10 m at Shinkawa river	5
Number of dimensions		-	2 (x, z)	2 (x, y)
Hydraulic conductivity, m s^{-1}	-	-	-	6 x E-4
Longitudinal pore water velocity	-	-	30 m $month^{-1}$	0.2 m day^{-1}
Vertical pore water velocity, m $month^{-1}$	-	-	0.3	-
Longitudinal dispersivity, m	-	-	-	10
Transverse dispersivity, m	-	-	-	1
Turnover rate of aquifer, a^{-1}	0.17	-	-	-
Dilution factor	-	0.3	-	-

5. COMPARISON OF PREDICTIONS WITH OBSERVATIONS

Before model performance was evaluated, the internal consistency of predictions and observations was examined and discussed.

5.1. Internal Consistency between Predictions of Each Model

The means of predicted to predicted (P_x/P_{air}) ratios of the yearly mean tritium concentration (P_x) for each endpoint (x) to that for air moisture were compared between models. The endpoints considered were rain, pine needle TFWT, pine needle OBT and ring OBT.

When the air concentration varies with time, the predicted concentration in each endpoint is expected to vary with time in a similar fashion, but the pattern and concentration levels may differ from those of air depending on factors in the tritium transport process such as isotopic dilution, the rate at which equilibrium is achieved, isotopic discrimination and time delays between adjacent compartments. The P_x/P_{air} ratio and the factors that influence it for each endpoint are listed in Table 6.

Table 6. Expected predicted to predicted (P_x/P_{air}) ratio of tritium concentrations in the scenario endpoints (x) and the concentration in air moisture in dynamic conditions

Endpoint (x)	Influence factors* for P_x/P_{air} ratio	Expected P_x/P_{air} ratio
Rain	Isotopic exchange rate with air HTO in the plume	< 1 (≥ 1)**
Plant TFWT	Rapid isotopic equilibrium with air HTO; contribution of soil HTO	< 1
Plant OBT	Isotopic discrimination, translocation of OBT, different photosynthesis rates between day and night	< 1, (≥ 1)**
Groundwater	Time delay from air HTO	< 1, (≥ 1)**

* Large isotopic dilution by less contaminated water pools always occurs.
** The ratio may be above unity for short times under dynamic conditions.

Even if elevated OBT concentrations are produced after an incidental release of tritium, the effect of isotopic discrimination and isotopic dilution by less contaminated OBT produced thereafter means that the P_{OBT}/P_{air} ratio rarely exceeds unity. Similarly, the large isotopic dilution that occurs as the HTO plume moves into the groundwater (GW) aquifer suggests that the P_{GW}/P_{air} ratio rarely exceeds unity even if the concentrations in rain are elevated. In all cases where the P_x/P_{air} ratio is above unity, the mechanisms should be clarified.

The mean P_x/P_{air} ratios for each endpoint for each model are presented in Tables 7 and 8 for sampling sites P3 and MS2, respectively. Also shown are the standard deviations (SD) in the ratios, which indicate the variation in the mean ratio from year to year. The SDs were used here to judge if the mean P_x/P_{air} ratio is less than or greater than unity when uncertainties are taken into account. The ratios for each endpoint at P3 and MS2 showed similar values or tendencies

among the models. When the SDs are taken into account, the P_{rain}/P_{air} and P_{TFWT}/P_{air} ratios predicted by NIRS, LLNL and IFIN are below unity and are considered to be reasonable. On the other hand, some of the ratios predicted by SRA and EDF are above unity when the SDs are taken into account. These are considered to be questionable and may need clarification.

Table 7. The means of predicted to predicted (P_x/P_{air}) ratios of yearly mean tritium concentration in each endpoint (x) to that in air at P3 averaged over 1982-1986.

	Rain to air		Needle TFWT to air		Needle OBT to air	
Modeler	Mean ratio*	SD	Mean ratio*	SD	Mean ratio*	SD
NIRS	0.27‡	0.06	0.76	0.08	0.77	0.17
SRA	1.22	0.22	1.00	0.04	1.14	0.69
LLNL	0.60	0.14	0.97	0.01	0.73	0.01
IFIN	0.55	0.14	0.97	0.03	0.50	0.04
EDF	5.62	3.66	np**	np**	np**	np**

* The mean P_x/P_{air} ratios and the standard deviations for 1982-1986 were calculated from the mean ratios for each year.

‡ Annual means calculated from monthly data.

** Not predicted.

Table 8. The means of predicted to predicted (P_x/P_{air}) ratios of yearly mean tritium concentration in each endpoint (x) to that in air at MS2 averaged over 1984-1987.

	Rain to air		Needle TFWT to air		Needle OBT to air		Ring OBT to air	
	Mean ratio*	SD	Mean ratio*	SD	Mean ratio*	SD	Mean ratio*	SD
NIRS	0.22	0.03	0.70	0.04	0.58	0.05	0.37	0.03
SRA	1.63	0.58	1.22	0.12	0.76	0.24	0.66	0.18
LLNL	0.69	0.27	0.98	0.02	0.73	0.02	0.42	0.01
IFIN	0.50	0.05	0.98	0.03	0.50	0.07	0.51	0.10
EDF	3.83	0.94	np**	np**	np**	np**	np**	np**

* The mean P_x/P_{air} ratio and the standard deviations for 1984-1987 were calculated from the mean ratios for each year.
** Not predicted.

5.2. Internal Consistency between Observations

The observed to observed (O_x/O_{air}) ratios of tritium concentration for each endpoint (rain, pine needle TFWT, pine needle OBT and ring OBT) to the concentration in air moisture are presented in Tables 9 and 10 for sampling sites P3 and MS2, respectively. The O_x/O_{air} ratios can be greater than unity in dynamic conditions but such values should be confirmed and the responsible mechanism clarified.

When discussing the O_x/O_{air} ratios, we must take into account the timing of the exposure of the samples to the air and the different OBT photosynthesis rates between daytime and night time. Since the air moisture was continuously collected for whole days, including daytime and night time, and the rain was accumulated monthly, the timing of the exposure is not an issue for the O_{rain}/O_{air} ratio. The mean O_{rain}/O_{air} ratios presented in Tables 9 and 10 are around 0.3, which is consistent with other measured values.

There are a number of reasons for O_{TFWT}/O_{air} and O_{OBT}/O_{air} ratios above unity. Firstly, O_{TFWT} reflects the daytime air concentration while O_{air} reflects the 24-hour air concentration. The pine needles were always collected around noontime and thus their TFWT and OBT concentrations were directly influenced by the daytime air and not the 24-hour air. Analyses of wind direction frequency data at JAERI for daytime (6hr-18hr) and nighttime (18-6hr) for four seasons from 1981 to 1987 showed that i) during both the day and night, winds from the NE were dominant in spring and summer, and winds from the NW were dominant in autumn and winter, and ii) the frequency of occurrence of winds from the NE and adjacent directions (onshore windw) increased a little during the day even in autumn and winter, and the frequency of winds from the NW and adjacent directions (offshore winds) increased a little at night even in spring and summer. Thus the probability that the pine needles were exposed to onshore winds (which brings contaminated air from the three tritium sources at JAERI over sampling points P3, MS2 and MP7) is higher during the day than at night throughout the year. Consequently, the daytime air concentration tends to be higher than that of the 24-hour air and the O_{TFWT}/O_{air} and O_{OBT}/O_{air} ratios tend to be higher than unity (called the "downwind effect" hereafter).

Secondly, the air over the sea is stable during the day due to cooling by sea water. When this air blows onshore, it becomes unstable due to warming by the land surface. The thickness of the unstable layer, which is called the internal boundary layer, increases with distance from the coast. When tritium is released into this internal boundary layer, upward dispersion is limited because the stable sea air caps any further vertical transport. The tritium is constrained to disperse within the internal boundary layer, which causes an elevation of the surface air concentration (called the "trapping effect" hereafter). As a result, the daytime O_{TFWT} value often tends to be higher than the nighttime value, in which case the observed O_{TFWT}/O_{air} ratio can be above unity (a maximum value of 4.2 was observed at P3 in 1985), as shown in Tables 9 and 10. The trapping effect is not an issue for the NFRP in JNC because of its large effective stack height.

Thirdly, during the day, the pine needles are biologically active and produce a large amount of OBT, whose concentration tends to be high due to exposure to the elevated air concentrations in effect during the day. However, at night, the pine needles are biologically less active and produce lesser amounts of OBT, whose concentration tends to be low due to exposure to air that blows mostly offshore and is essentially uncontaminated. As a result, the observed OBT concentration (O_{OBT}) at daytime tends to be higher than that of the 24-hour air concentration, and thus the O_{OBT}/O_{air} ratios tend to be higher than the P_{OBT}/P_{air} ratios, which are calculated for the whole day (called the photosynthesis rate effect hereafter). Thus the O_{OBT}/O_{air} ratios that sometimes lie above unity (a maximum of 1.35 was observed at P3 in 1985; Tables 9 and 10) are considered reasonable.

Table 9. Observed to observed ratios (O_x/O_{air}) of tritium concentration in each endpoint (x) at P3 to that of air at MP7

Endpoint	Ratio, 1984	Ratio, 1985	Ratio, 1986	Mean ratio	SD*
Rain	0.36	0.38	0.27	0.34	0.06
TFWT	1.88	4.20	0.71	2.26	1.78
Needle OBT	1.09	1.35	nd**	1.22	0.18

* Standard deviation of the mean from 1984 to 1986.
** No data.

Table 10. Observed to observed ratios (O_x/O_{air}) of tritium concentration in each endpoint (x) at MS2 to that of air at MP7

Enpoint	Ratio, 1984	Ratio, 1985	Ratio, 1986	Ratio, 1987	Mean ratio	SD*
Rain	0.43	0.43	0.13	0.18	0.29	0.16
TFWT	1.62	4.00	0.63	1.03	1.82	1.51
Needle OBT	0.68	1.05	0.38	1.08	0.80	0.33
Ring OBT	0.43	0.37	0.13	0.17	0.28	0.15

* Standard deviation of the mean from 1984 to 1987.

The means of observed to observed ratios of needle OBT to needle TFWT concentrations at P3 and MS2 (O_{OBT}/O_{TFWT}) have almost the same values (0.54 and 0.44, respectively; Table 11). The isotopic discrimination factor D_p in the formation of OBT from TFWT in controlled conditions ranges from 0.54 for barley to 0.83 for maize, with a mean of 0.70 ±0.12 (IAEA, 2008). This suggests that the value of 0.5 for the O_{OBT}/O_{TFWT} ratio in pine needles (which was obtained in dynamic conditions in the field) can be attributed primarily to isotopic discrimination. Given these interpretations, all the observations are believed to be internally consistent for dynamic conditions, and can be used with confidence for the discussion of the P/O ratios in the following sections.

Table 11. The means of observed to observed (O_{OBT}/O_{TFWT}) ratios of needle OBT to needle TFWT concentrations at P3 and MS2

	OBT/TFWT Ratio	SD
Mean ratio for 1984 and 1985 at P3	0.54	0.43
Mean ratio for 1984 and 1987 at MS2	0.44	0.41

5.3. Predictions and Observations of Tritium Concentrations in Air Moisture

Predicted monthly variations of tritium concentrations in air moisture at P3 are shown in Fig. 3, together with the observed concentrations at MP7. All the predictions vary almost coincidently with each other and with the observations over the entire study period, but the predictions for P3 generally underestimate the observations at MP7from 1984 to 1986. Predicted yearly variations of tritium concentrations in air moisture at MS2 are compared with each other and with the observations at MP7 in Fig.4. They also vary in parallel with each other and the predictions underestimate the observations.

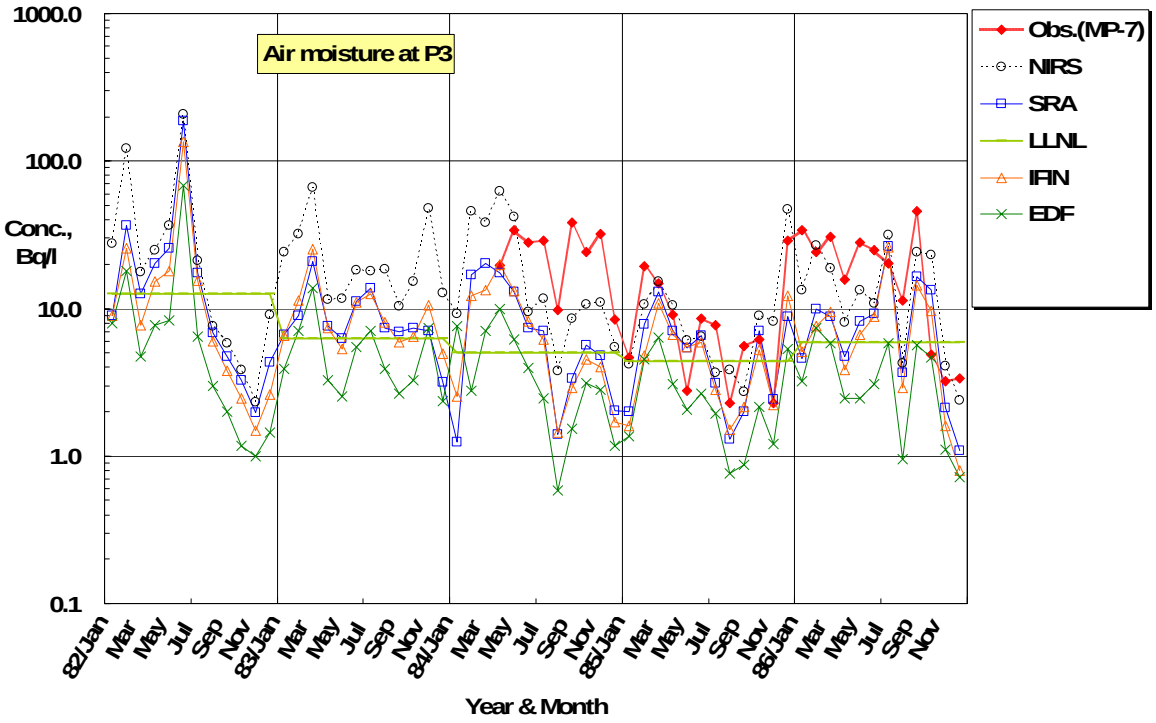

Figure 3. Predicted and observed monthly variations of tritium concentration in air moisture at P3 from 1982 to 1986

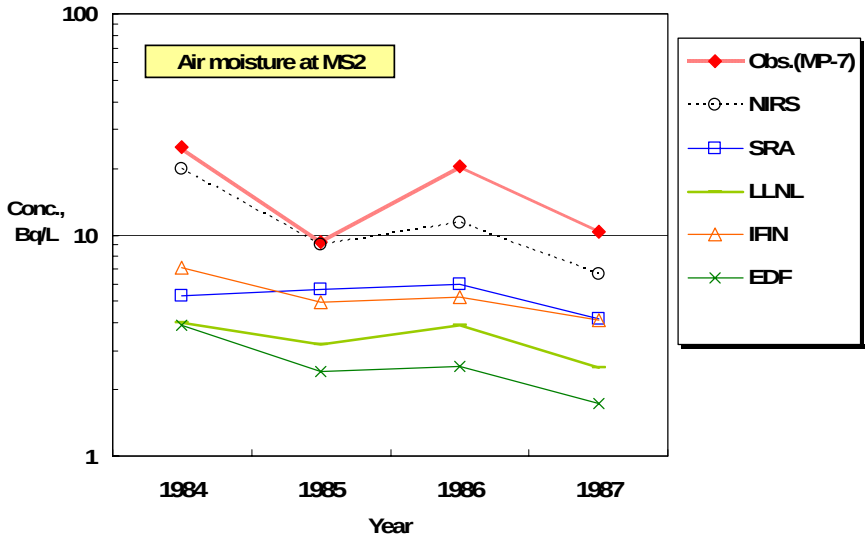

Figure 4. Predicted and observed yearly variations of tritium concentration in air moisture at MS2 from 1984 to 1987

The means of predicted to observed ratios (P_x/O_x) for each endpoint (x) were calculated from the yearly values for each year of the study, and are presented in Table 12 and Table 13 for sampling sites P3 and MS2, respectively. The means of P_{air}/O_{air} at P3 from 1984 to 1986 ranged from 0.92±0.21 for NIRS to 0.21±0.07 for EDF. The means of P_{air}/O_{air} at MS2 for 1984-1987 ranged from 0.74±0.18 for NIRS to 0.18±0.06 for EDF. The order of mean P_{air}/O_{air} ratios was NIRS > SRA> IFIN> LLNL> EDF for P3 and MS2. The concentrations predicted for MS2 were about 80% of the values predicted for P3.

Table 12. Means of predicted to observed (P_x/O_x) ratios of tritium concentration for each endpoint (x) at P3 for 1982 to 1986

	Air, 1984-1986		Rain, 1982-1986		TFWT, 1982-1986		Needle OBT, 1982-1986	
Modeler	Ratio	SD	Ratio	SD	Ratio	SD	Ratio	SD
NIRS	0.92	0.21	0.86	0.27	0.92	0.73	0.74	0.36
SRA	0.46	0.13	2.00	0.76	0.63	0.55	0.52	0.14
LLNL	0.32	0.14	0.58	0.15	0.35	0.24	0.21	0.07
IFIN	0.42	0.13	0.82	0.43	0.53	0.41	0.21	0.08
EDF	0.21	0.07	3.71	1.21	np*	np*	np*	np*

* Not predicted.

Table 13. Means of predicted to observed (P_x/O_x) ratios of tritium concentration for each endpoint (x) at MS2 for 1984-1987

	Air		Rain		TFWT		Needle OBT		Ring OBT	
Modeler	Ratio	SD	Ratio	SD	Ratio	SD	Ratio	SD	Ratio	SD
NIRS	0.74	0.18	0.66	0.30	0.39	0.19	0.61	0.23	1.15	0.46
SRA	0.38	0.17	2.31	1.07	0.34	0.19	0.35	0.06	1.08	0.67
LLNL	0.23	0.08	0.60	0.26	0.18	0.10	0.24	0.09	0.44	0.21
IFIN	0.37	0.13	0.76	0.39	0.27	0.14	0.24	0.06	0.86	0.51
EDF	0.18	0.06	2.72	1.40	np*	np*	np*	np*	np*	np*

* Not predicted.

Taking account of the standard deviation of the mean of the P_{air}/O_{air} ratios, and an estimated error of 30% to 80% when the observed air concentration at MP7 is assumed to apply at P3 and MS2, the NIRS model performed very well at both sampling sites. This agreement may be fortuitous and due in part to compensatory errors, since the NIRS model ignores plume rise (which could result in an overestimate of the concentrations) and trapping (which could result in an underestimate).

The other models underestimated the air moisture concentrations at P3 and MS2 by factors of 2 to 5, as shown in Tables 12 and 13. The reasons for this can be attributed to the parameter values in the atmospheric dispersion equations, as listed in Table 4. The relevant parameters are the wind speed at the effective stack height and the vertical dispersion parameter σ_z. The wind speed is normally estimated by extrapolating the wind data observed at different heights to the effective stack height using a power law function. However, data from the 10 m, 20 m and 40 m levels on the JAERI meteorological tower indicate a linear relationship between wind speed and height. Thus models with a power law function will estimate wind speeds that are too high and air HTO concentrations that are too low. In the EDF model, the wind speed at the effective stack height was estimated by extrapolating the speed observed 10 m above ground at JNC, rather than the speed at the greatest measurement height, viz. 40 m on the JAERI meteorological tower. This will probably amplify the errors in the power function extrapolation and may help to explain the low predictions of the EDF model.

The various modelers calculated the vertical dispersion parameter σ_z in different ways and obtained very different results in some cases. For example, the SRA and NIRS models gave smaller σ_z values than IFIN by a factor of 2-5, depending on the stability class and the distance from source to receptor. The prediction of higher air HTO concentrations by NIRS compared to IFIN may be attributed partly to the use of lower σ_z values.

Other causes for the underestimation may be the following:

- Ignoring differences in elevation between the base of the stacks and the target points. P3 and MS2 are located about 20 m and 35 m above sea level, respectively, whereas the three tritium sources at JAERI are located between about 10 m and 15 m above sea level. In ignoring these differences, the models will under-predict the air HTO concentrations because they overestimate the height of the plume as it passes over the target points.

- Ignoring trapping in coastal areas. A simulation of pollutant dispersal under typical conditions in coastal Japan has shown that when a continuous source with an effective stack height of 52.5 m is located at the coastline, the air concentration is largest 700-800 m from the source (Kimura and Takeuchi, 1978). Similar conditions may have sometimes happened at Tokaimura, leading to large concentrations at the target points P3 and MS2, but were not simulated by the models.

5.4. Predictions and Observations of Tritium Concentrations in Rain

Predicted and observed monthly tritium concentrations in rain from 1982 to 1986 at P3 and yearly concentrations at MS2 from 1984 to 1987are shown in Figs. 5 and 6, respectively. At both sites, the predictions scatter around the observations. The predictions of most models for P3 track each other well, including the sharp peak in June 1982 when an incidental HTO release occurred from JRR3. The EDF predictions stand apart due to their higher level and some sharp peaks in the middle of 1984.

The means of yearly P_{rain}/O_{rain} ratios at P3 from 1982 to 1986 and those at MS2 from 1984 to 1987 are shown in Tables 12 and 13, respectively. The models divide into two groups depending on whether the ratio is above or below unity. P_{rain}/O_{rain} ratios above unity are predicted by EDF and SRA, the models for which the P_{rain}/P_{air} ratios are also above unity. P_{rain}/O_{rain} ratios below unity are predicted by IFIN, NIRS and LLNL, the models that also predict P_{rain}/P_{air} ratios below unity. This systematic difference may be caused by the models and washout coefficients used to calculate concentrations in rain. The P_{rain}/O_{rain} ratios of 3.71 and 2.72 predicted by EDF are difficult to accept given that the P_{rain}/P_{air} ratios for this model are 5.62 and 3.83, more than 10 times higher than the mean O_{rain}/O_{air} ratios of 0.34 and 0.29. The P_{rain}/O_{rain} ratios of NIRS, IFIN and LLNL lie in the range 0.58 to 0.86, which agrees with the O_{rain}/O_{air} ratios within a factor of two to three and thus are more acceptable.

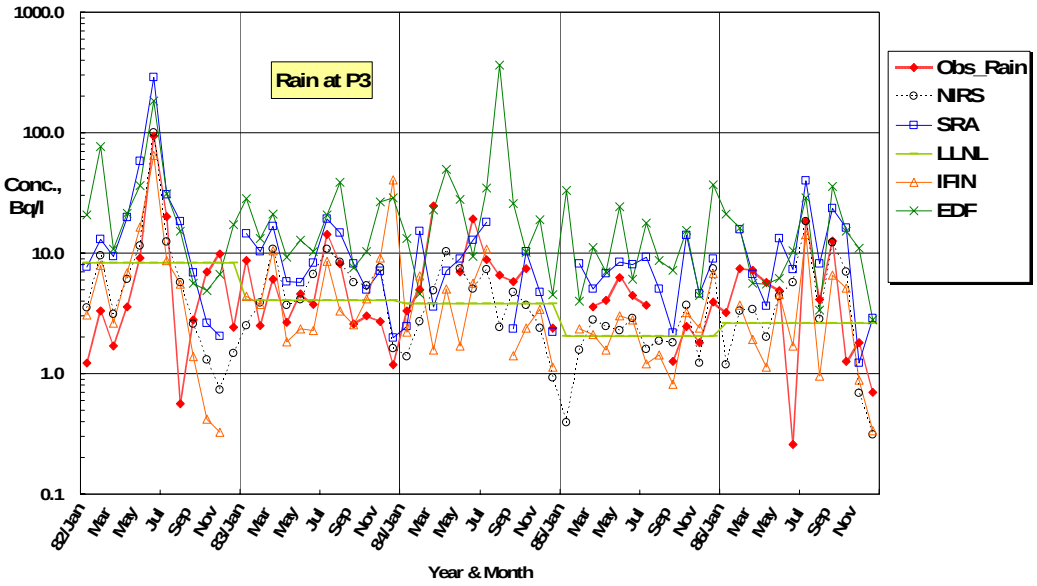

Figure 5. Predicted and observed monthly tritium concentrations in rain at P3 from 1982 to 1986.

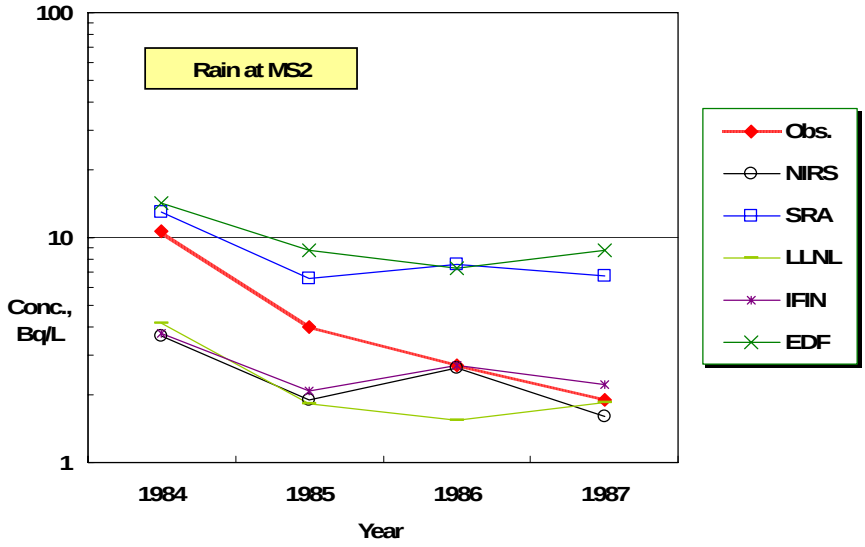

Figure 6. Predicted and observed yearly tritium concentrations in rain at MS2 from 1984 to 1987.

5.5. Predictions and Observations of TFWT Concentrations in Pine Needles

The predicted and observed monthly and yearly TFWT concentrations in pine needles at P3 and MS2 are shown in Figs. 7 and 8, respectively. The means of predicted to observed ratios (P_{TFWT}/O_{TFWT}) are listed in Tables 12 and Table 13. Since all models calculated the TFWT concentration using an equation similar to Eq. (1), the predicted monthly patterns of TFWT concentrations at P3 and MS2 are similar to those of the air HTO concentrations (Fig. 2 and Fig. 3).

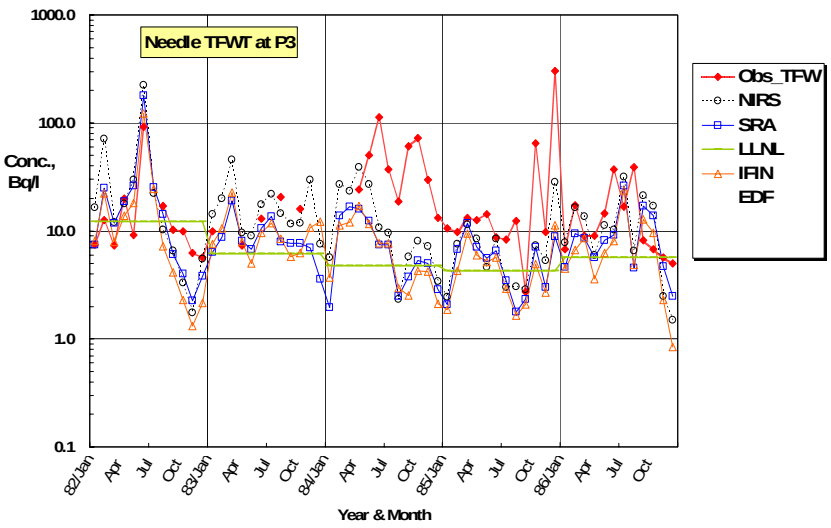

Figure 7. Predicted and observed monthly tritium concentrations (Bq/l) in pine needle at sampling point P3 from 1982 to 1986.

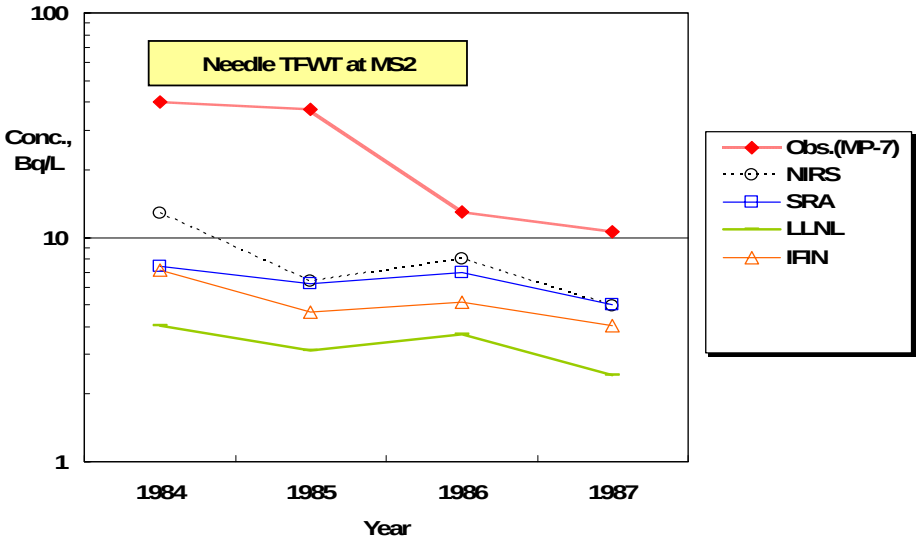

Figure 8. Predicted and observed yearly tritium concentrations in pine needles at sampling point MS2 from 1984 to 1987.

The mean observed TFWT concentrations were higher than the predictions both at P3 and MS2. Individual models underestimated the observations at P3 by up to a factor of 3 and at MS2 by up to a factor of 5. Since these factors are almost the same as the P/O ratios for air, the underestimate of the TFWT concentrations appears to be due primarily to the underprediction of the air concentrations.

The observed TFWT concentrations were higher than the predictions at both P3 (Fig.7) and MS2 (Fig.8) in 1984 and 1985, the years in which the observed mean O_{TFWT}/O_{air} ratios were much greater than 1 (Tables 9 and 10). Due to a combination of the downwind effect and the trapping effect associated with onshore winds during the day, which lead to high O_{TFWT}/O_{air} ratios (Section 5.2), the observed TFWT concentrations in pine needles collected near noontime tend to be higher than the predicted concentrations, which were calculated on a 24-hour basis.

5.6. Predictions and Observations of OBT Concentrations in Pine Needles

Predicted and observed monthly OBT concentrations at P3 from 1982 to 1986 and yearly concentrations at MS2 from 1984 to 1987 are shown in Figs. 9 and 10, respectively. The mean predicted to observed (P_{OBT}/O_{OBT}) ratios of yearly average OBT concentration at P3 and MS2 are presented in Tables 12 and 13, respectively. All of the models underpredicted the observed OBT concentrations by up to a factor of 5; the magnitude of the underprediction was similar at P3 and MS2. All models calculated the OBT concentration at a given time by multiplying the TFWT concentration by an isotopic discrimination factor between 0.6 and 0.8 (Table 4). One model assumed that the concentration in the new growth was made up partly of OBT produced in the current year and partly of OBT formed in the previous year and translocated to the new growth.

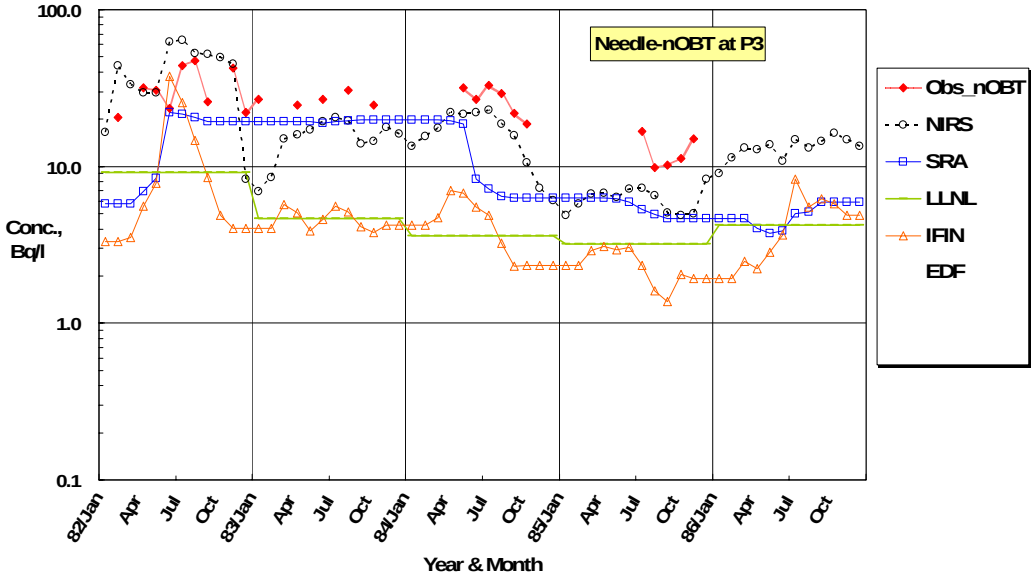

Figure 9. Predicted and observed monthly OBT concentrations (Bq/l) in pine needles at P3 from 1982 to 1986.

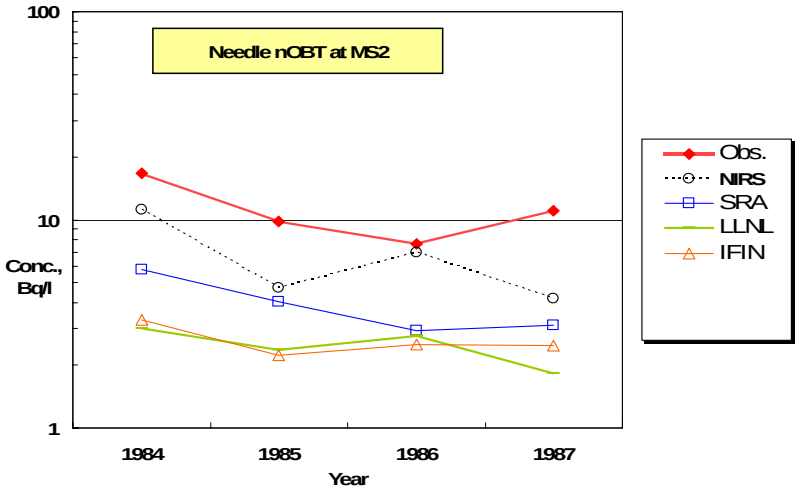

Figure 10. Predicted and observed yearly OBT concentrations (Bq/l) in pine needles at MS2 from 1984 to 1987.

The NIRS and SRA predictions of OBT were almost always several times higher than those of IFIN and LLNL (Fig. 9) whereas all predictions of TFWT concentrations were about the same (Fig.7). This result may have derived from the different assumptions made in the models regarding the photosynthesis period for OBT production, and the retention and translocation in pine trees, particularly as these relate to the high tritium concentration in air in June 1982. NIRS made the conservative assumptions that OBT is photosynthesized at the same rate throughout the year and that the OBT concentration at the time of sampling is an average over the 6 months before sampling. This resulted in predicted OBT concentrations of up to several tens of Bq/L in the second half of 1982, due to predicted TFWT concentrations that reached as high as about 200 Bq/L in June 1982.

The IFIN model was the only model that took account of the specific plant physiology of an evergreen conifer. The model estimated the average net photosynthetic rate from temperature and solar radiation intensity, which resulted in an OBT production period from April to October. In addition, the model assumed a low retention rate of newly photosynthesized OBT in leaves and a large translocation rate to roots and trunk. As a consequence, it assumed that the monthly average OBT concentration in needles during the summer consisted of equal parts old and new OBT, where the new OBT depended on the TFWT concentration. For example, the OBT concentration in needles in August was calculated as $OBT_{Aug} = 0.5 \times OBT_{py} + 0.5 \times 0.6 \times TFWT_{cy.}$, where OBT_{py} is the OBT concentration in the previous year, $TFWT_{cy}$ is the HTO concentration in needles in the current year (averaged over the previous few months), and 0.6 is the isotopic discrimination factor. The assumptions of a low contribution of new OBT and a rapid turnover of old OBT, together with predictions of low TFWT concentrations, may have resulted in OBT predictions by IFIN that were lower and changed more rapidly than those of NIRS or SRA.

The SRA model assumed that OBT was produced over the period from April to August and retained for two years. Although SRA and IFIN predicted similar time variations of TFWT concentrations, the long retention time adopted by SRA resulted in high OBT concentrations from June 1982 through May 1984, due to the influence of high air and TFWT concentrations in June 1982.

The LLNL model assumed that the OBT concentration was the TFWT concentration multiplied by an isotope discrimination factor of 0.7, without any assumptions concerning photosynthesis periods, retention or translocation of OBT. Thus its predicted yearly average OBT concentrations were simply 0.7 times the TFWT concentrations.

5.7. Predictions and Observations of OBT Concentrations in Tree Rings

Predicted and observed OBT concentrations in the annual rings of the pine tree collected at MS2 are shown in Fig. 11, together with the observed needle OBT concentration at MS2 for comparison. Since SRA and IFIN assumed no isotopic discrimination between needles and rings, the ring OBT concentrations predicted by these models were almost the same as the needle concentrations. Since NIRS and LLNL assumed an isotopic discrimination factor of 0.5 and 0.57 respectively, the OBT concentrations in rings predicted by NIRS and LLNL were about half the OBT concentrations in the needles.

As seen in Fig. 11, the ring OBT concentrations of each model agree fairly well with each other except for 1984, when the observed TFWT concentration was irregularly high. The predicted to observed ($P_{ringOBT}/O_{ringOBT}$) ratios for ring OBT concentrations averaged over the period 1984-1987 were 1.15 for NIRS, 1.08 for SRA, 0.44 for LLNL and 0.86 for IFIN. All of the models predicted the observed ring OBT concentration to within a factor of about 2.

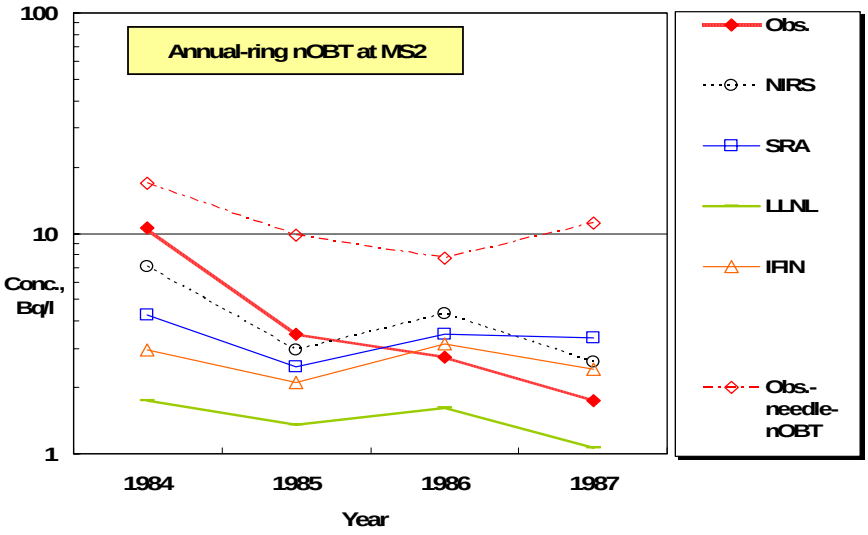

Figure 11. Observed and predicted yearly OBT concentrations in tree rings at MS2 from 1984 to 1987. Needle OBT concentrations observed at MS2 are also plotted for comparison.

It is worth noting that the data for 1984, 1985 and 1986 (but not 1987) show a yearly mean concentration ratio of ring OBT to needle OBT of about 0.5. This value is interpreted as an isotopic discrimination factor arising during translocation of needle OBT to ring OBT.

5.8.Predictions and Observations of Tritium Concentrations in Groundwater

The predicted and observed monthly tritium concentrations in groundwater at G4 from 1984 to 1987 are shown in Fig. 12. The yearly means of predicted to observed ratios of the groundwater concentrations are presented in Table 14.

The means of the P_{GW}/O_{GW} ratios for each model (the last two columns of Table 14) were based on the three years of data from 1985 to 1987, excluding the 1984 data, when most of the predicted concentrations were changing rapidly. Given that the tritium discharge rates and meteorological data were specified starting only in 1981, and that a delay time of about 3 years was assumed for wet-deposited tritium to reach the groundwater aquifer, the predicted time variation in 1984 varied strongly depending on the initial 1981 conditions assumed by the modelers. The peak concentration predicted by all models except that of IFIN occurred at the beginning or middle of 1985 as shown in Fig. 12, which corresponds most probably to the high release from JRR3 in June 1982.

The mean P_{GW}/O_{GW} ratios for 1985-1987 indicate that EDF overestimated the observed concentration by a factor of 1.65, and NIRS, SRA and IFIN underestimated by factors of 0.85, 0.47 and 0.28, respectively. In other words, all models predicted the observed groundwater concentration within a factor of about 3 except for 1984.

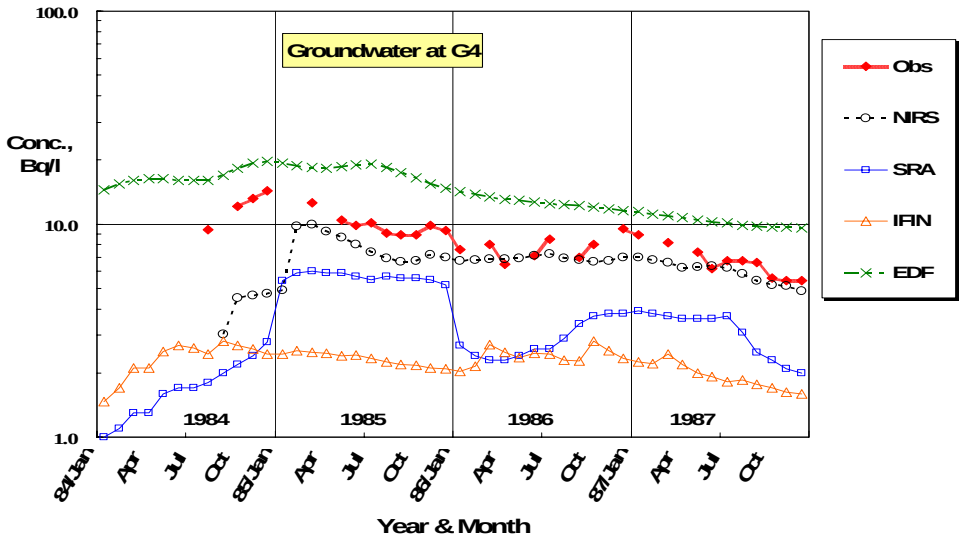

Figure 12. Predicted and observed monthly tritium concentrations in groundwater at G4.

Table 14. Predicted to observed (P_{GW}/O_{GW}) ratios of yearly mean tritium concentration in groundwater at G4 from 1984 to 1987 and the means of 1985 to 1987

	1984		1985		1986		1987		1985-1987	
	Ratio	SD	Ratio	SD	Ratio	SD	Ratio	SD	Mean	SD
NIRS	0.34	0.09	0.78	0.17	0.89	0.11	0.89	0.19	0.85	0.06
SRA	0.14	0.05	0.57	0.07	0.37	0.09	0.47	0.14	0.47	0.10
IFIN	0.19	0.05	0.24	0.03	0.31	0.05	0.29	0.07	0.28	0.04
EDF	1.37	0.27	1.80	0.26	1.63	0.22	1.53	0.28	1.65	0.14

The EDF results, which were obtained with the groundwater dispersion model ARGUS, overestimated the observations by an average of 65%. EDF demonstrated through additional calculations that this overestimate could be reduced by 30% by assuming an aquifer thickness of 7 m rather than 5 m. Part of the overprediction was also ascribed to the fact that EDF overestimated the observed rain concentration by a factor of 2.7 at MS2 (Table 13). As a conclusion, the sophisticated ARGUS model proved to be precise enough to predict the time variation of groundwater concentration as long as the input rain concentrations were predicted correctly. The good performance of the model was judged to be due to an appropriate assumption of a limited area of wet deposition and a suitable selection of parameter values based on the relatively detailed information on geological structure, infiltration rate, soil layer depth and groundwater flow rate given in the scenario description.

IFIN also applied a dispersion model to the groundwater calculations, but predicted concentrations that were consistently lower than those of any other model, as shown in Fig.11. This was due in part to an underestimate of the rain concentration at MS2, and in part to the assumption of a wide wet deposition area starting 2 km north of JRR2 to the Shinkawa river through G4, which resulted in excessive dilution of tritium by the southward movement of less contaminated groundwater.

NIRS and SRA used so-called piston models in their calculations. Wet-deposited tritium at MS2 was assumed to infiltrate the soil compartment, enter the groundwater aquifer and run off to the Shinkawa river with instant mixing and no dispersion in any compartment. Only a few parameters were required for their calculations, as listed in Table 5. The mean monthly groundwater concentrations predicted by NIRS were only 15% lower than the observations (Table 14). The success of this simple model may be due to the small, shallow nature of the groundwater system, with rapid mixing in an aquifer of limited area, in addition to the use of appropriate parameter values based on expertise accumulated by NIRS staff in the area concerned.

The mean monthly groundwater concentration predicted by SRA was about a factor of two lower than the observations in spite of the fact that the rain concentrations were overestimated by more than a factor of 2. If the dilution factor used in the model were increased from 0.3 to 0.6 (Table 5), the predicted groundwater concentrations would become closer to the observations, although the basis for selecting the value of the dilution factor is not clear.

5.9. 95% Confidence Intervals

Only LLNL carried out a rigorous uncertainty analysis and reported 95% confidence intervals for all scenario endpoints. IFIN reported 95% confidence intervals based on expert judgment without statistical analysis: a factor 3 for air moisture and a factor 5 for needle OBT and ring OBT. No factors were given for needle TFWT predictions, for which the uncertainty was expected to be large due to the fact that the measured value came from a single batch sample in a month. Other modelers did not report any uncertainties. In this situation, no conclusions can be drawn regarding the overall uncertainties for any of the endpoints in the scenario.

6. SUMMARY AND CONCLUSIONS

The Pine Tree scenario requested modelers to predict time-dependent monthly or yearly tritium concentrations in a variety of endpoints including air moisture, rain, TFWT and OBT in pine needles, OBT in annual tree rings and HTO in groundwater in the vicinity of multiple tritium sources located along the Pacific coast in Tokaimura, Japan. Monthly tritium release rates from three sources, yearly release rates from a fourth source, and hourly meteorological data were provided on a CD separately from the scenario description. Five models participated in the exercise. One model did not submit groundwater concentrations and predicted only mean yearly concentrations for the rest of the endpoints. Another model predicted concentrations in air moisture, rain and groundwater, but not in the pine tree.

All models were based on similar concepts but the equations and parameters used for tritium transfer in each process differed among models. Most modelers used a Gaussian plume model to calculate air concentrations but one participant used a random walk model. Similarly, simple piston compartment models and sophisticated dispersion compartment models were used for groundwater movement. The differences between predictions and observations proved to depend less on the differences in the models themselves and more on the choice of parameter values and the ways in which local conditions were taken into account, particularly the meteorological characteristics specific to the Pacific coast in Japan and the relationship between the sampling method used (continuous or batch) and the exposure timing (24 hours or daytime only) of each sample type. Some aspects of plant physiology, such as the difference in photosynthesis rate between day and night and between seasons, and the translocation of OBT, proved to be quite important in predicting the OBT concentration in plants.

For a given model, the accuracy of the predicted tritium concentrations in rain, needles, rings or groundwater depended on the ability of the model to predict the air concentrations accurately. Good agreement between predictions and observations for rain, needles, rings or groundwater was likely the result of compensatory errors if the model performed poorly with respect to the concentration in air.

The internal consistency of the predictions (P) of each model was examined based on the mean P_x/P_{air} ratios of yearly mean tritium concentration in a given endpoint (x) to the concentration in air. Most of the five models showed mean P_x/P_{air} ratios close to or below unity when the variance in the ratios was taken into account, indicating that most predictions were internally consistent. However, one model showed an unacceptably high P_{rain}/P_{air} ratio, suggesting that it may have a problem in modeling wet deposition.

The internal consistency of the observations (O) was also examined in terms of the O_x/O_{air} ratios of tritium concentrations in the various endpoints (x) to the concentration in air. The yearly mean O_{TFWT}/O_{air} ratios showed values much greater than unity at two target points in two years of the study. These high ratios likely arose from the fact that the pine needles were always sampled during the day. The air concentration during the day (and thus the observed TFWT concentration) tends to be high due to the frequent onshore winds that carry contaminated air to the target points and sometimes cause the trapping effect. In contrast, the 24-hour air concentration from which the TFWT concentrations were predicted tends to be lower because the frequency of offshore winds, which are associated with lower concentrations, increases at night.

The air moisture concentrations predicted by three of the five participating models lay within 40% to 80% of the observed concentrations, which is considered good modeling performance. The remaining two models underestimated the observed concentrations by a factor of 3 to 5, which suggests relatively poor performance, perhaps because the wind speeds or dispersion parameters used to calculate the air concentrations were overestimated. Ignoring the probable trapping effect is probably a common cause for all models to underestimate the air moisture concentration.

Since the scenario involved a simple groundwater system with relatively detailed information on the geological structure and water movement in the unsaturated and saturated soil layers, the complex dispersion compartment models were able to predict the time evolution of tritium concentrations in the groundwater to within a factor of 2 if appropriate assumptions and parameter values were applied. Even the simple piston compartment models that assumed instant mixing of input tritium performed well as long as key parameter values such as the turnover rate or dilution factor in the aquifer were known beforehand from other sources.

The key conclusions to come out of the Pine Tree scenario are: i) the air concentration, which drives concentrations of the other environmental compartments, is affected by local meteorology such as the trapping effect when the sources are located along the sea coast; ii) the measured TFWT and OBT concentrations, which were obtained from samples collected during the day, reflect daytime meteorological conditions; and iii) the plant OBT concentration is affected by the physiology of OBT production, OBT translocation and associated hydrogen isotope effects. All of these aspects are worthy of further study.

REFERENCES

Fuma, S. and Y. Inoue. 1995. Simplified and sensitive analysis of organically bound tritium in tree rings to retrospect environmental tritium levels. Appli. Radiat. Isot., **46**, 991-997.

Hisamtsu, S., T. Katsumata, Y. Takizawa, Y. Inoue and K. Isogai. 1990. Interlaboratory comparison of low-level organic tritium measurement in environmental samples. Radioisotopes, **39**, 457-463.

IAEA. 2008. Handbook of Parameter Values for the Prediction of Radionuclide Transfer in Temperate Environments. TRS 364, International Atomic Energy Agency, Vienna, Austria (in preparation).

Inoue, Y. and T. Iwakura. 1990. Tritium concentration in Japanese rice. Journal of Radiation Research, **31**, 311-323.

Inoue, Y., K. Miyamoto, S. Fuma and H. Takeda. 2005. Unique features of a pine tree for monitoring and modeling of environmental tritium. Fusion Science and Technology, **48,** 508-511.

Iwakura, T., S. Kasida and Y. Inoue. 1979. A low-background scintillation counter for measuring low-level tritium. In: Behaviour of Tritium in the Environment, IAEA-SM-232/32, 163-171.

Kimura, F. and K. Takeuchi. 1978. A numerical experiment on fumigation by sea breeze. Meteorology and Geophysics, **29**, 17-28.

Matsuura, K., Y. Sasa, C. Nakamura and H. Katagiri. 1995. Levels of tritium concentration in the environmental samples around JAERI Tokai. J. Radioanaly. and Nucl. Chem. Articles, **197,** 295-307.

Tanaka-Miyomoto, K., Y. Inoue and T. Iwakura. 1987. Tritium concentrations of groundwater in Naka Terrace, Ibaraki Prefecture, Japan. Journal of Environmental Radioactivity, **5**, 219-227.

APPENDIX A

Pine Tree Scenario Description

1. BACKGROUND

The main purpose of the pine tree scenario is to test models by comparing their prediction with observations of TFWT and OBT concentrations in pine trees, and HTO concentrations in groundwater. The major observed data were results of the NIRS monitoring program conducted monthly in the vicinity of nuclear sites in Tokaimura, Japan, where a few sources have released HTO vapor into the atmosphere continuously for many years. The scenario is characterized by such features as a subtropical environment, relatively simple wind direction frequencies (especially when it rains), reliable discharge rate data, and additional supportive measurements of tritium in air vapor and precipitation.

2. SITE DESCRIPTION AND MEASUREMENTS

2.1. Location of nuclear facilities

The Tokiamura village is basically a flat land of agriculture such as rice plant, vegetable and fruit plants. An overview of the Tokaimura village is shown in Fig 1. The population of Tokaimura is about 35,400. The Japan Atomic Energy Research Institute (JAERI), the Japan Nuclear Cycle Development Institute (JNC) (previously the Power Reactor and Nuclear Fuel Development

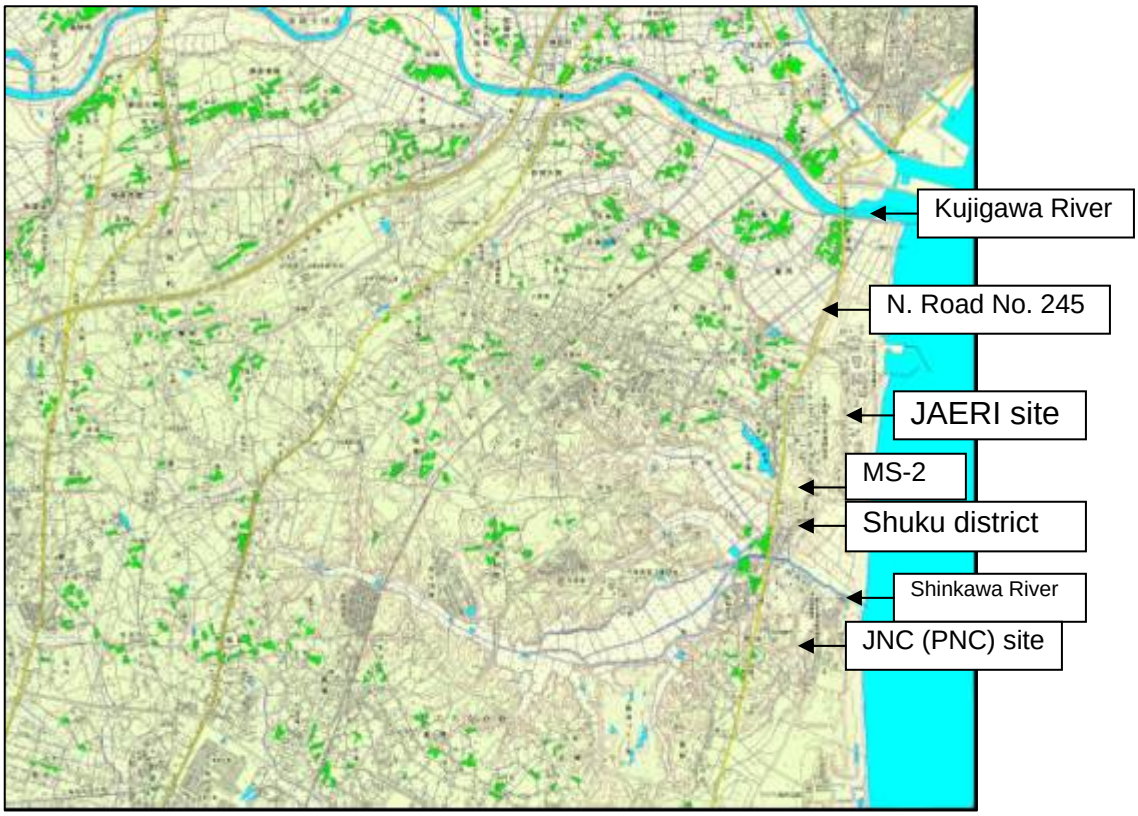

Fig. 1: Map of Tokaimura village with key nuclear facilities and landmarks

Corporation (PNC)), and other nuclear facilities are located in the east end of Tokaimura village (longitude 140.6E, latitude 36.5N), Ibaraki Prefecture Japan, facing the Pacific ocean. The locations of the main nuclear facilities and sampling sites are shown in Fig. 2.

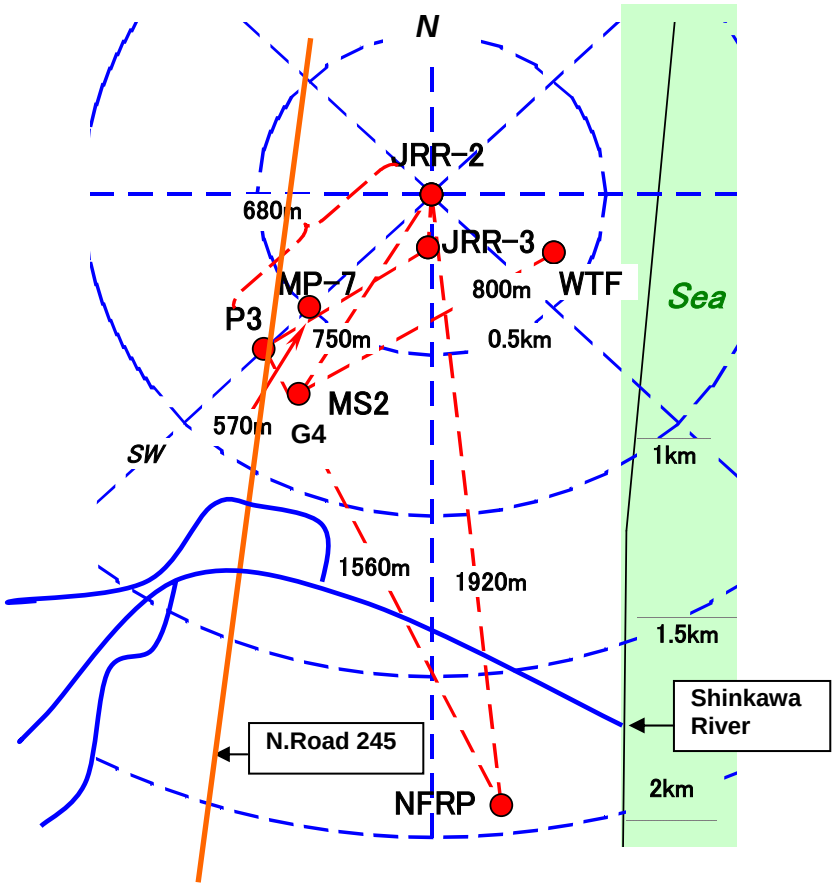

Fig. 2: Directions and distances of sampling points MP-7, P3, MS2 and G4 from the tritium discharge sources JRR-2, JRR-3, WTF and NFRP in Tokaimura, Ibaraki Prefecture. The distance between stacks of JRR-2 and JRR-3 is approximately 170m.

As seen in Figs. 1 and 2, the major nuclear facilities in Tokaimura are situated in a 1000-m wide zone between the east coast facing the Pacific Ocean and National Road No. 245, which runs north-south along the west boundaries of the JAERI and JNC sites. All the major tritium discharge sources, as well as the NIRS tritium sampling points in the scenario, are located within a rectangle 1 km east-west by 2 km north-south. The elevation of the sand dune terrain increases from sea level at the coast line to about 24 m above sea level at road 245. Most of the facility buildings at JAERI and JNC are located about 10-20 m above sea level. The highest hill top of the sand dunes is 35.7 m above sea level and located near the site boundary of JAERI in the SSW direction from the two heavy-water moderated research reactors JRR-2 and JRR-3. JAERI Monitoring Station 2 (MS-2) is located near the top of this hill.

2.2 Geological formation and a supposed groundwater aquifer in Shinkawa River Basin in Shuku district

The Tokaimura village is situated on part of the diluvial Naka Terrace. Three small streams are combined into the main Shinkawa River in the Shuku district, which flows along the north boundary of JNC (PNC) into the Pacific Ocean, as shown in Fig. 2. The Quaternary formation of Naka Terrace, consisting of silt or sandy gravel layers, overlies a hardened pelite layer (Miocene-Pliocene). The Pleistocene deposits of Naka terrace formed the broad wave-cut platform and the buried river channels of ancient rivers. Both the JAERI and JNC sites are situated on a shallow buried river channel that was cut by the ancient Shinkawa River. Later this was covered with quaternary formations when the area lay below sea level. Although groundwater is not so plentiful because of the thinness of soil deposits over the hardened pelite base rock, this groundwater, as well as water from the Kuji River (See Fig.1) supplied to the inhabitants in a local public water supply, is used for drinking or irrigation of fruit trees or upland rice fields.

Fig. 3 shows a supposed simplified geological cross-section and a groundwater aquifer along a line (the inner land line) connecting the points JRR2 at the north, G4 at the south-southwest and the Shinkawa river. Fig. 3 was drawn based on information from a limited number of soil cores in the area, taking into account a published, detailed geological section along a line (the seaside line) which runs about 500m east and almost parallel to the inner land line described above. Since the levels of both ground surface and base rock in the area surrounding JRR2 and JRR3 along the inner land line seem about 10 m higher than those along the seaside line, the groundwater may

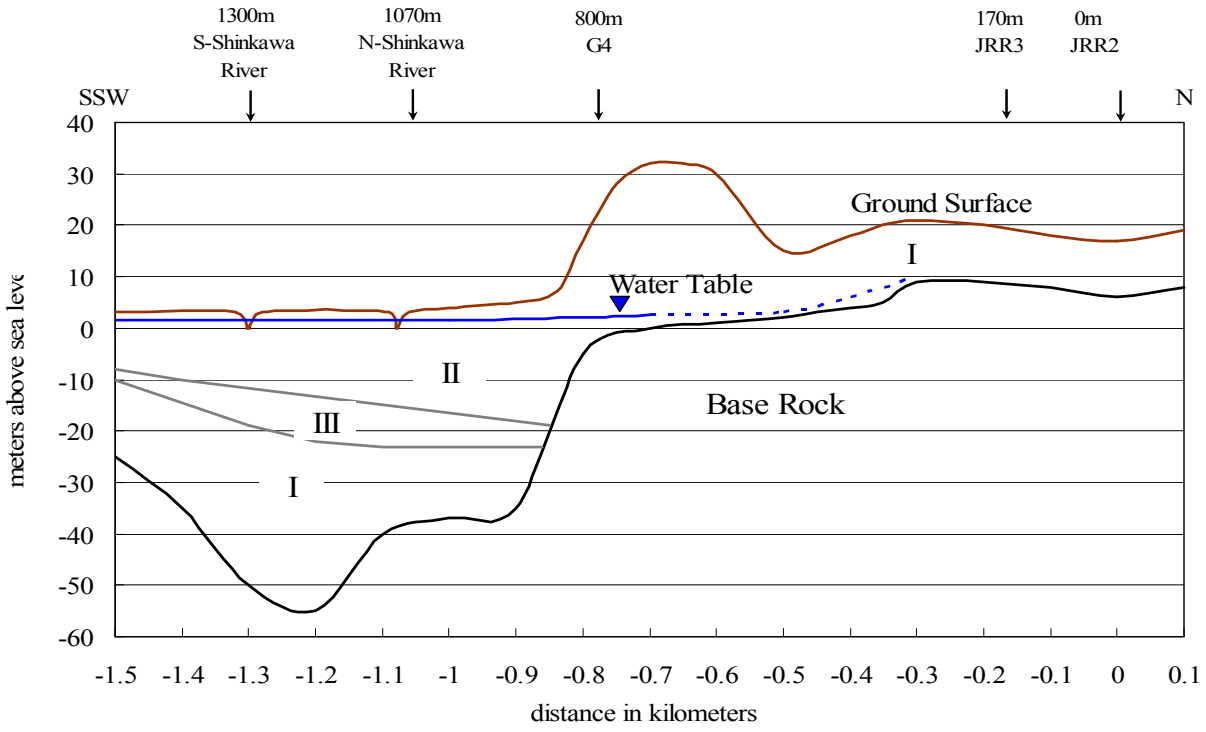

Fig.3 Supposed and simplified geological model along a line connecting the points of northern JRR2, south south-west G4, and Shinkawa River. I: Sand/Silt, II: Gravel/Sand, III: Silt/Clay

mainly flow eastward in the direction of the sea. Even if the groundwater flows southward from the JRR2 and JRR3 area, it might be blocked by ascending ground surface and base rock about 300 m south of JRR2, provided that the amount of groundwater is not so plentiful and the mean residence time of groundwater is relatively short, e.g. about half a year.

The infiltration rate of water into the unsaturated soil layer was estimated to be about half the annual precipitation of 500 – 700 mm (0.5 - 0.7 m). The vertical pore water velocity in the unsaturated soil layer was estimated to be about 5.5 m/y based on experimental data obtained by tracing HDO depth profiles for several months after mixing D_2O with surface soil in a field in the northern part of the JAERI site. The mean horizontal flow rate was estimated to be about 0.2 m/day based on Darcy's law applied to the area between a well close to G4 and a well close to the Shinkawa river, where groundwater flows southward into the Shinkawa River. Most of the well water in the Shuku district was probably taken from subsurface groundwater at a depth from several meters to 20 m. More than 10 monthly groundwater samples were taken from the resident wells in the area outside the south boundary of the JAERI for tritium analyses. The distribution or contour lines of tritium concentration in subsurface groundwater in the area showed an evident relationship between the excess tritium concentration and the distance in a southwest direction from JAERI. A horizontal gradient in the tritium concentration suggested that tritium reaching the groundwater layer gradually drains into the ocean through the Shinkawa basin due to an inflow of groundwater from the upper inland basin. The groundwater sampling well at G4 in Fig. 3, where groundwater tritium concentration is requested for prediction in this scenario, was bored in the early 1980s at a point halfway down the southern slope of the 35.7-m sand dune hill, about 800 m SSW of JRR-2, as indicated in Fig. 3. At G4, the depth from the soil surface to the top of the groundwater aquifer is estimated to be 15 – 20 m.

2.3. Surface soil characteristics

Both the JAERI and JNC (PNC) sites are located in an area covered with sand dunes along the coast. The environment surrounding both sites is a grove mainly of pine trees on sandy soil with a total porosity of 0.53 (the volume ratio of the air-filled and liquid-filled pore space to the total, which includes the solid phase space). The soil characteristics from the surface to 20 cm depth are shown in Table 1a, and the water content of the surface soil from 0-60 cm, as observed at MS2 in 1986, is shown in Table 1b. The profiles of soil water content from 5 cm to 100 cm depth were almost constant at each sampling.

Table 1a. Typical soil characteristics of the surface soil layer around JAERI.

Depth (cm)	Texture (%)				Soil pH		Organic matter
	Silt	Sand			Gravel (%)	KCl	H_2O
		Fine	Coarse				
	(<0.075)	(0.075-0.25)	(0.25-2.0)	(>2 mm)			
0 – 5	2.8	17.1	79.9	0.2	5.1	5.7	2.5
5 – 10	1.9	16.2	81.7	0.2	-	-	-
10 – 15	1.6	16.4	81.9	0.1	-	-	-
15 – 20	1.5	16.6	81.8	0.1	6.3	7.1	1.0

Table 1b. Soil water content (% by weight) in surface soil from 0 to 60 cm depth at MS2 in 1986

Date (1986)	20-Jan	23-Jun*	8-Jul	16-Jul	18-Sep	2-Oct	21-Oct	13-Nov	2-Dec	Mean
Water content (%)	2.20	1.90	2.93	2.70	4.46	3.23	2.46	3.59	2.05	2.84

* Soil depth 0 – 40 cm

2.4. Parameter values related to groundwater flows

Parameter values which may be applicable to groundwater flows in the area are listed in Table 2. The locations where the parameter values were obtained or estimated are also indicated.

Table 2. Parameter values suggested for predicting groundwater flows

Parameter	Value	Remarks
Porosity for coastal soil Total porosity of surface soil	0.4 0.53	 Tokaimura coast
Evaporation/Evapotranspiration rate	~ 62% of annual precipitation	Ibaraki Prefecture
Potential recharge	~ 0.7 m/y	Ibaraki Prefecture
Vertical pore water velocity in unsaturated soil layer	~ 5.5 m/y	JAERI site
Estimated depth from soil surface to the top of groundwater aquifer at G4	~ 15 to 20 m	Rough estimate for the point G4
Hydraulic conductivity, K	~ 6 x 10^{-4} m/s	Between G4 and Shinkawa River
Longitudinal pore water velocity, U_x	~ 0.2 m/d	Between G4 and Shinkawa River
Empirical longitudinal dispersivity on a field scale of 1km	~ 10 m	General text book value

2.5. Vegetation

There are various species of vegetation in the area, but Japanese red and black pine trees about 10-m high are the dominant species. The depth of pine tree roots is observed to be mostly within about 1m of the soil surface. Pine tree needle samples were taken monthly about 1.0-1.5 m above the ground at several points around the JAERI site from 1982. As the pine tree branch and needles grow actively from spring to summer and stay for a few years, pine needles grown in individual years are easily identified and were separately collected at sampling. A pine tree trunk sample was taken near MS-2 near the top of the 35.7-m sand dune. A view of a typical pine tree grove is shown in Fig. 4. It is likely that tritium reaches the trees from both air and root pathways.

Fig. 4: A view of a pine tree grove on the sand dunes looking toward the Pacific Ocean from the east boundary of the JAERI site.

2.6. Detection limit, precision and uncertainty of tritium measurement

The lower detection limit is evaluated to be 1.2 Bq/L based on 3 standard deviations (SD) of the net counting rate when 8 ml of combustion water are counted. All the OBT concentration data exceeded the lower detection limit except for the tree rings in Chiba city in the late 1980s (a natural or background level sample). The precision (reproducibility) was evaluated to be 11-20% (2 SDs of the mean) on the basis of 2 or 3 replicate analyses of identical tree ring samples obtained in different years. Uncertainties (as 2 SDs of OBT concentrations in tree rings at MS2 from 1984 to 1987) ranged from 11% to 31%.

3. TRITIUM DISCHARGE SOURCES AND SAMPLING POINTS

The major tritium sources that affected tritium levels in the Shuku district near MS-2 were the two heavy-water moderated research reactors JRR-2 and JRR-3 and a waste treatment facility (WTF) on the JAERI site in the north-east, and a small-scale nuclear fuel reprocessing plant (NFRP) at JNC (PNC) in the south. The JRR-2, JRR-3 and WTF discharged HTO continuously into the atmosphere whereas the NFRP discharged HT as well as HTO. The average discharge rate of HT was recently studied and proved to be in the range of 20-30% of the total tritium when spent nuclear fuels were being reprocessed and almost 0% when reprocessing was not occurring. Thus the conversion to HTO resulting from the oxidation of HT by the surface soil could be ignored.

The stack height and discharge parameter 3WD of each HTO discharge source are indicated in Table 3. Plume rise should be calculated by applying the monthly mean wind speed to the equation $\Delta H = 3WD/U$, where ΔH is plume rise (m); W is the exit velocity of the stack gases (m/s); D is the inside diameter of the stack (m); and U is the monthly mean wind speed (m/s). Then the effective stack height can be derived by adding ΔH to the physical height of the stack.

Table 3. The discharge sources and their discharge parameters

	Discharge sources			
	JRR-2	JRR-3	WTF	NFRP
Stack height, m	40	40	30	90
3WD, m	28.5	31.5	26.5	139.2

From the end of 1981, NIRS started a tritium monitoring program in the general Tokaimura area, with intensive measurements near the nuclear site boundaries, including the Shuku district. Samples of precipitation, river water, seawater, groundwater and plants such as pine needles and moss were collected on a monthly basis. NIRS often found a relatively good relationship between elevated tritium concentrations in the Shuku district and the distance of the sampling locations from the tritium discharge sources at JAERI. The monthly TFWT and OBT concentrations in pine needles, monthly precipitation and groundwater were determined in the Shuku district intensively for the period 1982 to 1986. Additionally, a pine tree trunk was sampled near MS-2 near the top of the sand dune in December 1987. OBT concentrations in this sample made it possible to determine the past environmental tritium levels retrospectively to 1961. These data are offered for testing models that predict the long-term average tritium concentrations in the environment due to chronic atmospheric releases. Near some of NIRS sampling points, JAERI also measured monthly tritium concentrations in air vapor and precipitation, and tissue free water in pine needles. Tritium samples and their sampling locations are summarized in Table 4 in relation to the four tritium sources.

Table 4. Tritium samples and their sampling locations

Sampling points (Fig.2)	Samples	Tritium forms measured	Responsible organization	Direction and distance (m) from the tritium discharge sources			
				JRR-2	JRR-3	WTF	NFRP
MP-7	air vapor	HTO	JAERI				
	rain	HTO	JAERI	SSW	SW	WSW	NNW
	pine needles	TFWT	JAERI	510	400	720	1610
P3	rain	HTO	NIRS	SW	SW	WSW	NNW
	pine needles	TFWT & OBT	NIRS	680	570	820	1560
MS2	rain	HTO	NIRS	SSW	SSW	SW	NNW
	pine needles	TFWT & OBT	NIRS	750	580	800	1300
	tree-rings	OBT	NIRS				
G4	groundwater	HTO	NIRS	SSW 800	SSW 630	SW 850	NWN 1260

4. TRITIUM DISCHARGE RATES

JNC provided monthly HTO discharge rates from NFRP from January to December each year. JAERI provided similar data for JRR-2 and JRR-3, but for the Waste Treatment Facility (WTF) only yearly data were provided starting in April and ending in March of the following year. The monthly discharge rates from 1981 to 1987 are plotted in Fig 5a (JRR-2), 5b (JRR-3) and 5c (NFRP). The annual discharge rates of the four tritium sources are shown in Fig. 5d. The numerical values are summarized in Tables A1 and A2 in Annex 1. The WTF discharge rates will cause an error in model predictions to a certain extent when the annual rates are divided into monthly rates and assigned to individual months.

Note that an incidental release of HTO with a small leakage of D_2O from a pipe occurred in JRR-3 during a week in June in 1982. This led to a monthly discharge rate of 1.6×10^{12} Bq, which was one order of magnitude higher than the usual monthly discharge rate (Fig. 5b). This incident may have affected the tritium concentration in precipitation, groundwater and pine needles in the months immediately following.

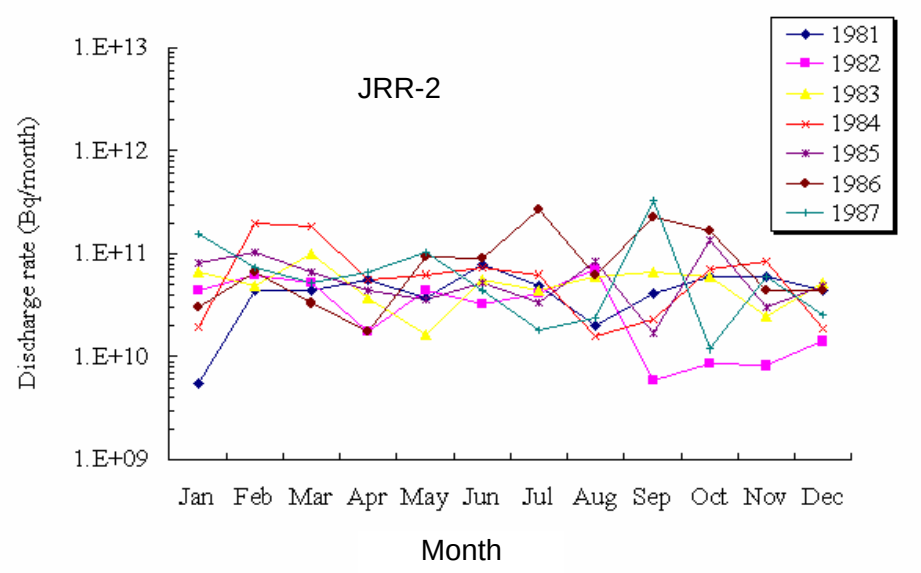

Fig. 5a: Monthly atmospheric discharge rates of HTO from JRR-2

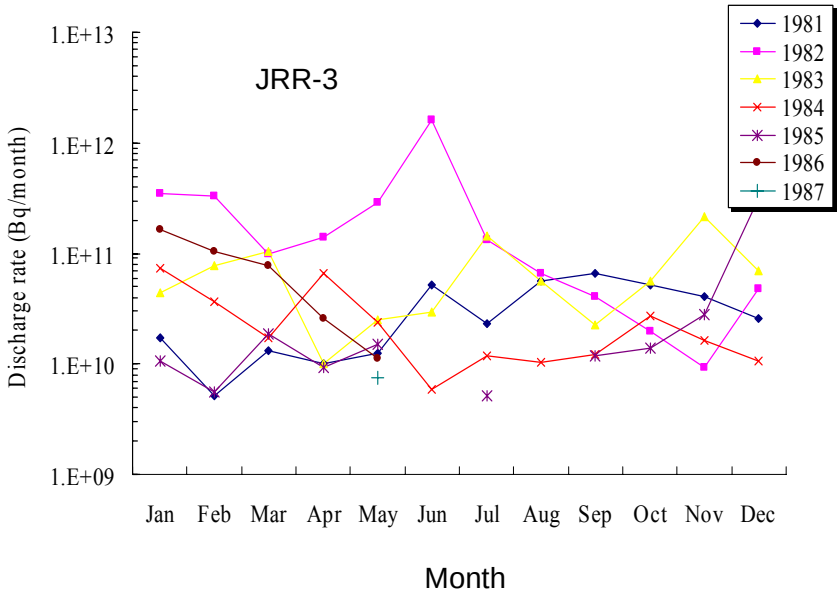

Fig. 5b: Monthly atmospheric discharge rates of HTO from JRR-3

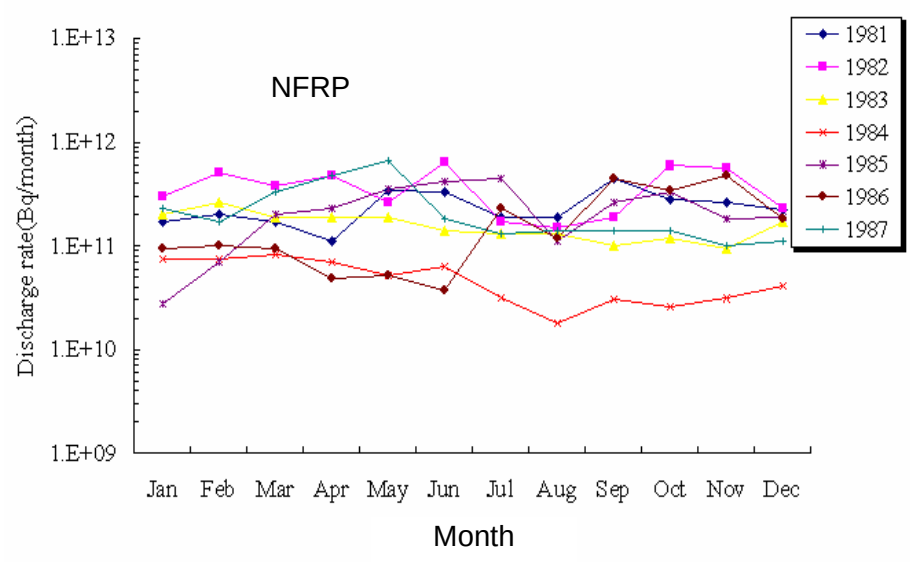

Fig. 5c: Monthly atmospheric discharge rates of HTO from NFRP

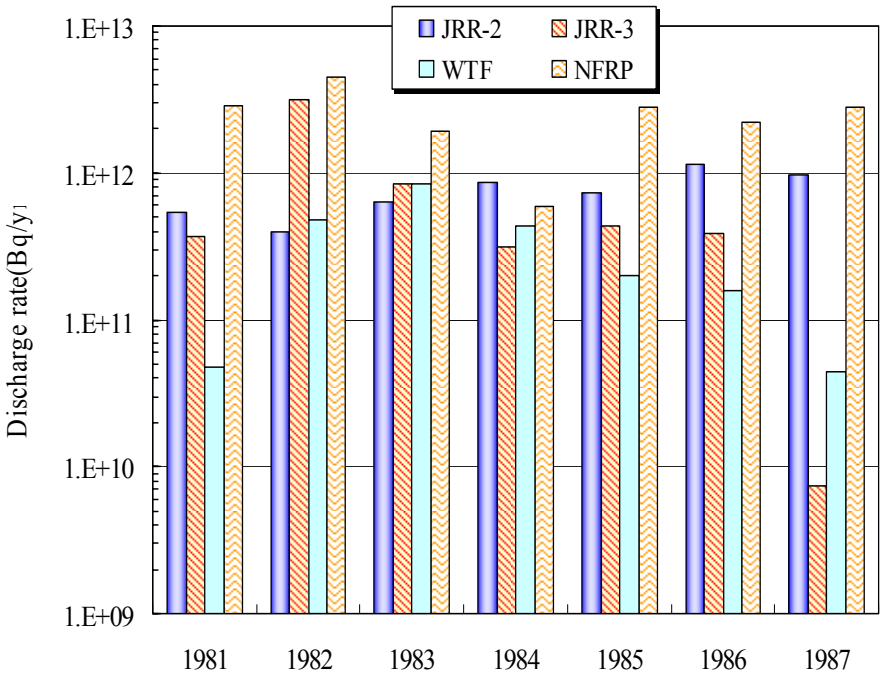

Fig. 5d. Annual discharge rates of the four tritium sources. The WTF data were obtained for annual periods starting in April and ending in March of the following year.

5. METEROLOGICAL DATA

Both monthly and annual average meteorological data from 1981 to 1987 for JAERI (File name: JAERI_met_aver3.xls) and JNC (JNC_met_aver7.xls) were tabulated by averaging the original hourly data from JAERI and the 10-minute data from JNC observed at different heights on their respective meteorological towers. The JNC data are provided with the scenario text in electronic form. The JAERI data will be provided on request for each modeler who carries out calculations. The datasets contain wind roses (16 directions) and wind speeds measured at different heights, stability classes (A to G), precipitation intensities, precipitation frequencies, air temperatures, relative humidities (JNC) or dew point temperatures (JAERI), net radiation (JNC) or solar radiation and radiation balance (JAERI), and so on. The method used to classify atmospheric stability is shown in Table 5. The JAERI measurements of atmospheric stability class are indicated using numbers from 1 to 10, which correspond to stability classes A to G as shown in a separate file (JAERI_met_cmnt.txt).

The wind roses observed at JAERI and JNC were quite similar to each other, and the roses observed at 70m at JNC (PNC) during fine and rainy weather are shown as examples in Figs. 6a and 6b, respectively. The annual mean wind rose fluctuated less from year to year during fine weather than during rainy weather. The NE sector (wind blowing from northeast to southwest) was by far the dominant wind direction (20 to 38%) during rain and this is a special feature of weather in the area. Stability classes D and G were dominant at the JAERI site but D was overwhelming frequent at JNC (PNC) from 1981-1987. Washout may play a key role in the prediction of tritium concentration in precipitation, groundwater, and so on. Two washout factors Λ were reported by separate research groups in field studies around the nuclear facilities, one on the Japan coast and the other on the Pacific side of Tokaimura. The reported values were 7.3 x 10^{-5} s^{-1} and 4.6 x 10^{-4} s^{-1} respectively, both at precipitation intensities of 2 mm/h.

Table 5. Classification of atmospheric stability for safety assessment of nuclear power plants in Japan

Wind speed* (U) m/s	Solar radiation** (T) kW/m^2				Radiation balance** (Q) kW/m^2		
	T≥0.60	0.60>T≥ 0.30	0.30>T≥ 0.15	0.15>T	Q≥- 0.020	-0.020> Q ≥ -0.040	-0.040>Q
U<2	A	A-B	B	D	D	G	G
2≤U<3	A-B	B	C	D	D	E	F
3≤U<4	B	B-C	C	D	D	D	E
4≤U<6	C	C-D	D	D	D	D	D
6≤U	C	D	D	D	D	D	D

* measured at the ground surface

** solar radiation used during the day and radiation balance at night

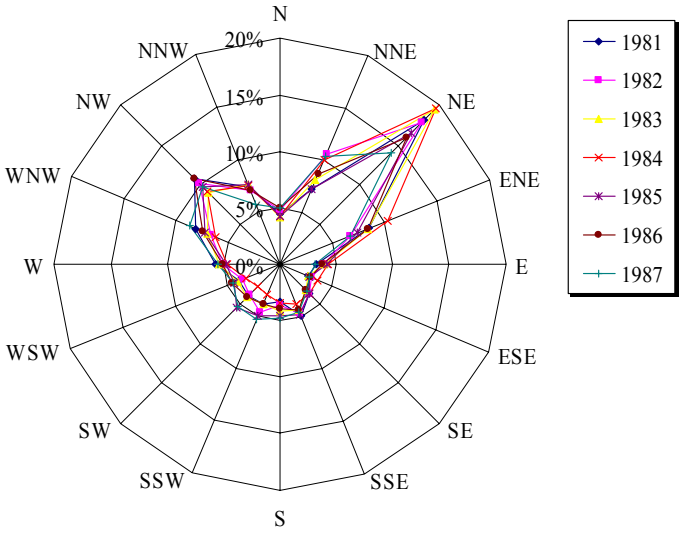

Fig. 6a: Annual average wind rose at 70 m at the JNC (PNC) Tokai site from 1981-1987 during fine weather

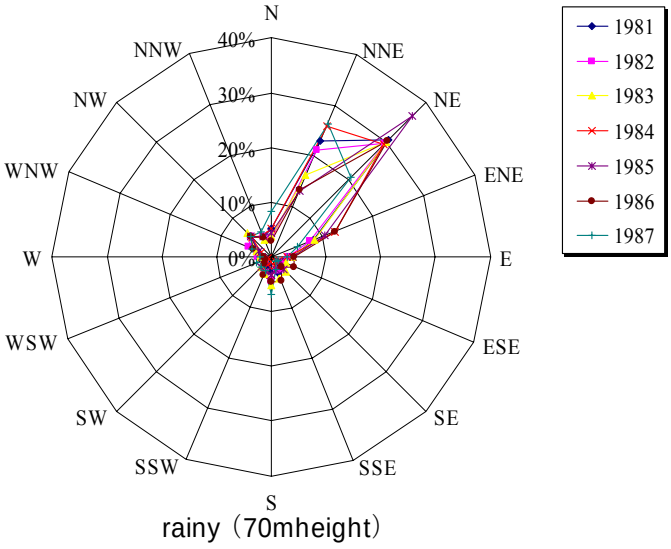

Fig 6b: Annual average wind rose at 70 m at the JNC (PNC) Tokai site from 1981-1987 during rainy weather.

6. CALCULATION END POINTS

Using the HTO discharge rates for the four tritium sources, and the meteorological data given with the scenario text, modelers are requested to calculate the following end points:

1. Monthly tritium concentrations in air moisture, precipitation, tissue free water (TFWT) and non-exchangeable OBT (nOBT) in pine tree needles from 1982 to 1986 at P3;
2. Yearly tritium concentrations in air moisture, precipitation and nOBT in pine tree trunk year-rings, and TFWT and nOBT in needles of pine trees collected separately from the trunk at MS2. All predictions are to be for the period from 1984 to 1987 at MS-2.
3. Monthly tritium concentrations in groundwater at the well G4 from 1984 to 1987;
4. 95% confidence intervals on each prediction.

All results should be reported for the excess tritium concentration caused by the atmospheric HTO discharges from the four sources, not including the contribution from natural and fallout tritium. These will be compared with observations from which background levels have been subtracted. The predictions should be presented in Bq/L water or water equivalent, taking into account the fact that the OBT samples were washed with tritium free water and dried before combustion. Please contact Yoshikazu Inoue (y_inoue@nirs.go.jp) or Kiriko Miyamoto (kiriko@nirs.go.jp) if you have any questions.

Acknowledgement
The author is grateful to the Japan Atomic Energy Research Institute (JAERI) and the Japan Nuclear Cycle Development Institute (JNC) (which were unified into the Japan Atomic Energy Agency (JAEA) as of 1st October 2005) for their cooperation in providing their source data in electronic form.

ANNEX 1

Table A1: Monthly discharge rates of HTO from JRR-2 and JRR-3, and the annual discharge rate of HTO from WTF at JAERI.

Year	Facilities	Jan	Feb	Mar	Apr	May	Jun	Jul	Aug	Sep	Oct	Nov	Dec	Annual
		Bq/month												Bq/year
1981	JRR-2	5.6E+09	4.4E+10	4.4E+10	5.6E+10	3.7E+10	7.8E+10	4.8E+10	2.0E+10	4.1E+10	5.9E+10	5.9E+10	4.4E+10	5.4E+11
	JRR-3	1.7E+10	5.2E+09	1.3E+10	1.0E+10	1.3E+10	5.2E+10	2.3E+10	5.6E+10	6.7E+10	5.2E+10	4.1E+10	2.6E+10	3.7E+11
	WTF													4.8E+10
1982	JRR-2	4.4E+10	6.3E+10	5.2E+10	1.7E+10	4.4E+10	3.2E+10	4.1E+10	7.0E+10	5.9E+09	8.5E+09	8.1E+09	1.4E+10	4.0E+11
	JRR-3	3.4E+11	3.3E+11	1.0E+11	1.4E+11	2.9E+11	1.6E+12	1.3E+11	6.7E+10	4.1E+10	2.0E+10	9.3E+09	4.8E+10	3.2E+12
	WTF													4.8E+11
1983	JRR-2	6.7E+10	4.8E+10	1.0E+11	3.7E+10	1.7E+10	5.6E+10	4.4E+10	5.9E+10	6.7E+10	5.9E+10	2.5E+10	5.2E+10	6.3E+11
	JRR-3	4.4E+10	7.8E+10	1.0E+11	1.0E+10	2.5E+10	2.9E+10	1.4E+11	5.6E+10	2.3E+10	5.6E+10	2.1E+11	7.0E+10	8.5E+11
	WTF													8.5E+11
1984	JRR-2	2.0E+10	2.0E+11	1.8E+11	5.6E+10	6.3E+10	7.4E+10	6.3E+10	1.6E+10	2.3E+10	7.0E+10	8.5E+10	1.9E+10	8.7E+11
	JRR-3	7.4E+10	3.7E+10	1.7E+10	6.7E+10	2.4E+10	5.9E+09	1.2E+10	1.0E+10	1.2E+10	2.7E+10	1.6E+10	1.1E+10	3.1E+11
	WTF													4.4E+11
1985	JRR-2	8.1E+10	1.0E+11	6.7E+10	4.4E+10	3.6E+10	5.2E+10	3.3E+10	8.5E+10	1.7E+10	1.4E+11	3.0E+10	4.8E+10	7.3E+11
	JRR-3	1.1E+10	5.6E+09	1.9E+10	9.3E+09	1.5E+10	0.0E+00	5.2E+09	0.0E+00	1.2E+10	1.4E+10	2.8E+10	3.1E+11	4.3E+11
	WTF													2E+11
1986	JRR-2	3.1E+10	6.7E+10	3.3E+10	1.8E+10	9.3E+10	8.9E+10	2.7E+11	6.3E+10	2.3E+11	1.7E+11	4.4E+10	4.4E+10	1.1E+12
	JRR-3	1.7E+11	1.0E+11	7.8E+10	2.6E+10	1.1E+10	0	0	0	0	0	0	0	3.8E+11
	WTF													1.6E+11
1987	JRR-2	1.6E+11	7.4E+10	5.2E+10	6.7E+10	1.0E+11	4.4E+10	1.8E+10	2.4E+10	3.3E+11	1.2E+10	5.9E+10	2.5E+10	9.6E+11
	JRR-3	0	0	0	0	7.4E+09	0	0	0	0	0	0	0	7.4E+09
	WTF													4.4E+10

Note 1: No tritium releases occurred after June 1986 because of JRR-3 reconstruction.
Note 2: Monthly discharge rate data for the WTF are not available, and the annual data for WTF are for the period April to March.

Table A2: Monthly atmospheric discharge rates of HTO from NFRP at JNC (PNC)

	Jan	Feb	Mar	Apr	May	Jun	Jul	Aug	Sep	Oct	Nov	Dec	Annual
1981	1.7E+11	2.0E+11	1.7E+11	1.1E+11	3.4E+11	3.3E+11	1.9E+11	1.9E+11	4.4E+11	2.8E+11	2.6E+11	2.2E+11	2.9E+12
1982	3.0E+11	5.1E+11	3.8E+11	4.7E+11	2.6E+11	6.5E+11	1.7E+11	1.5E+11	1.9E+11	5.9E+11	5.6E+11	2.3E+11	4.5E+12
1983	2.0E+11	2.6E+11	1.9E+11	1.9E+11	1.9E+11	1.4E+11	1.3E+11	1.3E+11	1.0E+11	1.2E+11	9.3E+10	1.7E+11	1.9E+12
1984	7.4E+10	7.4E+10	8.1E+10	7.0E+10	5.2E+10	6.3E+10	3.2E+10	1.8E+10	3.0E+10	2.6E+10	3.1E+10	4.1E+10	5.9E+11
1985	2.8E+10	7.0E+10	2.0E+11	2.3E+11	3.5E+11	4.1E+11	4.4E+11	1.1E+11	2.6E+11	3.3E+11	1.8E+11	1.9E+11	2.8E+12
1986	9.3E+10	1.0E+11	9.3E+10	4.8E+10	5.2E+10	3.7E+10	2.3E+11	1.2E+11	4.4E+11	3.4E+11	4.8E+11	1.8E+11	2.2E+12
1987	2.3E+11	1.7E+11	3.3E+11	4.8E+11	6.7E+11	1.8E+11	1.3E+11	1.4E+11	1.4E+11	1.4E+11	1.0E+11	1.1E+11	2.8E+12

APPENDIX B

MODEL DESCRIPTIONS

6 September 2007

NIRS Model

1. Introduction

We developed the Easy Evaluation System for Atmospheric Dispersion for tritium (Tritium-EESAD) code based on the random walk method (RWM). It can deal with hourly changes of weather conditions and tritium release rates, which makes it possible to assess accidental releases. The RWM, which was used in the SPEEDI system [1], [2], expresses transfer of a radioactive cloud by movement of many particles, and estimates the behavior of the plume more effectively than the Gaussian plume model for short-term releases. The Tritium-EESAD code is able to calculate the deposition and the change of chemical form of tritium based on each particle. The process of re-emission from the ground surface soil and infiltration into deeper soil are calculated in each mesh division of the computation domain.

The atmospheric dispersion, deposition and re-emission processes in the tritium-EESAD code were validated using data from BIOMASS (IAEA Biosphere Modeling and Assessment Program). It was first validated for the endpoints of the Canadian Scenario (Scenario 3[3]) which focused on simulation of the phenomena caused by continuous and long-term tritium release. Tritium-EESAD was secondly validated for the Russian Scenario [4], in which additional data of tritium concentrations in atmospheric moisture, snow and soil water samples collected over shorter time intervals were provided by the Scenario developer [5].

2. Basic Assumptions

- Two heavy water moderated reactors (JRR-2 and JRR-3) and a waste treatment facility (WTF) in JAERI were selected as the sources of tritium (HTO). The Tokai Repressing Plant (TRP) in JNC was neglected, because the contribution to air contamination at the receptors was considered to be small.
- Two locations (receptors) for calculating endpoints (P3 and MS2) were regarded as two different locations whose tritium concentrations were calculated independently.
- The three sources were regarded as three independent release points, and their locations were set up in the mesh coordinates relative to the locations of the two receptors.
- Monthly tritium discharge rates for JRR-2 and JRR-3 were used as inputs. For the WTF, only yearly discharge data were provided and thus monthly tritium discharge rates were calculated by dividing the yearly tritium discharge rates by 12.
- The scale of the mesh coordinates was 100 m by 100 m.

3. Calculation of Atmospheric Moisture Concentration

Monthly mean tritium concentrations in atmospheric moisture were calculated from the arithmetic mean of the tritium activity in a unit volume of the air for the month, and the absolute humidity (the amount of water in a unit volume of air). Tritium activity in a unit volume of air was calculated by Tritium-EESAD as follows:

3.1. Atmospheric dispersion and deposition on the ground surface

3.1.1 Equations

Movement of particles is expressed by the sum of movements by wind velocity and diffusion due to air turbulence. The position of a particle at time t+Δt after release, ($x_{t+\Delta t}$, $y_{t+\Delta t}$, $z_{t+\Delta t}$), is expressed by the following equations using particles located at time t after release (x_t, y_t ,z_t):

$$\left.\begin{aligned} x_{t+\Delta t} &= x_t + u_x \Delta t + dx \\ y_{t+\Delta t} &= y_t + u_y \Delta t + dy \\ z_{t+\Delta t} &= z_t + u_z \Delta t + dz \end{aligned}\right\} \quad (1)$$

u_x, u_y, u_z : Wind velocity in the x, y, z directions
dx, dy, dz : Turbulent displacement in the x, y, z directions

The turbulent displacements were calculated as a function of uniform random numbers and diffusion coefficients. Each diffusion coefficient was calculated using the Pasquill-Meade equation [6, 7]. The contribution to the concentration at a given location from a particle at that location was calculated by the Kernel Density Estimator (KDE) method [8].

The deposition (wet and dry) to the ground surface during the time step Δt was calculated for each particle by the following equations (2) and (3), where deposition depends on the spatial position of each particle.

$$G_W = \sum_{n=1}^{N} \alpha_n Q_n \left\{ 1 - \exp(-\Lambda \Delta t) \right\} \quad (2)$$

G_W :Wet deposition amount in a mesh cell, Bq
N :Number of particles distributed over the mesh
α_n :Contribution ratio of particle n
Q_n :Activity of particle n in the current time step, Bq
Δt :Time step, s
Λ :Washout coefficient, s^{-1} (a function of rain intensity J (mm/h))

$$G_d = \sum_{n=1}^{N} \alpha_n Q_n \left\{ 1 - \exp(-k v_g \Delta t) \right\} \quad (3)$$

G_d :Dry deposition in a mesh cell, Bq
v_g :Deposition velocity, m/s
k :Contribution to deposition in the height, m

$$k = 2.0 \cdot \left(1 - \frac{h_p}{\Delta z} \right) \Big/ \Delta z$$

h_p :Particle height, m
Δz :Height contributing to deposition, m

3.1.2 Important parameter values

Variable	Value	Reference
Λ (Washout coefficient)	5.0×10^{-5} $J^{0.8}$ s^{-1}	BIOMASS [5]
v_g (Deposition velocity)	0.005 m/s	Field experimental data [9, 10]

3.1.3 Meteorological data

The hourly data on wind direction and wind velocity at a height of 40 m, precipitation intensity, air temperature, dew point and atmospheric stability class supplied by JAERI were used. Except for wind direction and stability class, the meteorological data sets for each month were prepared by averaging the hourly data for each parameter over the month. The stability classes were determined from the maximum frequencies and the wind direction was the monthly mean frequency. The resulting data were processed to fit the input format of Tritium-EESAD.

3.2. Infiltration of tritium from surface soil to lower soil layers

3.2.1 Equations

Tritium deposited on the surface soil infiltrates to lower soil layers at a certain rate. The tritium concentration on the surface soil layer at time t after deposition is shown by the following equation.

$$q_{grn}(x,y)(t) = q_{grn}(x,y)(0)\left\{\ 1-\exp\left(-K_{perm}\cdot t\right)\right\}$$

$q_{grn}(x,y)(0)$:Tritium activity deposited in mesh cell (x, y), Bq
$q_{grn}(x,y)(t)$:Tritium activity in mesh cell (x, y) at time t after deposition, Bq
K_{perm} :Infiltration rate, h^{-1}

3.2.2 Parameter values

Regarding K_{perm}, the peak concentration of tritium deposited on the surface soil layer moved downward at a maximum of 2 cm/day (= 0.0833 cm/h) [11]. If we assume the surface layer depth is 5 cm and tritium is present homogeneously, an infiltration rate is calculated as 0.0833 (cm/h) / 5(cm) = 1.67% h^{-1}.

3.3. Re-emission of tritium from surface soil to the air

3.3.1 Equations

Generally, re-emission from surface soil to the air is driven by the tritium concentration difference between air and soil, and by evaporation caused by solar heating. Modeling evaporation phenomena needs many detailed meteorological data, for example, air temperature and moisture pressure at the soil surface. The re-emission rate from surface soil to the air has been reported from some field experiments. The Tritium-EESAD code considers re-emission only due to differences between the soil and air tritium concentrations:

$$q_{re} = (q_{grn} - q_{air}) [1 - \exp(-re_{HTO}\, t)] \quad (5)$$

q_{re} :Total re-emission in a mesh cell, Bq
re_{HTO} :Re-emission rate , h^{-1}
q_{grn} :HTO activity in soil surface, Bq
q_{air} :HTO activity in air at the ground surface, Bq

Locations where re-emission occurs should become a secondary release source. In Tritium-EESAD, when re-emission occurs, its activity is added to the air concentration only once, but in the next hour, re-emission activity disappears from the air.

3.3.2 Parameter values

Ogram et al. [12] reported an re_{HTO} value of about 2% h^{-1} for the first 24 hours after tritium release and about 0.6 for the first 2 weeks. Foerstel [13] reported an average value of about 3% h^{-1}, which was not limited to a certain time after release.

4. Rain Water

Tritium concentrations in the monthly rain were calculated from the arithmetic mean of the tritium activity wet deposited for the month, and the amount of the monthly rainfall.

5. TFWT and OBT in pine needles

Tritium in pine needles was assumed to originate from the direct uptake of atmospheric moisture through the stomata of the leaves, and also from root uptake of soil water. The tritium concentration in soil water for a given month was calculated from the total amount of tritium deposited on the ground in the month and the mean water content in the surface soil of 5 cm depth. The calculated tritium concentrations in atmospheric moisture and soil water for each month were used to calculate the TFWT in pine needles for the month:

$$PN_{TFWT} = A\, R_a / (R_a + R_b) + B\, R_b / (R_a + R_b)$$
$$= 0.57\, A + 0.43\, B \quad (6)$$

PN_{TFWT} : TFWT concentration in pine needles, Bq/L
A : Tritium concentration in air moisture, Bq/L
B : Tritium concentration in soil water, Bq/L
R_a : TFWT in plants/tritium concentration in air moisture observed in steady-state conditions (= 0.8 from literature survey[14])
R_b : TFWT in plants/tritium concentration in soil water observed in steady-state condition (= 0.6 from literature survey[15])

The OBT concentration was calculated by Equation (7). The arithmetic mean value of TFWT concentration for the previous six months was used to calculate the OBT concentration at a given time, because OBT is considered to be metabolized slowly in the plant body independent of season.

$$PN_{OBT} = Rc\ PN_{TFWT} \quad (7)$$

PN_{OBT} : OBT concentration in pine needles at time t, Bq/L
R_c : concentration ratio of OBT/TFWT in plants observed in steady-state conditions (= 0.8 from literature survey[16])
PN_{TFWT} : Mean value of TFWT concentration in pine needles over the six months prior to t, Bq/L

6. OBT in Annual Rings of a Pine Tree

The OBT concentration in annual tree rings was considered to be half the mean value of yearly OBT concentration in pine needles, based on the observation by NIRS.

$$PR_{OBT} = PN_{OBT}/2 \quad (8)$$

PR_{OBT} : OBT concentration in annual tree rings, Bq/L
PN_{OBT} : Mean annual value of OBT concentration in pine needles, Bq/L

7. Groundwater

The assumed geological characteristics of the area, including the point G4, are shown in Fig. 3 in the scenario description. The well water at G4 is pumped out from the shallow groundwater layer in the narrow area of a small river basin near a seacoast, where slow vertical infiltration and fast horizontal flow of the groundwater were presumed.

Based on field studies by NIRS [17], the volume of storage water in this area is so small that the tritium concentration of the groundwater has a quick time response to tritium input by rainwater. Tritium in the rainwater is considered to mainly come from the nuclear facilities in JAERI, which are located to the northeast of the receptors. The tritium is deposited on the soil surface where it infiltrates the groundwater aquifer, and gradually drains out to the ocean through the river basin.

Monthly rain water at MS2 infiltrates vertically over a distance of 15 m to recharge groundwater at G4. Vertical infiltration of monthly rain water (at a rate of 5.5 m/y) reaches the groundwater aquifer 32 months later.

$$15\ m \div 5.5\ m/y = 2.7\ years = 32\ months$$

Ten percent of the volume of the groundwater aquifer was assumed to run off monthly into the river (Fig.1):

$$T_{Vn} = (T_{Vn-1} - a\ T_{Vn-1}) + T_{Rn}\ x \quad (9)$$

T_{Vn} : Tritium concentration in the groundwater layer for the n^{th} month, Bq/L
T_{Rn} : Tritium concentration in monthly rainwater at MS2 for the n^{th} month, Bq/L
a : the fraction of water that runs off into the river from the layer at the end of the $(n-1)^{th}$ month (= 0.1)
x : a turnover rate constant for water in the layer (= rainfall volume/layer volume = 0.17)

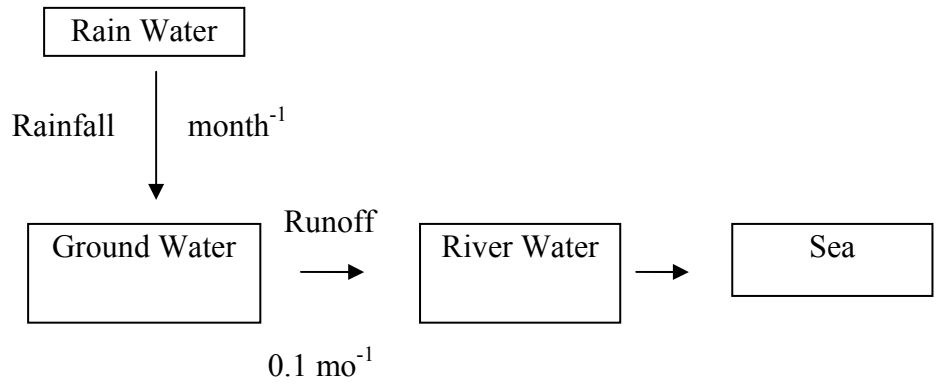

Fig.1. A model of river runoff in the Tokai area.

References

[1] Chino, M., et al., Dose evaluation model on complex topography by random walk model using 3 dimension wind speed , AESJ, 26, 526-534 (1984).

[2] Chino, M., et al., WSPEEDI (World wide version of SPEEDI); A computer code system for the prediction of radiological impacts on Japanese due to a nuclear accident in foreign countries, JAERI-M, 1334 (1995)

[3] IAEA, Tritium Working Group. A test of chronic atmospheric release models using Canadian data, BIOMASS theme 3 Tritium Working Group Working Document: 3 November (2000)

[4] IAEA, Tritium Working Group. A test of chronic atmospheric release models using Russian data, BIOMASS theme 3 Tritium Working Group Working Document: 4 November (2000)

[5] K. Yamamoto, Sakashita, T. and Miyamoto, K., Development and Validation of an Atmospheric Dispersion Model for Tritium using the IAEA BIOMASS Scenario, Fusion Science & Technology, 48, 500-503 (2005).

[6] Maede, P.J. ,The Effects of Meteorological Factors on the Dispersion of Airborne Material, Rassegns Internasionale Elettronica e Nucleare 6 Rassegna Rome 1959, 11, 107-130 (1959).

[7] Pasquill, F., The Estimation of the Dispersion of Windborne Material, Meteorol. Mag. 90, 33-49 (1961).

[8] Lorimer, G. S., The Kernel for Air quality modeling (I), Mathematical formulation, Atmos. Environ., 20, 1447-1452 (1986).

[9] Garland, J. A., Cox, L. C.,The absorption of tritium gas by English soils, plantsand the sea, Water Air Soil Poll., 14, 103-114 (1980).

[10] Noguchi, H. et al., Tritium behavier observed in the Canadian release study, Fusion Tech., 14, 1287-1292 (1988).

[11] Sasscer, et al., Dynamic model of water movement in soil under various climatological condition, in “Tritium”, Messenger Graphics, Las Vegas, Nevada, 485-495 (1973).

[12] Ogram, G.L. et al., Field studies of the HT behavior in the environment: 2 The interaction with soil, Fusion Tech., 14, 1170-1175 (1988).

[13] Forestel, H., HT to HTO conversion in the soil and subsequent tritium pathway: Field release data and laboratory experiments, Fusion Tech., 14, 1241-1246 (1988).

[14] Diabate, S. and Strack, S., Organically bound tritium in wheat after short-term exposure to atmospheric tritium under laboratory conditions. J. Environ. Radioactivity, 36, 157-175 (1997).

[15] Belot, Y., Tritium in plants: A review, Radiation Protection Dosimetry, 16, 101-105 (1986).

[16] McFarlane, J. C., Tritium fractionation in plants. Envirn. Exp. Botany, 16, 9-14 (1976). Garland, J. A. and Ameen, M. Incorporation of tritium in grain plants. Health Phys., 36, 35-38 (1979).

[17] K. Miyamoto, Y. Inoue, T. Iwakura, H. Takeda,S. Fuma, K. Yanagisawa and N. Ishii. Fusion Science & Technology, 41, 483-487 (2002).

SRA Model

1. Atmospheric Diffusion of HTO

The atmospheric diffusion of tritium in the primary plume is described by a Gaussian plume model. The wind blows with equal probability within a given sector. The HTO concentration in the primary plume is calculated by assuming the common frequency of individual atmospheric stability and the corresponding average wind velocity. The interference of neighboring sectors was neglected. The sector-averaged tritium concentration on the ground surface is then approximately given by the following formula[1)]:

$$\chi(x) = \sum_{S=A}^{F} \sqrt{\frac{2}{\pi}} \frac{F(s)Q}{\sigma_{ZS} U_S (2\pi x / 16)} \bullet \exp\left(-\frac{H^2}{2\sigma_{ZS}^2} \right) \qquad (1)$$

where:

x = the distance from the release point (m)
$\chi(x)$ = air tritium concentration at distance x (Bq/m^3)
S = stability index of the atmosphere
F(S) = the frequency rate of wind blowing for stability class S
σ_{ZS} = vertical dispersion parameter (m)
U_S = the average wind velocity for stability class S (m/s)
Q = the release rate (Bq/s)
H = the stack height (m)

The secondary emission of HTO after dry deposition of HTO is assumed to take place instantaneously after deposition. The tritium depletion by dry or wet deposition of atmospheric HTO is neglected. The dispersion parameters were calculated using Brigg's formula.

2. Tritium Transfer from Atmosphere to Soil

Atmospheric HTO is deposited to soil and vegetation through two processes. One is the dry deposition process where the atmospheric HTO moisture molecule exchanges with free water molecules in the soil and plant leaves. The other process is the scavenging of atmospheric HTO by rain, snow and frost. The washout of atmospheric HTO by rain is the major cause of increasing tritium levels in precipitation. Hereafter, solely the washout by rain will be considered as the cause of wet deposition.

The washout velocity is estimated by the following equation [2)].

$$V_{wash} = \frac{8\Lambda Q}{\pi\, xU} \qquad (2)$$

where V_{wash} = the velocity of wet deposition ($Bq/(m^2.s)$)
Λ= the washout constant (s^{-1})
Q = the tritium release rate (Bq/s)
U = the wind velocity (m/s)
x = the distance to the estimation point from the release point (m)

The value of Λ is related to precipitation intensity, J (mm/a), and a proportionality constant S_{precip} (a / (mm.s)) as :

$$\Lambda = J\, S_{precip}. \tag{3}$$

Inoue and others determined the value of S_{precip} as 2.6×10^{-8}. [2] This value will be used in this report.

The specific concentration of tritium in soil water is estimated as follows. At first, the contribution to the soil HTO from the primary atmospheric HTO by dry deposition is considered. The dry deposition is assumed to occur only during fine or cloudy weather.

Generally, the specific activity of the soil water C_s is described by the following equation.

$$\frac{dC_S}{dt} = -\left(\frac{I_P}{V}\right)C_S + \left(\frac{I_P}{V}\right)C_P + \left(\frac{I_{dry}}{V}\right) \tag{4}$$

where Cs = the specific activity of the soil water (Bq/kg)
C_P = the specific activity of the precipitation (Bq/kg)
I_P = the annual precipitation rate (kg/(y.m^2))
I_{dry} = the tritium flux of dry deposition (Bq/(y.m^2))
V = the area density of soil water (kg/m^2)

At equilibrium, C_S is given by

$$C_S = C_P + \frac{I_{dry}}{I_P}$$

In the case of HTO release, C_P and I_{dry} are given by:

$$C_P = \left(\sum_S \frac{F(S)}{U_S}\right) \times \left(\frac{8\Lambda Q}{\pi x \bullet I_p}\right) \times (8.64 \times 10^4 \times rainDay) \tag{6}$$

and

$$I_{dry} = \text{DryHTO} \times C_{air,HTO} \times 8.64 \times 10^4 \times (365 - \text{rainDay}) \tag{7}$$

respectively, where

DryHTO = dry deposition velocity of atmospheric HTO (3×10^{-3} m/s)
$C_{air,HTO}$ = atmospheric HTO concentration (Bq/m^3)
rainDay = number of rainy days per year

3. Tritium Transfer from the Atmosphere and Soil to the Pine Trees

If there is no supply of tritium from the soil, the tritium concentration in the plant leaves is described by the following equation of Belot [3].

$$\frac{dC_L}{dt} = \frac{C_a}{\mu r} - \left(\frac{\rho_s}{\alpha \mu r}\right) C_L \tag{8}$$

where C_L = tritium concentration in the plant leaves (Bq/kg)
C_a = atmospheric HTO concentration (Bq/m^3)
ρ_s= saturation moisture density (kg/m^3)
μ=leaf water content (kg/m^2)
r = resistance to moisture exchange between atmosphere and stomata (s/m)
α = 1.1 is the ratio of the vapour pressure for water vapour to that of HTO

Under the circumstance that tritium is supplied from the soil water, an additional term must be added to the above equation:

$$\frac{dC_L}{dt} = \frac{C_a}{\mu r} - \left(\frac{\rho_s}{\alpha \mu r}\right) C_L + \frac{C_{soil} I_W}{\mu} \tag{9}$$

where C_{soil}= tritium concentration in the soil water(Bq/kg)
I_W = evapotranspiration velocity of the plant leaves (kg/(m^2.s))

At equilibrium, the leaf tritium concentration is given by

$$C_L = \frac{\alpha r}{\rho_s}\left(\frac{C_a}{r} + C_{soil} I_W\right) \tag{10}$$

Let the tritium concentration of the air moisture be C_a^*. By using the relationships $C_a = C_a^* \rho$ and $I_W = \frac{\rho_s - \rho}{r}$, the above equation is reduced to

$$C_L = \alpha\left(C_a^* f + C_{soil}(1-f)\right)$$

where f is the relative humidity of the atmosphere.

4. OBT Formation in Pine Trees

The physiological condition of pine trees is unclear. In the present model, it is assumed that free water tritium in pine trees is converted to OBT only in April through August. The average lifespan of pine tree needles is believably above 2 years. The newly synthesized OBT in the needles is assumed to be retained for two years. The OBT produced in the needles in the growth period is assumed to be transferred to trunks and accumulated as the OBT of the tree rings. The value of the tritium discrimination factor used was 0.73 obtained as an average value from two reference sources[4, 5].

5. Tritium Concentration in Groundwater

The depth of the G4 well was assumed to be 15 m with some uncertainty. The precipitation containing HTO reaches the aquifer 3 years after deposition. Thus the predicted tritium concentration in the groundwater reflects the tritium concentration of the surface soil water that was recorded about 3 years before. Naturally, convection and diffusion of HTO may take place during migration. The extent of the influence of these phenomena to the tritium level in the well water is unclear at the moment. Therefore, it was assumed that the HTO concentration represents that of surface soil water deposited on the soil surface 2.5 – 3.5 years before sampling. Furthermore, it was assumed that the contaminated groundwater is diluted by the clean water that is supplied from the surrounding aquifer. Tentatively the dilution factor (DF) was assumed to be 0.3. If there is no dilution (DF=1), the level of groundwater tritium is on the order of that of rain. The choice of the factor DF is a point of debate. The figure below shows the effect of varying DF from 0.3 to 1.0.

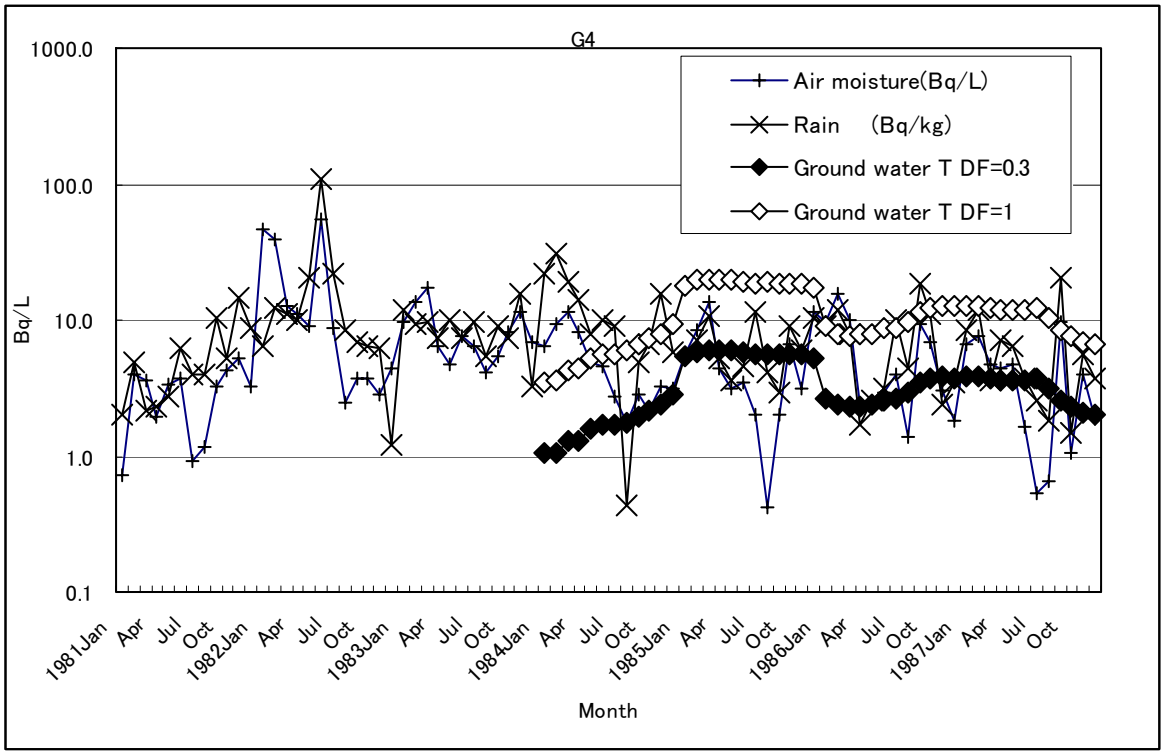

References

1) Nuclear Safety Commission of Japan, Meteorological Guideline for the Safety Analysis of Nuclear Power Plants (Hatudenyougenshiroshisetu no anzenkaisekinikansuru kishoushishin, in Japanese) p.398, Taiseishuppansha, Tokyo, 2000

2) Inoue, Y, Iwakura,T. and Miyamoto, K., Environmental Aspects of Tritium Released into the Atmosphere in the Vicinity of Nuclear Facilities in Japan. NIRS-M-52, pp.296-315 (1983)

3) Belot,Y., Gauthier,H., Camus,H., and Caput,C., Prediction of the flux of tritiated water from air to plant leaves. Health Physics 37, 576-583 (1979).

4) Garland J.A. and Ameen M. Incorporation of tritium in grain plants. Health Physics. 36. 35-38(1979).

5) Kim M.A. and Baumgärtner F. Equilibrium and non-equilibrium partition of tritium between organics and tissue water of different biological systems. Anal.Radiat. Isot. 45. 351-353 (1994).

LLNL Model

1. Introduction

DCART (**D**oses from **C**hronic **A**tmospheric **R**eleases of **T**ritium) was developed as a stochastic assessment model to be used in a dose reconstruction for tritium releases from the Lawrence Livermore National Laboratory. It is a steady-state, analytical compartment model that calculates uncertainties using parameter distributions and Latin Hypercube Sampling. DCART accounts for inhalation and ingestion pathways to dose, but for the Pine Tree Scenario, only the compartments for air, air moisture, soil, tissue free-water tritium (TFWT) of pine needles and organically bound tritium (OBT) in pine needles and wood were calculated. Concentrations in rain were also calculated.

To estimate tritium concentrations in pine needles and wood, processes include uptake of HTO from soil water and air moisture and conversion to OBT. For the Pine Tree Scenario, dispersion modeling was used to calculate concentrations of tritiated water (HTO) in air (Bq m^{-3}) from atmospheric releases from specified facilities. From these predicted air concentrations, concentrations in air moisture, TFWT in pine needles, and OBT in pine needles and wood were predicted.

DCART is described in detail in:

Peterson, S-R. Historical Doses from Tritiated Water and Tritiated Hydrogen Gas Released to the Atmosphere from Lawrence Livermore National Laboratory (LLNL) Part 1. Description of Tritium Dose Model (DCART) for Chronic Releases from LLNL. Lawrence Livermore National Laboratory, Livermore, CA. UCRL-TR-205083-REV-1. October 2006. A copy may be obtained by searching the reports library at LLNL (http://library-r.llnl.gov/uhtbin/cgisirsi/i5V55DaK0I/MAIN/230100017/9).

2. Key Assumptions

DCART should be used to calculate annual or long-term mean concentrations and dose. Thus, as a more meaningful test of DCART, instead of the monthly predictions that were requested, only predictions for mean annual environmental concentrations of tritium were submitted.

To prepare the input file for the dispersion model, the meteorological data provided by the Japan Nuclear Cycle Development Institute (JNC) and the Japan Atomic Energy Research Institute (JAERI) had to be manipulated into hourly averages (for JNC) with six (instead of ten) stability classes (for both JAERI and JNC data). The conversion from ten stability classes to six was accomplished in Excel® without using macros as follows:

1. The Japanese data were sorted first by stability class.
2. The column containing stability classes was moved to a separate worksheet so that the "replace" function could be used to replace numbers (1 – 10) with letters (a – j) (i.e., 1 = a; 2 = b; ….10 = j).
3. The letters then had to be converted back to numbers of just six stability classes (i.e., a = 1; b = 1 or 2, c = 2; d = 2 or 3; e = 3; f = 3 or 4; g = 4; h = 5; i and j = 6). For Japanese stability classes 2 (b), 4 (d), 6 (f) that had to be broken into two classes, each set of replacement classes (1-2; 3-4; 5-6) was alternated hour by hour and inserted in blocks.
4. The revised column was then put back with the rest of the meteorological data and sorted by time.

The meteorological data provided for JAERI and JNC for all years was combined to produce a single wind file for each site to use as input to the dispersion model. Thus one wind file, based on all years of data provided, was used to calculate tritium concentrations in air moisture and pine needles each year for the JAERI releases, and, similarly, another wind file was used to calculate concentrations each year from the JNC releases.

For the preparation of the meteorological files, wind speeds and wind directions for 40 m were used because the JAERI stacks were 40 and 30 m tall. For JNC, 70 m wind speeds and directions were used because the JNC stack is 90 m tall. No adjustment of wind speed was made to account for the difference between the heights of the measured data and heights of release.

The annual meteorological data provided by JAERI and JNC were sorted for the hours it rained. Rainfall rate was determined from total rainfall divided by the total time it rained in a year, based on whether rain was recorded in 10 minute (JNC) or hourly (JAERI) time-periods. Washout coefficients took into account stack height and distance from stack and were adjusted for the rainfall rate.

Because of the elevated week-long release in June 1982 from stack JRR-3, annual mean air concentrations and concentrations in rain at location P3 were calculated two ways. The first used the total released for 1982, including June. The second assumed a June release that was 10% that observed (and comparable to the releases of the other months). The second assumption was necessary in case the annual wind file for the dispersion model could not account for the semi-acute release. The submitted prediction included the mean and upper confidence limit based on the first assumption and the lower confidence limit based on the second assumption.

The source terms for the rainfall model in DCART and for the other pathways in DCART are slightly different from each other. The monthly source terms for estimating tritium concentrations in rain were weighted based on the duration of rainfall during each month.

3. Modeling Approaches (Conceptual and Mathematical)

CAP88-PC, a model approved by the United States Environmental Protection Agency for regulatory compliance, was used as the dispersion model from which χ/Q was obtained as input for DCART. CAP88-PC is a simple Gaussian model for flat terrain that uses conservative assumptions to increase the probability that air concentrations at a given location will be overestimated. One of the conservative assumptions is that the input wind file should be derived from wind measurements take at 10 m; another is that the roughness length is 0.01 m. With these assumptions, CAP88-PC normally predicts concentrations in air to within a factor of three with a tendency to overestimate rather than underestimate.

In DCART, annual wet deposition of HTO is calculated:

$$\omega = \frac{\Lambda Q \Delta T \exp(-\Lambda x / \mu)}{x \mu \Lambda \theta}$$

where:

ω = wet deposition (Bq m^{-2} a^{-1})
Λ = washout coefficient (s^{-1}) (variable, depending on distance from source, stack height, and wind speed during rain)
Q = release rate (Bq s^{-1})
x = downwind distance in meters from the source
u = mean wind speed (m s^{-1}) for when it rains; sector, release height and year specific data are used when available
ΔT = duration of rainfall when plume is present (s a^{-1}); (calculated from fraction of time wind blows into a sector times fraction of time it rains times seconds in a year)
$\Delta\theta$ = sector width (radians); 0.393

The annual mean concentration of HTO in precipitation is calculated:

$$C_{precip} = (\omega / P)(0.001 m^3 / L)$$

where:

C_{precip} = HTO concentration in precipitation (Bq L^{-1})
P = mean annual precipitation (m^3 m^{-2} or m)

Concentrations in air moisture are calculated by dividing the tritium concentration in air volume predicted by the dispersion model by the estimated annual mean absolute humidity.

The annual mean concentrations of HTO in TFWT of pine needles is given by the equation:

$$C_{pw} = 1/\gamma \ [R_H \, C_{a\_HTO} / H_a + (1 - R_H) \, C_{sw}]$$

where:

C_{pw} = concentration of tritium in the plant water (Bq L^{-1} or Bq kg^{-1})
γ = ratio of vapor pressure between HTO and H_2O (0.909)
R_H = relative humidity
C_{a_HTO} = concentration of HTO in air (Bq m^{-3})
H_a = absolute humidity (kg m^{-3})
C_{sw} = concentration of tritium in soil moisture (Bq L^{-1})

Concentration of OBT in needles and tree rings (Bq L^{-1} water equivalent) equals the concentration in TFWT reduced by a discrimination factor that arises from isotopic effects during OBT formation.

Default soil moisture concentrations in DCART are normally set equal to 30% of the tritium concentration in air moisture. However, for this scenario, when air concentrations were obtained from dispersion modeling, the concentration in wet deposition always exceeded 30% of air moisture. Consequently it was felt that soil concentrations would be underestimated if the default ratio were used, and it was assumed that the best estimated soil concentration would equal the concentration of the wet deposition (i.e., the precipitation).

4. Parameter Values and Associated Uncertainties

The parameter values and uncertainties used in the precipitation model are found in Table A1 in the Annex; the parameter values, used in DCART to estimate concentrations in needles and wood, that varied from year to year or location to location are found in Table A2.

Isotopic discrimination for pine needles was 0.7. The distribution was an extreme value distribution with md = 0.067 and scl = 0.014. Isotopic discrimination for tree rings was calculated using a triangular distribution (0.2 – 0.4 – 0.7).

For the Pine Tree Scenario, the concentration in soil water was set equal to the concentration in precipitation. The extremes were then set at best estimate (BE) plus 0.2 and BE minus a multiple of 0.1 that brought the lower limit to about 0.2. Values for the ratio are found in Table A2.

5. Sensitivity

Even though the parameter values to which a model is sensitive are related directly to one particular scenario and endpoint, sensitivity analyses were not carried out for each location and each year because of the similarity between years.

When calculating concentrations in rain, the model was sensitive to the source term and the washout coefficient. When calculating air moisture and TFWT, the parameters to which the model was sensitive were source terms, specifically for JRR2 and JRR3, and χ/Q, for JRR3. When calculating OBT in pine needles and in wood, the model was most sensitive to the isotopic discrimination parameter.

6. Application of the Model to the Scenario

The stack heights, stack diameters and exit velocities supplied in Table 2 of the scenario description were used in the dispersion model. The distances and directions given in Table 3 of the scenario description were used in the determination of χ/Q.

All wind speed, wind direction, stability class, and rainfall data provided for all years were used to prepare input files for the dispersion model and for the rain model. In addition, the temperature (both JAERI and JNC) and the relative humidity (JNC) or dewpoint (from JAERI – used to estimate relative humidity) were used to calculate absolute humidity.

Annual source terms were obtained by summing the monthly releases.

The washout coefficients provided were used to determine uncertainty bounds on the best estimates; each distribution was adjusted to include the two values provided.

7. Predictions

Air concentrations were calculated using the χ/Q from the dispersion model, CAP88-PC, and estimated annual release rates. Predicted to observed (P/O) ratios at the three sampling locations for concentrations of tritium in air moisture and precipitation are shown in Table 1 and Table 2, respectively.

Table 1. Predicted to observed ratios in air moisture

Year	MP-7	P3	MS2
1984	0.16	0.22	0.18
1985	0.43	0.59	0.44
1986	0.21	0.32	0.21
1987	0.25		0.29

All air moisture concentrations are underestimated and the upper confidence limit on the predictions does not include the observations; the mean of all P/O ratios is 0.3. If the results from 1985 (which are noticeably higher) are excluded from the mean, the mean P/O ratio becomes 0.23. These results are surprising given that CAP88-PC, in at least three independent tests, has been shown to predict air concentrations within a factor of 3 and to overestimate air concentrations more than half the time.

Table 2. Predicted to observed ratios in precipitation. Shaded areas indicate when the upper confidence limit was below the observed concentration

Year	MP-7	P3	MS2
1982		0.63	
1983		0.81	
1984	0.44	0.42	0.39
1985	0.80	0.65	0.45
1986	0.33	0.47	0.57
1987	0.48		0.97

Based on the relative success of predictions of tritium concentrations in rainfall (Table 2), the source terms used in the model are probably reasonable. The over-all P/O ratio for concentrations of tritium in rain was 0.57, and just over half of the observations were included within the confidence intervals of the predictions.

Rather than the use of incorrect source terms, it is likely that the failure to correctly predict air moisture concentrations may be traced to the many errors that could have been introduced during the process by which the ten stability classes were reduced to six while preparing the input wind file for CAP88-PC, but some of the under-prediction may be due to having prepared the input wind file from the 40 and 70 m wind data rather than from 10 m data as recommended by CAP88-PC. The unusually high soil moisture to air moisture ratios (Table A2) that were derived for these calculations are probably symptomatic of the underestimated air concentrations.

Because air moisture concentrations were underestimated, DCART's predictions of TFWT and OBT in pine needles and OBT in tree rings were also underestimated.

8. Conclusions

Predictions from the rain model in DCART were uniformly underestimated, and the reason for this is not known as of this writing. The confidence placed in the parameter values of the rain equation should be reevaluated given that about half of the predicted confidence intervals failed to include the observations.

For whatever reason, the air concentrations calculated from the χ/Q obtained from the dispersion model were unacceptably low, with the result that all initial predictions were also unacceptably

low. However, as an exercise, when the observed air moisture concentrations were used as the driving input in DCART, most of DCART's predictions of TFWT in pine needles and OBT in pine needles and tree rings were within a factor of two of the observations.

The observations themselves were not internally consistent, and there were insufficient results to justify reconsidering any of the transfer parameter values in DCART. The degree of confidence in the predictions appears to be justified.

ANNEX – SUPPLEMENTARY TABLES

A1. Input data summary to rain model in DCART; distributions are normal unless noted

	1982	1983	1984	1985	1986	1987
Source term for the rain model in DCART (Bq s^{-1} ± 20%)						
JRR- 2	1.22E+04	2.06E+04	2.92E+04	2.26E+04	4.12E+04	3.22E+04
JRR-3	1.19E+05	2.55E+04	9.11E+03	7.81E+03	8.54E+03	2.54E+02
WTF	1.29E+04	2.45E+04	1.69E+04	8.45E+03	5.34E+03	2.31E+03
NFRP	1.43E+05	5.91E+04	2.08E+04	9.85E+04	6.40E+04	9.50E+04
Mean wind speed (m s^{-1} ± 5% for the 40 m JAERI towers and ± 10% for the other two towers)						
JRR-2; JRR-3	5.27	4.50	4.98	4.83	5.84	4.89
WTF	4.51	3.85	4.26	4.13	4.99	4.18
NFRP	10.4	10.2	9.72	8.02	9.09	8.59
Fraction of time when raining that the wind blows towards MP-7; no uncertainty						
JRR-2	0.232	0.120	0.307	0.211	0.152	0.286
JRR-3	0.290	0.304	0.320	0.295	0.297	0.219
WTF	0.0548	0.101	0.0727	0.0843	0.096	0.043
NFRP	0.0261	0.0410	0.0155	0.0251	0.0472	0.0242
Fraction of time when raining that the wind blows towards P-3; no uncertainty						
JRR-2; JRR-3	0.290	0.304	0.320	0.295	0.297	0.219
WTF	0.0548	0.101	0.0727	0.0843	0.0962	0.0435
NFRP	0.0261	0.0410	0.0155	0.0251	0.0472	0.0242
Fraction of time when raining that the wind blows towards MS-2; no uncertainty						
JRR-2; JRR-3	0.232	0.120	0.307	0.211	0.152	0.286
WTF	0.290	0.304	0.320	0.295	0.297	0.219
NFRP	0.0261	0.0410	0.0155	0.0251	0.0472	0.0242
Frequency of rain - best estimate is mean between frequency at JAERI and frequency at JNC; uncertainty is rectangular with JAERI and JNC values as extremes						
JAERI	0.0713	0.0776	0.0502	0.0866	0.0653	0.0683
JNC	0.0557	0.0631	0.0405	0.0553	0.0560	0.0527
Mean	0.0635	0.0704	0.0453	0.0710	0.0606	0.0605
Annual precipitation (m) is the average of JAERI and JNC with an uncertainty of +/- 25%						
Mean	1.15	1.07	0.611	1.14	1.16	0.980
Washout coefficients (s^{-1}) for all locations; distribution is lognormal with a GSD of about 1.8						
JRR-2; JRR-3	1.14E-04	1.01E-04	9.12E-05	1.01E-04	1.18E-04	1.04E-04
WTF	1.22E-04	1.08E-04	9.77E-05	1.08E-04	1.26E-04	1.12E-04
NFRP	8.49E-05	7.86E-05	7.04E-05	8.29E-05	8.90E-05	7.98E-05

A2. Input data for DCART's predicted concentrations in pine needles and wood

	1982	1983	1984	1985	1986	1987
Source term for DCART (Bq s^{-1} ± 20% on a normal distribution)						
JRR-2	1.27E+04	2.00E+04	2.75E+04	2.32E+04	3.65E+04	3.06E+04
JRR-3	9.88E+04	2.67E+04	9.89E+03	1.36E+04	1.22E+04	2.35E+02
WTF	1.18E+04	2.40E+04	1.72E+04	8.24E+03	5.39E+03	2.31E+03
NFRP	1.41E+05	6.07E+04	1.87E+04	8.87E+04	7.02E+04	8.94E+04
Relative humidity; the best estimate is the midpoint of a rectangular distribution with endpoints from JAERI and JNC						
JAERI	0.760	0.764	0.736	0.748	0.782	0.743
JNC	0.812	0.828	0.829	0.861	0.824	0.808
midpoint	0.786	0.796	0.783	0.805	0.803	0.776
Absolute humidity`(kg m^{-3}); the best estimate is the midpoint of a rectangular distribution with endpoints from JAERI and JNC						
JAERI	0.00951	0.00969	0.00929	0.00972	0.00875	0.00960
JNC	0.0102	0.0101	0.00955	0.0108	0.00973	0.0103
midpoint	0.00986	0.00989	0.00942	0.0102	0.00924	0.0100
Ratio of soil moisture/air moisture; uncertainty is triangular: BE + 0.2 or BE – 0.2, 0.3, 0.4, 0.5, or 0.6						
MP-7	-	-	0.82	0.56	0.45	0.94
P3	0.52	0.51	0.45	0.37	0.35	-
MS2	-	-	0.68	0.45	0.31	0.59

χ/Q (s m^{-3} ± 30% on a lognormal distribution)

	MP-7	P3	MS2
JRR-2	5.03E-07	9.92E-07	5.60E-07
JRR-3	8.64E-07	9.81E-07	5.32E-07
WTF	6.08E-07	5.50E-07	9.48E-07
NFRP	4.52E-08	4.68E-08	5.67E-08

IFIN Model

1. Method

We adapted the methods used in BIOMASS, considering the specific scenario data. Since the receptor- source positions were given by sector, and since monthly average concentrations were requested, we used the sector average Gaussian model to calculate atmospheric dispersion and wet deposition. The scenario description identified 10 atmospheric stability classes whereas it is traditional to specify only 6 (A to F). We established a correspondence by assuming that $1 \rightarrow$ A, $7 \rightarrow$ D and $9 \rightarrow$ F. We used the SCK/MOL scheme to calculate the vertical dispersion parameter, σ_z:

$$\sigma_z = \alpha\, x^{0.711}$$

where the parameter α depends on stability class with values of 1.31, 1.24, 1.13, 0.99, 0.83, 0.66, 0.50, 0.38, 0.32 and 0.3 for classes 1 to 10 respectively.

For a given receptor in sector i, we added the contributions from the various sources *j*. Using the hourly meteorological data from JAERI, we determined the monthly frequency (f_{ij}) with which the wind blew into the sector encompassing the receptor. For each case where the wind blew from source j to sector i, we calculated the hourly, sector-averaged air concentration, and later the average over all cases. Finally we converted the concentration in air to the concentration in air moisture using the monthly atmospheric humidity.

The average concentration in precipitation was assessed from the total monthly wet deposition and the total precipitation. The scavenging rate considered was $\Lambda = 1 \times 10^{-4}\, I^{0.8}\ s^{-1}$, where I is precipitation intensity in mm/h. The effect of temperature on washout was disregarded.

The HTO concentration in soil water was a superposition of the concentration in precipitation with a small (0.1) contribution from air moisture.

In order to assess the HTO and OBT concentrations in pine needles, we must consider the specific characteristics of evergreen conifers. This is the first time we are faced with such a case. The change in the leaf water concentration depends on the exchange velocity. For evergreen conifers, this is lower than for agricultural crops by a factor 3-5 (Dorman and Sellers 1989, Schultze et al. 1994). However, as we are asked to predict monthly mean concentrations, this slow transfer is irrelevant and we preserve the simple formalism used for crops, as in the BIOMASS study:

$$C_{leaf\_water} = 1.1\ [RH\ C_{air\_moisture} + (1\text{-}RH)\ C_{soil\_water}]$$

As a simplification, the relative humidity RH was set to its annual average value. In order to calculate the OBT concentration in pine needles or wood, we must consider some characteristics of pine trees. The needles found on the trees are of various ages, from new ones formed in the current year to those up to 7 years old; the needle loss rate is $0.33\ y^{-1}$ (Friend et al. 1997). Old leaves have low photosynthetic activity. In periods of low temperature ($<5^{o}$ C), the tree is dormant and we have practically no OBT production. Considering the average air temperature and radiation from 1981-1987, we deduce an average net relative photosynthesis rate. This is shown in Table 1 together with information on air temperature, solar radiation and leaf area index.

Table 1. Air temperature, solar radiation, leaf area index and average net relative photosynthesis rate

Month	Average air temperature (C)	Average radiation (W/m^2)	Average net relative photosynthesis rate	Leaf area index
Jan	2.16	100.93	0.000	6
Feb	3.06	118.75	0.000	6
Mar	5.86	134.72	0.017	6.5
Apr	10.70	171.82	0.067	7
May	15.19	193.58	0.150	7.5
Jun	17.52	167.63	0.167	8
Jul	21.99	173.66	0.167	8
Aug	24.49	188.74	0.167	7.5
Sep	20.98	130.51	0.117	7
Oct	15.83	114.71	0.100	6.5
Nov	9.85	89.55	0.042	6
Dec	5.08	83.64	0.000	6

In December, January and February we have no OBT production and no change in leaf OBT concentration. In March and November, the production of OBT is low and influences the average OBT concentration in the needles only marginally. For the rest of the season, the OBT concentration in needles depends on the relative contributions of old and newly-produced OBT. The yearly carbon production in evergreen conifers can be partitioned between needles, fine roots and wood, for a total production of about 2.1 $kgC/(y\ m^2)$ (Friend et al. 1997). Needle production contributes about 20% of this value. In the summer period (April-October), the daily carbon (and OBT) production rate (0.02 kgC/m^2) is less than the amount of carbon (and OBT) stored in the needles (0.8 kgC/m^2). Little carbon is retained in the needles and much is translocated to roots and trunk.

As a consequence of these considerations, the monthly average OBT concentration in needles in summer is assumed to be given by the arithmetic average of the concentration of old and newly-produced OBT. The concentration of newly-produced OBT is assumed to equal the HTO concentration in needle water apart from an isotopic discrimination factor of 0.6. For example, in August, the OBT concentration (in Bq/L water equivalent) in the needles is

$$OBT_{Aug} = (OBT_{Jul} + 0.6\ HTO_{Aug}) / 2$$

Only the new OBT contributes to the concentration in tree rings, but we must consider the monthly contribution to the annual average, as shown in Table 2.

Table 2. Relative contribution of the monthly OBT concentration to the annual average concentration

May	0.173
Jun	0.192
Jul	0.192
Aug	0.192
Sep	0.135
Oct	0.115

2. Uncertainties

Using a sector-averaged dispersion model and selecting a specific vertical dispersion parameter induces inherent uncertainties of a factor 3 in the air concentration. This factor is marginally increased for the predicted air moisture concentration (we use yearly averaged relative humidity of 0.7 but it fluctuates between 0.6 and 0.9), but for OBT in needles the uncertainty increases to a factor 5, since our estimate of the contribution of old and new OBT is preliminary. A factor 5 is also assessed for the OBT concentration in tree rings.

The above uncertainties refer to our calculations. In comparing with observations we must consider also potential errors in the data. Usually air moisture and precipitation are collected continuously and the observed monthly mean is a good estimate of the real value. Pine needles can be collected a few times a month, at various hours and under various plume conditions. This affects the average measured HTO concentration in pine needles. If we take the example of December 1983, from 744 hours we have good meteorological records for 712, but in only 48 of those hours did the wind blow from one of the release points to the sampling site P3. About half of those cases occurred during the work day. If only a few samples were taken per month (1-5), the average can be severely biased (Kim et al. 2000). A "perfect" monthly average must be constructed from at least 2 samples per day (one taken during the night and one during daylight hours) each day in the month. We expect a large spread between modeled and observed HTO concentrations in pine needles. The observed OBT concentrations will be less biased, as OBT is an integral of past HTO concentrations.

References

Kim, C-K. et al. 2000. Environmental distribution and behaviour of ^{3}H and ^{14}C around Wolsong NPP. Health Phys 78, 693.

Friend, A.D. et al. 1997. A process-based, terrestrial biosphere model of ecosystem dynamics. Ecological modeling 95, 249.

Dorman, J.L. and P.J. Sellers. 1989. A global climatology of albedo, roughness length and stomatal resistance. J. App. Meteorology 28, 833.

Schultze, E.D. et al. 1994. Relationships among maximum stomatal conductance, ecosystem surface conductance, carbon assimilation rate, and plant nitrogen nutrition: a global ecology scaling exercise Annu. Rev. Ecol. Syst 25, 629.

Results

Predicted HTO concentrations in air moisture, precipitation and pine needles, and OBT concentrations in needles and tree rings are given in the following figures for P3. Predictions for P3 and MS2 are shown in tabular form following the figures.

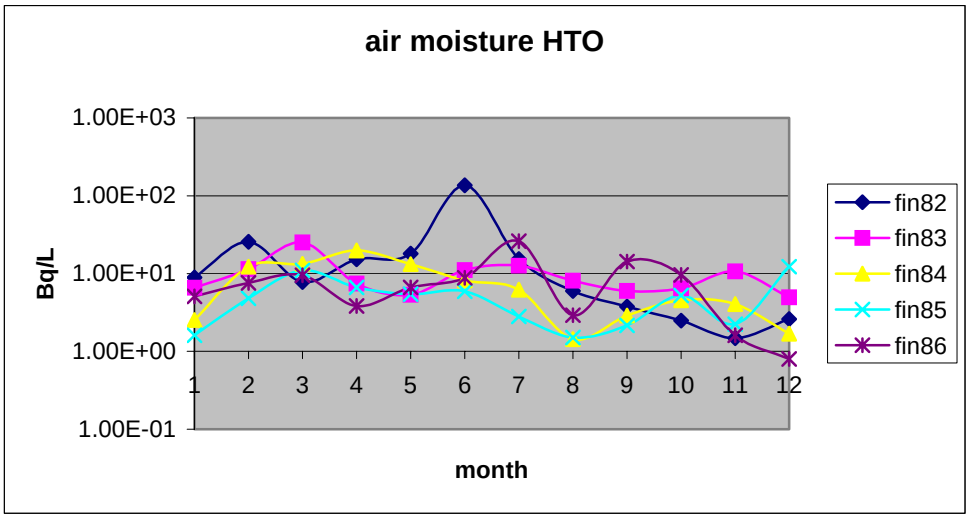
air moisture HTO
1.00E+03
1.00E+02
1.00E+01
1.00E+00
1.00E-01
Bq/L
1 2 3 4 5 6 7 8 9 10 11 12
month
fin82
fin83
fin84
fin85
fin86

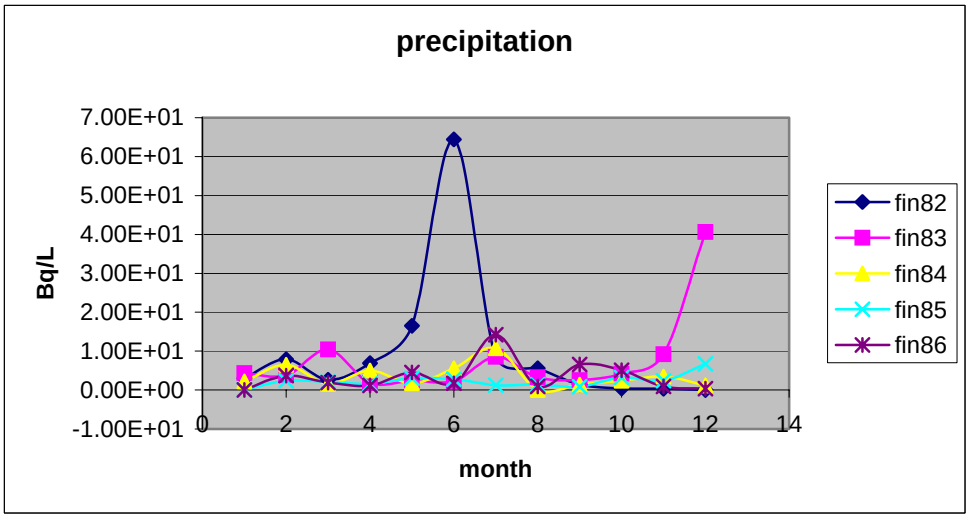
precipitation
7.00E+01
6.00E+01
5.00E+01
4.00E+01
3.00E+01
2.00E+01
1.00E+01
0.00E+00
-1.00E+01
Bq/L
0 2 4 6 8 10 12 14
month
fin82
fin83
fin84
fin85
fin86

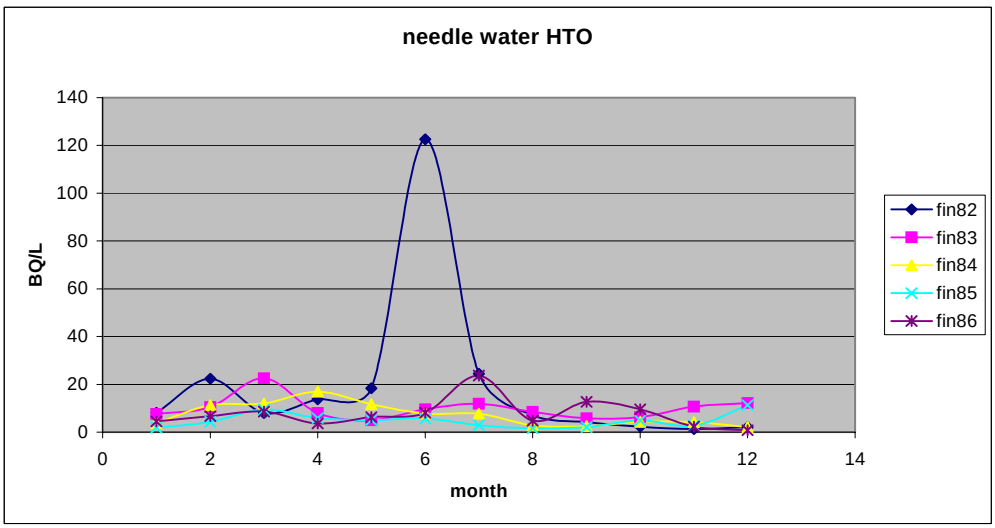
needle water HTO
140
120
100
80
60
40
20
0
BQ/L
0 2 4 6 8 10 12 14
month
fin82
fin83
fin84
fin85
fin86

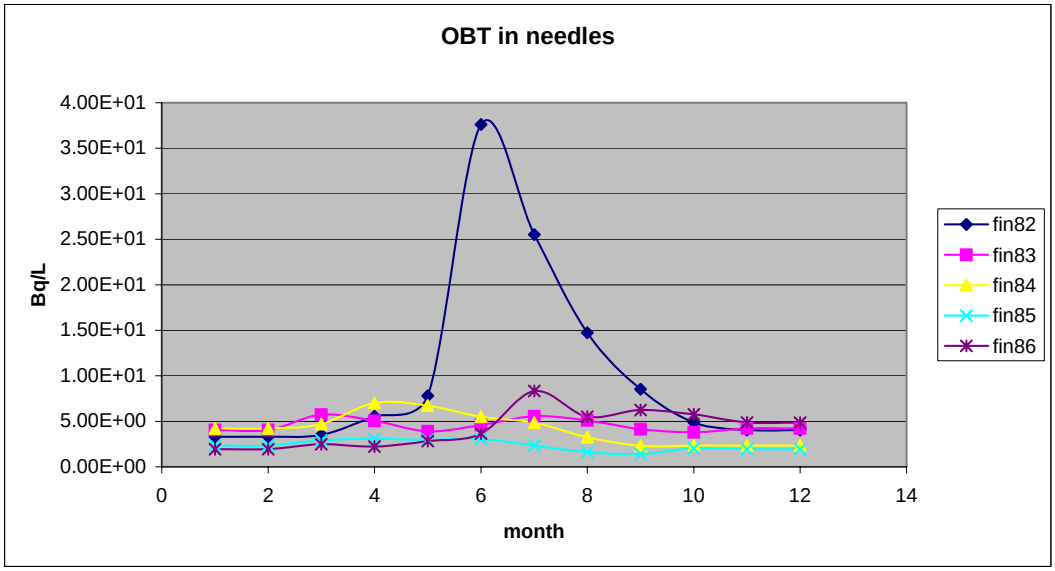
OBT in needles
4.00E+01
3.50E+01
3.00E+01
2.50E+01
2.00E+01
1.50E+01
1.00E+01
5.00E+00
0.00E+00
Bq/L
0
2
4
6
8
10
12
14
month
fin82
fin83
fin84
fin85
fin86

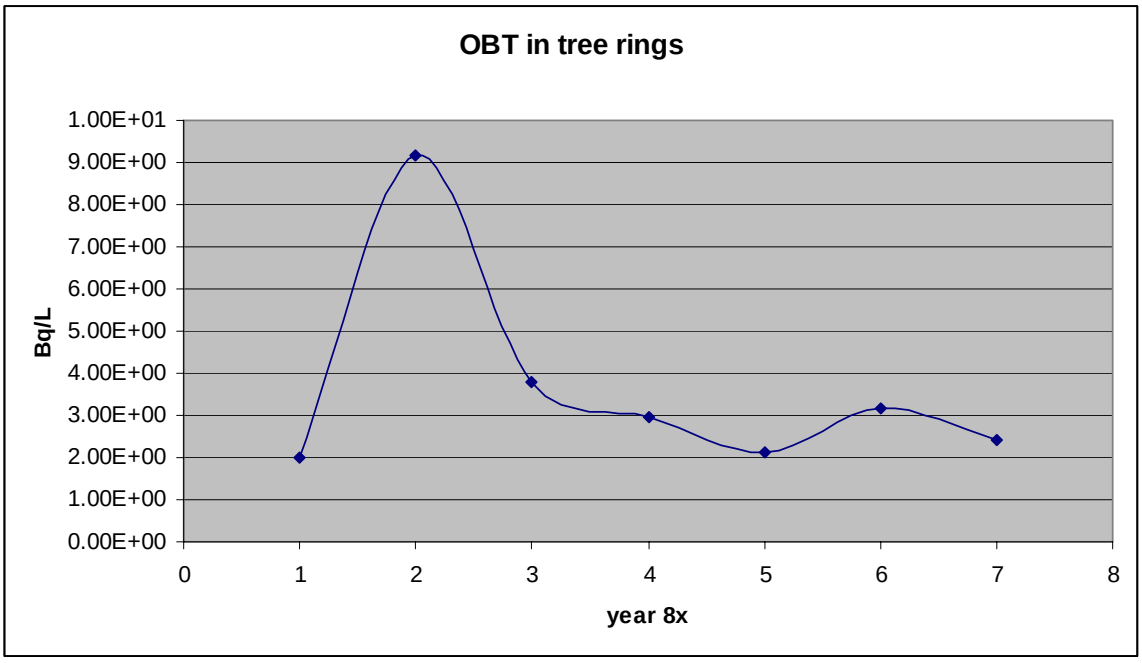
OBT in tree rings
1.00E+01
9.00E+00
8.00E+00
7.00E+00
6.00E+00
5.00E+00
4.00E+00
3.00E+00
2.00E+00
1.00E+00
0.00E+00
Bq/L
0
1
2
3
4
5
6
7
8
year 8x

P3

Air moisture HTO (Bq/L)

	Jan	Feb	Mar	Apr	May	Jun	Jul	Aug	Sep	Oct	Nov	Dec	Annual
1982	8.90E+00	2.56E+01	7.77E+00	1.52E+01	1.80E+01	1.36E+02	1.54E+01	6.00E+00	3.76E+00	2.48E+00	1.48E+00	2.60E+00	2.03E+01
1983	6.56E+00	1.14E+01	2.52E+01	7.41E+00	5.34E+00	1.10E+01	1.26E+01	8.12E+00	5.95E+00	6.45E+00	1.06E+01	4.93E+00	9.63E+00
1984	2.53E+00	1.22E+01	1.33E+01	1.98E+01	1.32E+01	8.13E+00	6.18E+00	1.44E+00	2.88E+00	4.53E+00	4.04E+00	1.69E+00	7.49E+00
1985	1.60E+00	4.80E+00	1.09E+01	6.63E+00	5.45E+00	5.93E+00	2.81E+00	1.50E+00	2.15E+00	5.26E+00	2.23E+00	1.22E+01	5.12E+00
1986	5.08E+00	7.57E+00	9.49E+00	3.82E+00	6.61E+00	8.84E+00	2.62E+01	2.91E+00	1.43E+01	9.58E+00	1.61E+00	7.97E-01	8.07E+00

Precipitation HTO (Bq/L)

	Jan	Feb	Mar	Apr	May	Jun	Jul	Aug	Sep	Oct	Nov	Dec	Annual
1982	3.08E+00	7.86E+00	2.61E+00	6.89E+00	1.65E+01	6.44E+01	8.70E+00	5.55E+00	1.39E+00	4.19E-01	3.28E-01	0.00E+00	9.81E+00
1983	4.39E+00	3.76E+00	1.04E+01	1.84E+00	2.36E+00	2.29E+00	8.56E+00	3.32E+00	2.53E+00	4.17E+00	9.17E+00	4.06E+01	7.78E+00
1984	2.22E+00	6.48E+00	1.58E+00	5.05E+00	1.71E+00	5.61E+00	1.08E+01	0.00E+00	1.40E+00	2.38E+00	3.44E+00	1.14E+00	3.48E+00
1985	0.00E+00	2.37E+00	2.10E+00	1.57E+00	3.01E+00	2.79E+00	1.21E+00	1.43E+00	8.18E-01	3.22E+00	2.38E+00	6.76E+00	2.30E+00
1986	0.00E+00	3.70E+00	1.93E+00	1.13E+00	4.50E+00	1.70E+00	1.42E+01	9.53E-01	6.55E+00	5.10E+00	8.84E-01	3.34E-01	3.42E+00

Pine needle HTO (Bq/L)

	Jan	Feb	Mar	Apr	May	Jun	Jul	Aug	Sep	Oct	Nov	Dec	Annual
1982	8.06E+00	2.24E+01	7.97E+00	1.38E+01	1.83E+01	1.23E+02	2.44E+01	7.17E+00	4.16E+00	2.29E+00	1.31E+00	2.14E+00	1.95E+01
1983	7.61E+00	1.05E+01	2.26E+01	7.97E+00	4.98E+00	9.60E+00	1.19E+01	8.48E+00	5.74E+00	6.28E+00	1.07E+01	1.22E+01	9.88E+00
1984	3.68E+00	1.12E+01	1.20E+01	1.70E+01	1.17E+01	7.74E+00	7.67E+00	2.94E+00	2.54E+00	4.26E+00	4.20E+00	2.11E+00	7.26E+00
1985	1.86E+00	4.25E+00	9.49E+00	5.93E+00	5.13E+00	5.72E+00	2.92E+00	1.64E+00	2.10E+00	4.89E+00	2.71E+00	1.13E+01	4.83E+00
1986	4.46E+00	6.69E+00	8.55E+00	3.57E+00	6.24E+00	8.12E+00	2.37E+01	4.84E+00	1.27E+01	9.61E+00	2.28E+00	8.41E-01	7.63E+00

Pine needle OBT (Bq/L)

	Jan	Feb	Mar	Apr	May	Jun	Jul	Aug	Sep	Oct	Nov	Dec	Annual
1982	3.30E+00	3.30E+00	3.52E+00	5.55E+00	7.81E+00	3.76E+01	2.55E+01	1.47E+01	8.51E+00	4.89E+00	4.05E+00	4.05E+00	1.02E+01
1983	4.05E+00	4.05E+00	5.72E+00	5.05E+00	3.90E+00	4.59E+00	5.57E+00	5.12E+00	4.14E+00	3.80E+00	4.22E+00	4.22E+00	4.53E+00
1984	4.22E+00	4.22E+00	4.70E+00	7.02E+00	6.73E+00	5.49E+00	4.86E+00	3.24E+00	2.32E+00	2.33E+00	2.33E+00	2.33E+00	4.15E+00
1985	2.33E+00	2.33E+00	2.91E+00	3.08E+00	2.95E+00	3.05E+00	2.33E+00	1.61E+00	1.38E+00	2.04E+00	1.93E+00	1.93E+00	2.32E+00
1986	1.93E+00	1.93E+00	2.48E+00	2.22E+00	2.83E+00	3.65E+00	8.33E+00	5.50E+00	6.25E+00	5.77E+00	4.86E+00	4.86E+00	4.22E+00

MS2

Air moisture HTO (Bq/L)

	Jan	Feb	Mar	Apr	May	Jun	Jul	Aug	Sep	Oct	Nov	Dec	Annual
1982	47.00	40.50	11.30	9.93	7.86	45.30	8.62	2.27	3.47	3.29	2.20	3.33	15.42
1983	9.80	13.80	19.20	6.71	4.01	7.61	6.12	4.17	5.80	7.32	9.51	7.77	8.49
1984	8.09	16.00	13.30	13.00	7.33	5.40	3.00	1.18	2.84	6.20	5.41	3.08	7.07
1985	3.89	6.86	11.60	4.34	3.65	3.81	2.24	0.75	2.20	7.38	3.24	9.72	4.97
1986	8.83	12.10	7.54	2.18	2.27	3.35	4.61	1.41	10.10	5.96	2.87	1.80	5.25
1987	6.99	7.44	3.59	4.86	5.26	2.18	0.64	0.79	11.60	1.08	3.49	1.70	4.13

Precipitation HTO (Bq/L)

	Jan	Feb	Mar	Apr	May	Jun	Jul	Aug	Sep	Oct	Nov	Dec	Annual
1982	2.94	4.10	5.51	4.00	6.27	24.40	6.28	2.42	1.43	0.92	1.48	0.88	5.05
1983	3.92	4.76	3.62	1.94	2.99	2.19	3.07	1.65	3.42	2.22	8.90	18.30	4.75
1984	5.20	9.35	7.04	4.06	1.06	4.48	4.36	0.00	1.90	2.36	3.56	1.58	3.75
1985	0.00	1.27	3.58	1.98	2.48	1.92	0.88	1.17	1.01	4.68	1.31	4.84	2.09
1986	2.31	4.16	1.97	0.50	0.59	4.05	7.11	0.53	7.19	3.10	0.34	0.70	2.71
1987	2.81	4.39	0.32	2.63	4.52	0.82	3.67	0.46	4.03	0.31	1.53	1.12	2.22

Pine needle HTO (Bq/L)

	Jan	Feb	Mar	Apr	May	Jun	Jul	Aug	Sep	Oct	Nov	Dec	Annual
1982	38.84	33.68	10.66	9.54	8.01	41.44	11.98	3.26	3.42	3.03	2.16	3.06	14.09
1983	8.66	12.51	16.80	6.31	4.03	6.97	5.78	4.13	5.49	6.81	9.47	10.73	8.14
1984	10.37	15.25	13.38	12.27	6.73	5.25	3.87	1.67	2.59	5.68	5.32	3.32	7.14
1985	3.38	5.72	10.12	4.40	3.67	3.79	2.26	0.94	2.13	6.86	3.59	8.82	4.64
1986	8.27	10.78	7.07	2.16	2.00	3.45	5.54	2.39	9.38	6.48	2.87	1.62	5.17
1987	6.19	7.16	3.66	4.39	5.40	2.63	1.25	1.31	10.06	1.58	3.11	1.80	4.05

Pine needle OBT (Bq/L water equivalent)

	Jan	Feb	Mar	Apr	May	Jun	Jul	Aug	Sep	Oct	Nov	Dec	Annual
1982	2.94	2.94	3.52	4.39	4.39	13.59	10.09	5.94	3.91	2.79	2.47	2.47	4.95
1983	2.47	2.47	3.82	3.65	2.93	3.38	3.28	2.78	2.90	3.32	3.70	3.70	3.20
1984	3.70	3.70	4.43	5.59	4.65	3.77	2.95	1.93	1.68	2.40	2.51	2.50	3.32

1985	2.50	2.50	3.11	2.77	2.39	2.24	1.74	1.13	1.15	2.46	2.36	2.36	2.23
1986	2.36	2.36	2.67	1.93	1.51	1.71	2.38	1.85	3.50	3.53	3.14	3.14	2.51
1987	3.14	3.14	2.91	2.66	2.82	2.13	1.41	1.07	3.30	2.08	2.01	3.14	2.49

Annual OBT in tree rings
(Bq/L water equivalent)

1981	2.01E+00
1982	9.15E+00
1983	3.80E+00
1984	2.95E+00
1985	2.11E+00
1986	3.15E+00
1987	2.42E+00

EDF Model

1. Atmospheric Dispersion

For this exercise, the model ADMS3 was used for atmospheric dispersion. This tool was developed by Cambridge Environmental Research Consultants (http://www.cerc.co.uk). Many companies and regulatory authorities in Europe use this model for impact studies. Nevertheless, this tool has not been used at EDF for nuclear impact studies before now. Here we use the Gaussian plume model of the tool.

As for any other plume model, the meteorological conditions are assumed to be constant in time and space for each hourly time step of the simulations. Moreover, no spatial variations of wind parameters have been modeled, as the region was considered to be flat.

The key parameters are the roughness length (0.5 m), the physical characteristics of the emission sources (height, diameter, emission velocity), and the washout coefficient ($7.3\ 10^{-5}\ s^{-1}$, as suggested in the scenario description). Four different emission sources corresponding to the JRR-2, JRR-3, WTF and NFRP installations were taken into account. The model calculates the effective release height of the plume using its own equations. The output grid resolution is 100 x 100 m.

For the meteorological conditions, we used the JNC data. From these, we calculated hourly-averaged meteorological conditions at 10-m height for input to the model.

The model can perform either short-term simulations, which assume steady-state conditions over one-hour periods, or long-term calculations for impact studies. In this last case, the model outputs mean concentrations or high-order percentiles such as 98 or 99%. For this scenario, monthly concentrations were determined by averaging the hourly predictions for each month of the 7-year study period.

2. Tritium Concentration in Air Moisture and Precipitation

ADMS outputs are air concentration in Bq m^{-3} and ground deposit in Bq $m^{-2}\ s^{-1}$. These quantities were divided by air moisture content and volume of precipitation, respectively, to obtain tritium concentrations in air moisture and precipitation

Air moisture content was calculated from monthly statistics on air temperature and relative humidity given in the JNC_met_ave_r7.xls Excel file, for the NFRP site. The JNC file was preferred because it contained data on relative humidity whereas the JAERI file contained dew point data.

Monthly precipitation amounts were taken from the JNC dataset.

3. Groundwater Concentrations

The outputs of the ADMS3 model were used as inputs to the groundwater calculations, which were performed with ARGUS, an operational tool developed by the EDF Research and Development Division. The aims of the tool are:

- to provides EDF operational sites and engineering units with a crisis assessment and management tool for the treatment of soil and groundwater pollution incidents,
- to help operators dealing with environmental management of sites to increase their knowledge of the subsoil / groundwater levels through a better integration of groundwater related data.

ARGUS is designed to provide pollutant transport results in the short term in order to answer rapidly questions from local and national authorities about the fate of pollutants in groundwater. Therefore, a conservative approach based on a semi-analytical solution of the transport equations is considered. The model is based on a compartment approach and is able to solve the transport equations in the unsaturated and saturated layers, and also the dispersion of a pollutant source term in rivers.

Due to the lack of knowledge concerning pollutant transport in the unsaturated zone, conservative constant flow parameters are used in this compartment. Adsorption (the reversible partitioning of a solute between the aqueous phase and the surfaces of solids) is described by a linear isotherm, and a constant adsorption distribution coefficient (K_d) is used. As a result, time-dependant concentrations of the pollutant plume can be calculated and plotted.

The aim of this study was to calculate the transfer of HTO deposited on the ground through the unsaturated and saturated layers and finally to evaluate the time-dependent HTO concentration at point G4.

3.1 Key assumptions

A simplified model of the geological formation around the study area is shown in Figure 1, which is taken from the scenario description. Since the levels of both ground surface and base rock in the area surrounding JRR-2 and JRR-3 along the inner land line seem about 10 m higher than those along the seaside line, the groundwater may mainly flow eastward in the direction of the sea. Even if the groundwater flows southward from JRR-2 and JRR-3, it might be blocked by an ascending ground surface and base rock about 300 m south of JRR-2, provided that the amount of groundwater is not so plentiful and the mean residence time of groundwater is relatively short, e.g. about half a year.

For this study, a water table starting 300 m south from the JRR-2 and JRR-3 area is considered. The 500 m long calculation area, where a ground deposit source term is taken into account, is presented in Figure 2. The width of the area is set to 200 m, assuming that ground deposit outside this range would not affect the concentration at point G4. Actually, lateral dispersion over a distance of 500 m, which is the maximum distance between an injection point and point G4, would probably not exceed 10 to 20 m.

Compartments corresponding to the unsaturated layer and the water table are considered in this study.

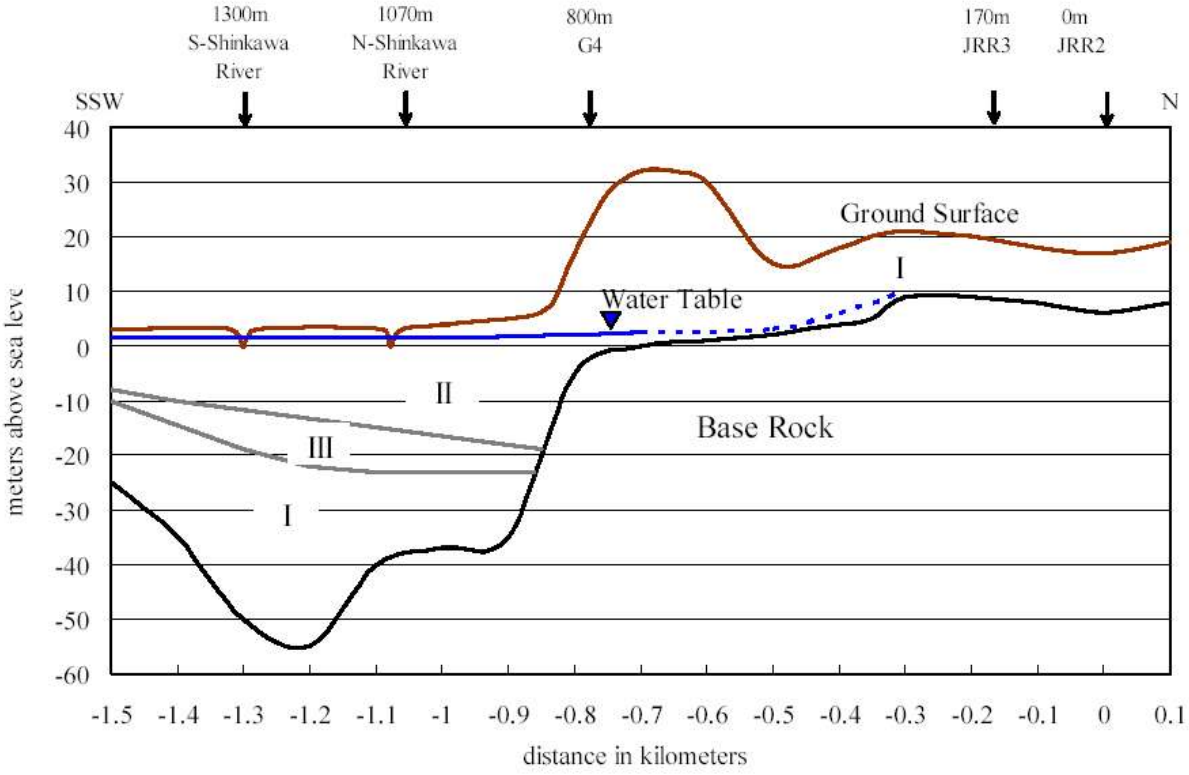

Figure1. Simplified geological model along a line connecting the points of northern JRR-2, south south-west G4, and the Shinkawa River. I: Sand/Silt, II: Gravel/Sand, III: Silt/Clay

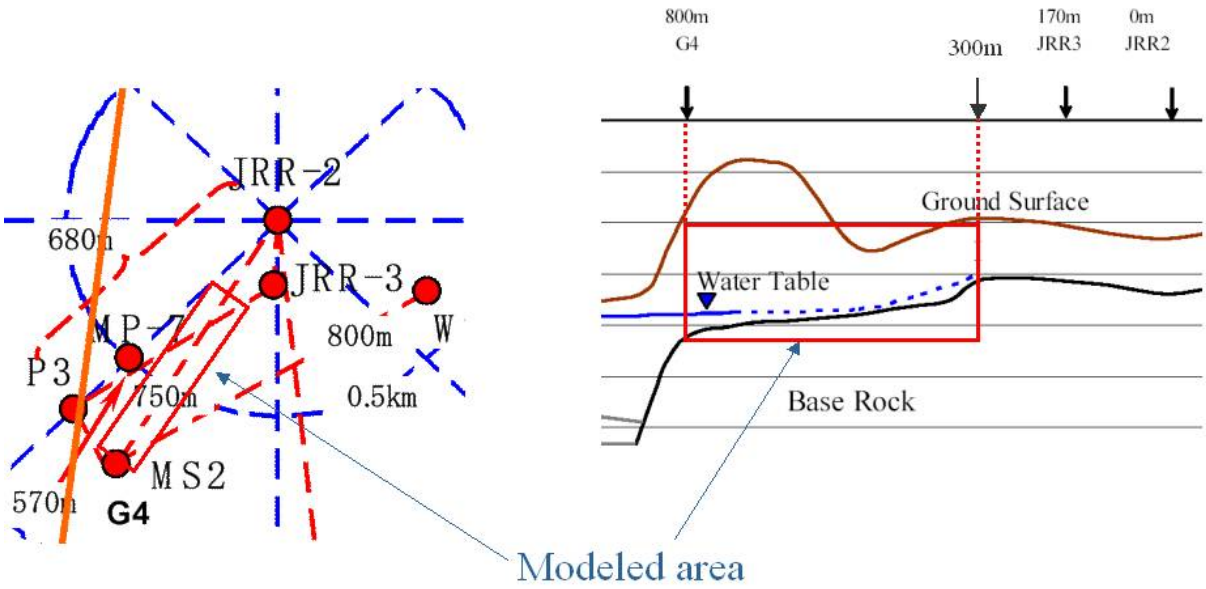

Figure 2. Description of the modeled area for the concentration calculation

3.2 Modeling approaches and application of the model to the scenario

Injection in the soil: In ARGUS, the pollution source is modeled as a single point, time-dependant, multi-pollutant source term. In this study, the atmospheric deposits are distributed over the whole area. The modeled area was therefore divided up into six injection zones. The radioactivity is assumed to be injected at the center point of each zone (see Figure 3 for more details). The source term injected at point 1, which is a result from the atmospheric dispersion simulations, is plotted on Figure 4 for illustrative purposes. Finally, the concentration at point G4 is calculated by summing up the contributions of each of the six injection points.

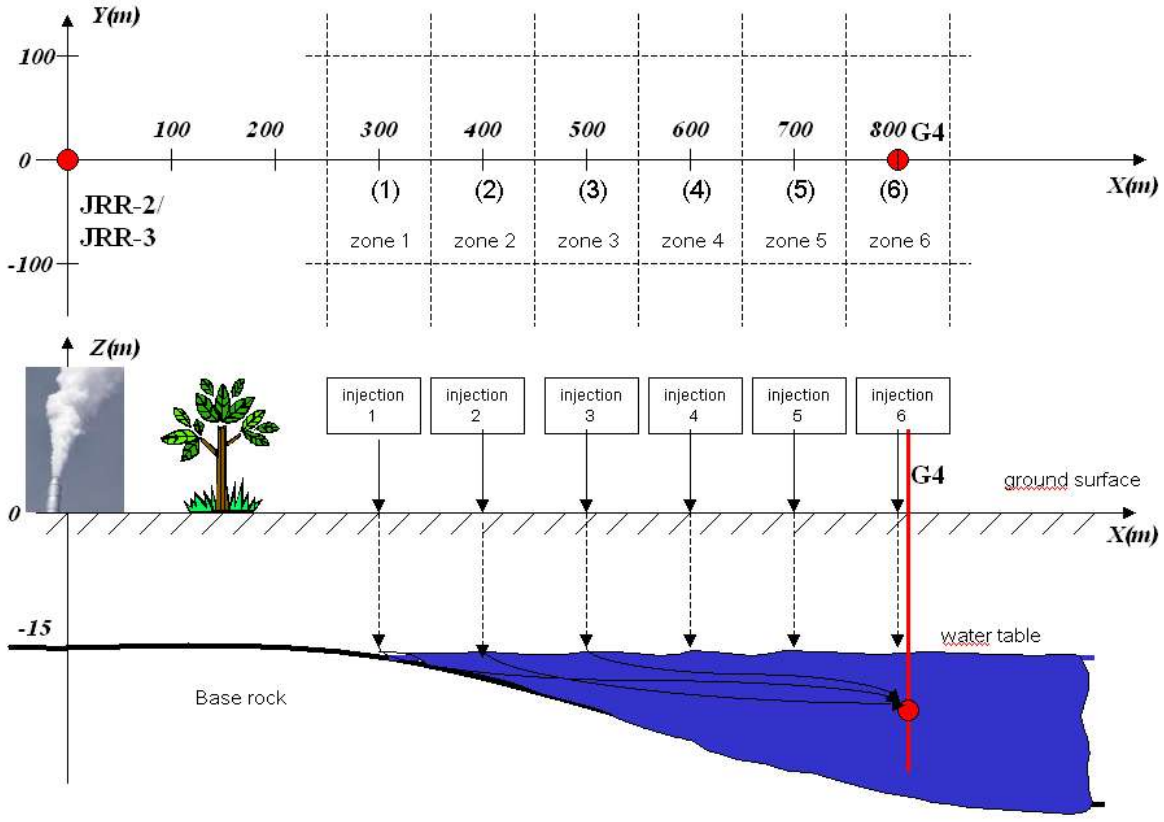

Figure 3. Schematic illustration of the multipoint injection principle used with the ARGUS software: 6 injection areas are modeled between the JR-R2/JRR-3 tritium discharge source area and point G4 (injection points 1 to 6 are located at the center of each area)

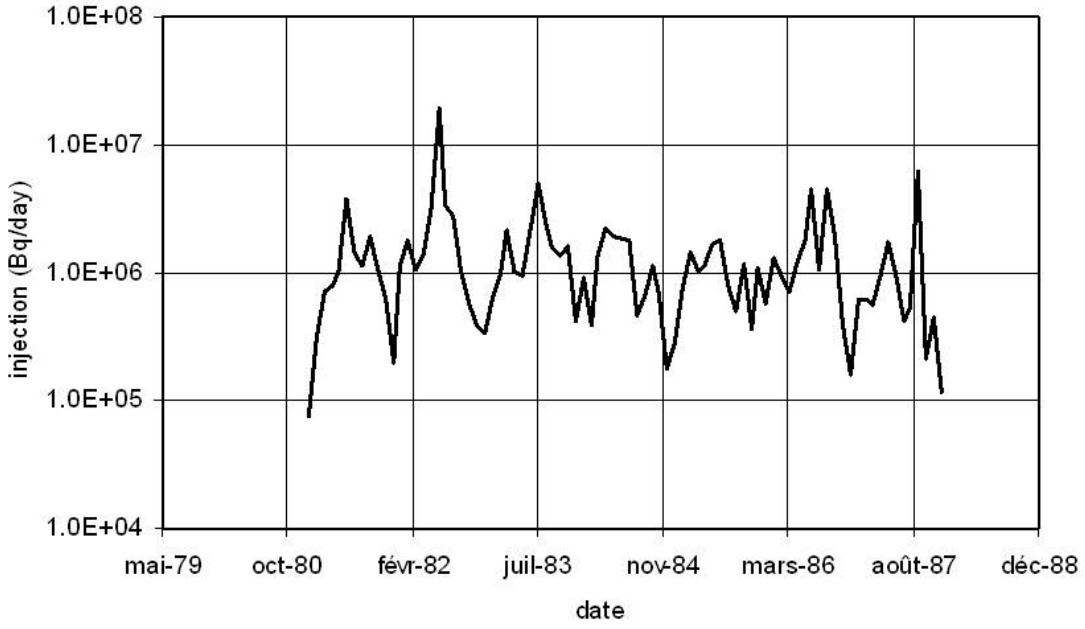

Figure 4. Injection profile at point 1 (Bq/day)

1-D transfer in the unsaturated layer: The transfer through the unsaturated layer is simulated by solving the following 1-D transport equation:

$$R\theta\frac{\partial C}{\partial t} + V_D\frac{\partial C}{\partial z} - D_L\frac{\partial^2 C}{\partial z^2} + R\theta\lambda.C = \dot{A}(t).\delta(x)\delta(y)\delta(z) \qquad (1)$$

where:
- C(t) is the concentration at the interface between the unsaturated layer and the water table
- R is the retardation coefficient
- θ is the mean moisture content
- V_D is the Darcy vertical velocity
- D_L is the dispersion/diffusion coefficient
- λ is the radioactive decay constant
- A(t) is the injection term

The dispersion/diffusion coefficient D_L is given by:

$$D_L = \alpha V_D + D_0 \psi \theta \qquad (2)$$

where the tortuosity is given by $\Psi = \frac{\theta^{10/3}}{\omega^2}$ and α is the dispersion coefficient.

The analytical solution of Equation 1 is given by:

$$C(x,y,h_{ZNS},t) = \frac{1}{\sqrt{\theta\, R}} \int_0^t d\tau \; \frac{e^{-\frac{(V.\frac{(t-\tau)}{\theta R} - h_{ZNS})^2}{4 D_L.(t-\tau)/\theta.R} - \lambda.(t-\tau)}}{\sqrt{4\pi.\, D_L.\,(t-\tau)}} \; \dot{A}(\tau).\delta(x)\delta(y) \qquad (3)$$

The infiltration rate of water into the unsaturated soil layer was estimated to be about half the annual precipitation of 500~700mm per year. A vertical pore water velocity in the unsaturated soil layer was estimated to be about 5.5 m/y based on an experiment carried out by the JAERI researchers. At G4, the estimated depth from the soil surface to the top of the groundwater aquifer was estimated to be roughly 15~20 m. The mean water content of the top 60 cm of soil was set to 2.84%, the value observed at MS2 in 1986.

The parameter values used for solving Equation (2) are summarized in Table 1. Concerning the dispersivity coefficient, an empirical value equal to 10% of the covered distance is usually considered. In our case, a conservative value of 1 m has been chosen.

Table 1 – Parameter values used for solving the transfer equation for the unsaturated zone

	Parameter	Value	Comment
UNSATURATED LAYER	Total porosity of surface soil	0.53	
	Water content	28.4 %	mean value
	Vertical pore water velocity in the unsaturated soil layer	5.5 m/y	
	Depth from soil surface to the top of the groundwater aquifer at G4	15 m	conservative value (15-20 m)
	Vertical dispersivity in the unsaturated zone	1 m	empirical

The temporal variation of activity at the interface between the unsaturated layer and the water table below injection point 1 is plotted in Figure 5 for illustrative purposes.

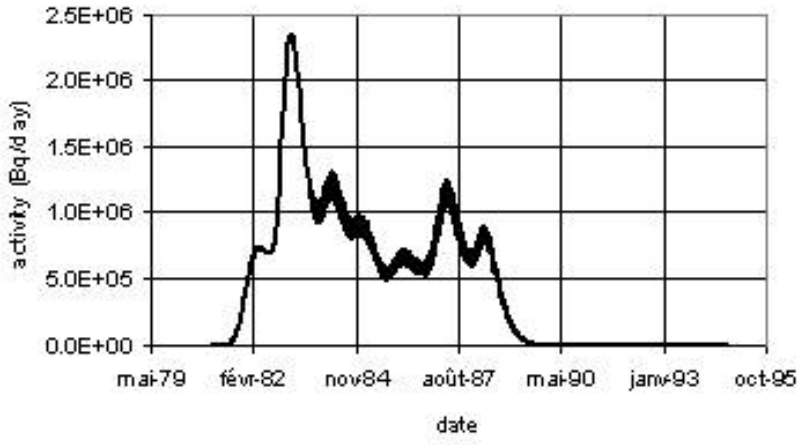

Figure 5. Time-dependent H^3 activity (Bq) at the interface between the unsaturated layer and the water table : contribution of injection at point 1

2-D transfer in the saturated layer

The output of the unsaturated layer compartment is injected into the saturated layer compartment. In the aquifer, a horizontal, constant flow velocity is considered. The problem can be considered two-dimensional or three-dimensional. In this case, as the depth of the water table is not well known, the 2-D transport equation was selected:

$$\omega R \frac{\partial C}{\partial t} + U.\frac{\partial C}{\partial x} - D_L.\frac{\partial^2 C}{\partial x^2} - D_T.\frac{\partial^2 C}{\partial y^2} + \omega R\lambda.C = \dot{A}(t)\delta(x)\delta(y)$$

where:

- U is the Darcy horizontal velocity
- D_L and D_T are respectively the longitudinal and transverse dispersion/diffusion coefficients

The 2-D analytical solution is given by an equation similar to that presented above for the 1-D transport equation:

$$C(x,y,t) = \int_0^t d\tau \; \frac{e^{-\frac{\frac{(U.\frac{(t-\tau)}{\omega R} - x)^2}{D_L} + \frac{y}{D_T}}{4(t-\tau)/\omega R} - \lambda.(t-\tau)}}{\sqrt{(64\pi)^2 D_L D_T (t-\tau)^2}} \dot{A}(\tau) \qquad (4)$$

The parameter values used for simulating transport through the water table are presented in Table 2. According to the scenario description, the mean horizontal flow rate was estimated to be about 0.2 m/day based on Darcy's law applied to the area between a well close to G4 and the point where groundwater flows southward into the Shinkawa River. At this location, the water table is deeper than in the area between JRR-2/JRR-3 and G4. Therefore, a higher value of the groundwater velocity should perhaps have been selected.

Table 2 – Parameter values for solving the 2-D saturated layer transport equation

	Parameter	Value	Comment
WATER TABLE	Hydraulic conductivity	K ~ 6 x 10^{-4} m/s	
	Longitudinal pore water velocity	Ux ~ 0.2 m/d	
	Longitudinal dispersivity	α_x = 10 m	empirical
	Transverse dispersivity	α_x = 1 m	empirical

An example of the ARGUS interface for the definition of the water table coefficients is shown in Figure 6. The plane concentration at point G4 resulting from injection at point 1 is plotted in Figure 7Figure and the HTO concentration plume calculated after 2500 days is plotted on Figure 8.

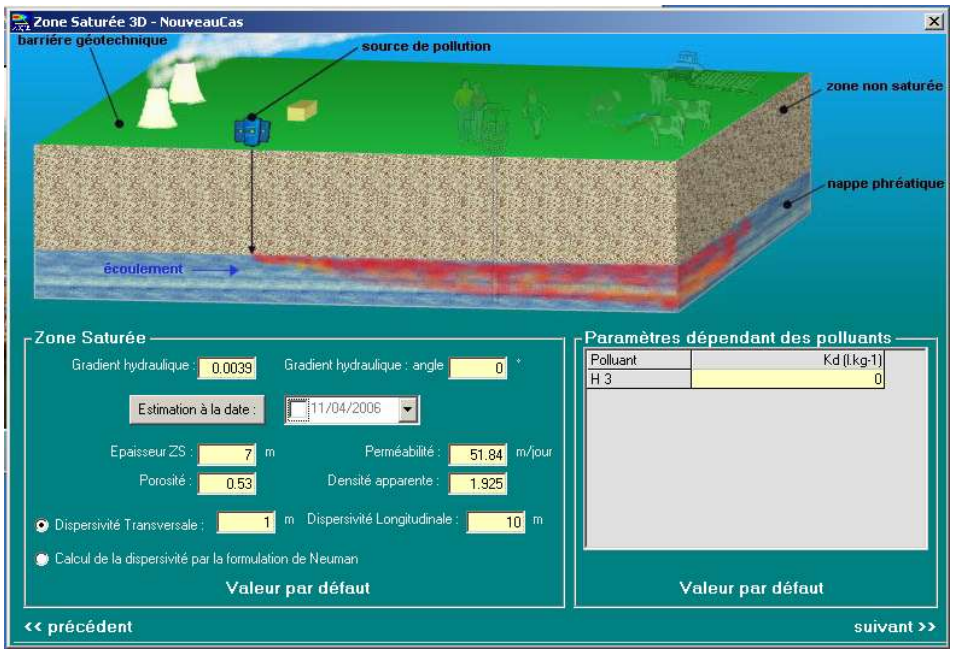

Figure 6. Example of the ARGUS software interface: definition of the hydrogeological parameters for the water table hydraulic gradient, permeability, porosity and dispersivity

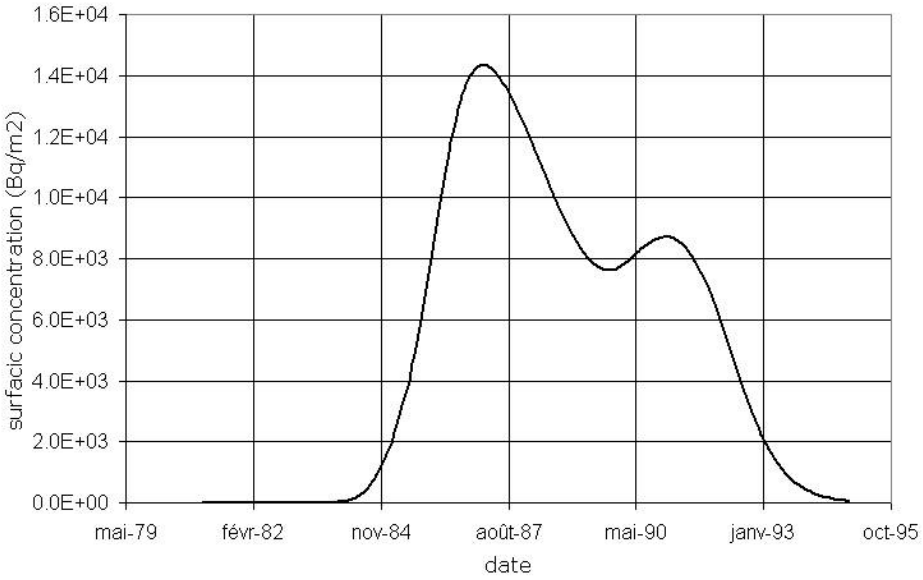

Figure 7. Time-dependent plane concentration at point G4 resulting from injection at point 1

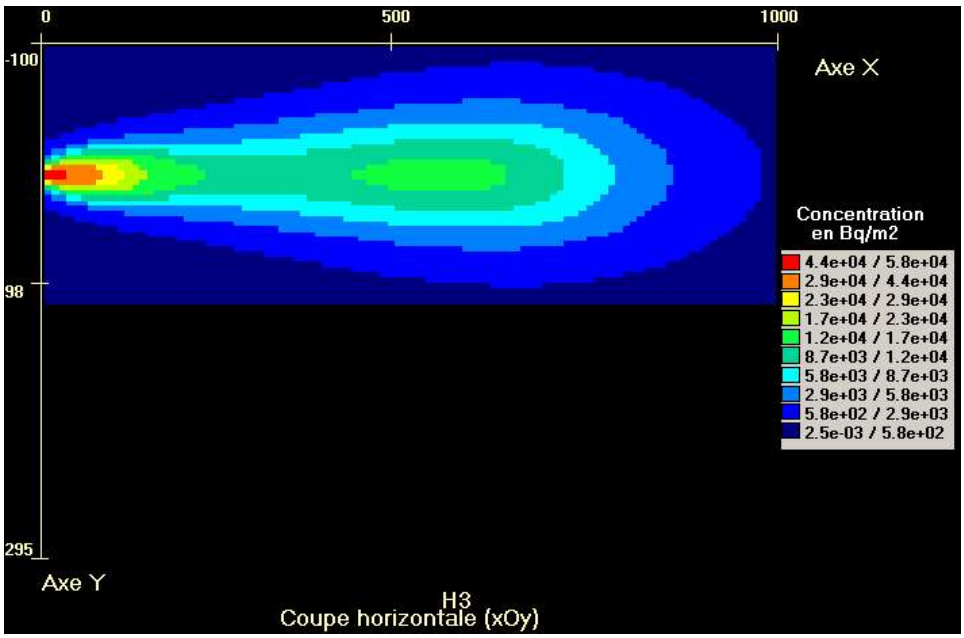

Figure 8. Plane concentration plume resulting from injection at point 1 (x=0, y=0) after 2500 days (Point G4 is located at x =500 and y=0)

Results at point G4: A plane concentration (Bq/m^2) was obtained as a result of using a 2-D model to calculate tritium transfer in the aquifer. The volumetric concentration (Bq/m^3 or Bq/L) can be estimated by taking into account the thickness of the aquifer at point G4. According to the geological scheme presented in Figure 1, a thickness of 5 m has been adopted.

The concentration at point G4 is obtained by summing the contributions from each of the six injection points. The contributions of injections 1 to 6 and the total concentration at point G4 are plotted in Figure 9. Over the studied period from 1984 to 1987, the concentration at point G4 varied from 10 to 19.5 Bq/L, with the peak occurring in November 1984. With a 7-m thick aquifer, the maximum concentration would have been around 14 Bq/L.

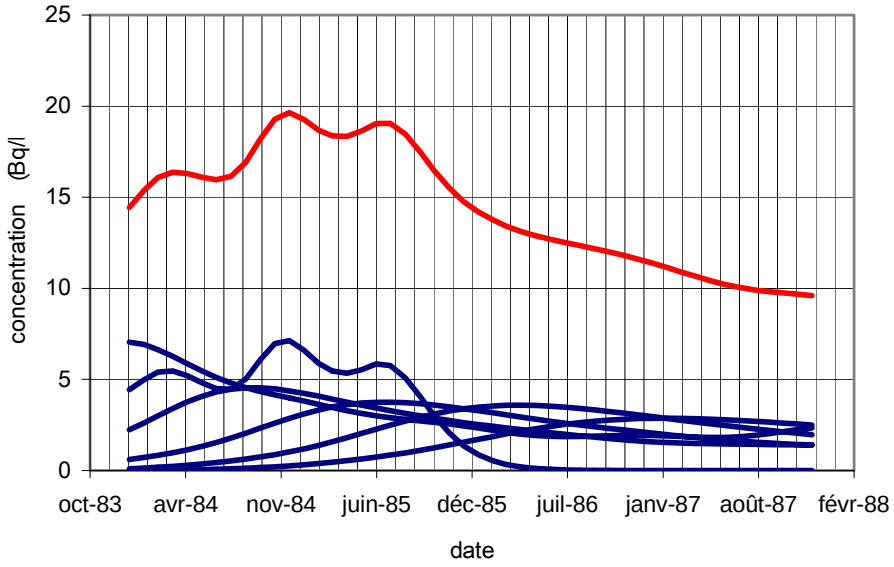

Figure 9 – Time-dependent H-3 concentration at point G4 (Bq/L): sum of the contributions of injection points 1 to 6 obtained for a 5 m thick aquifer (— contribution of injections 1 to 6; — cumulative value)